

Washington University in St. Louis
Washington University Open Scholarship

All Theses and Dissertations (ETDs)

January 2010

Structure And Function Of The FMO Protein From The Photosynthetic Green Sulfur Bacteria

Jianzhong Wen

Washington University in St. Louis

Follow this and additional works at: <https://openscholarship.wustl.edu/etd>

Recommended Citation

Wen, Jianzhong, "Structure And Function Of The FMO Protein From The Photosynthetic Green Sulfur Bacteria" (2010). *All Theses and Dissertations (ETDs)*. 374.

<https://openscholarship.wustl.edu/etd/374>

This Dissertation is brought to you for free and open access by Washington University Open Scholarship. It has been accepted for inclusion in All Theses and Dissertations (ETDs) by an authorized administrator of Washington University Open Scholarship. For more information, please contact digital@wumail.wustl.edu.

WASHINGTON UNIVERSITY IN ST. LOUIS

Department of Chemistry

Dissertation Examination Committee:

Robert E. Blankenship, Chair

Michael L. Gross

Dewey Holten

Cynthia Lo

John-Stephen Taylor

Yan-mei Wang

STRUCTURE AND FUNCTION OF THE FMO PROTEIN FROM THE
PHOTOSYNTHETIC GREEN SULFUR BACTERIA

By

Jianzhong Wen

A Dissertation Presented to the Graduate School
of Arts and Sciences of Washington University
in Partial Fulfillment of the Requirements
for the Degree of Doctor of Philosophy

August 2010

Saint Louis, Missouri

Copyright by
Jianzhong Wen
2010

STRUCTURE AND FUNCTION OF THE FMO PROTEIN FROM THE
PHOTOSYNTHETIC GREEN SULFUR BACTERIA

By

Jianzhong Wen

Research advisor:

Prof. Robert E. Blankenship
Lucille P. Markey Distinguished Professor of Biology and Chemistry
Washington University in St. Louis
St. Louis, MO 63130
Tel (314) 935-7971
Fax (314) 935-4432
Blankenship@wustl.edu

Committee members:

Prof. Robert E. Blankenship (Department of Chemistry, Department of Biology)
Prof. Michael L. Gross (Department of Chemistry)
Prof. Dewey Holten (Department of Chemistry)
Prof. John-Stephen Taylor (Department of Chemistry)
Prof. Cynthia Lo (Department of Energy, Environmental & Chemical Engineering)
Prof. Yan-mei Wang (Department of Physics)

ABSTRACT

Photosynthesis is a central biological process that produces all our food and the majority of energy used by human beings. Intense attention has been focused on using photosynthetic organisms or mechanisms adapted from photosynthesis as sources to produce cheap, clean and renewable energy. A deep understanding of the molecular mechanism of the photosynthetic processes is essential as part of that effort.

Photosynthetic prokaryotes called green sulfur bacteria (GSB) have been used as model species to understand the mechanism of the energy capture and storage and the molecular structures of the complexes that mediate this process. The photosystem of GSB includes a large antenna complex called a chlorosome. After light is captured by the chlorosome, the photon energy is transferred through two pigment-binding proteins, the baseplate protein and the Fenna-Matthews-Olson or FMO protein, to the reaction center where excitation energy is converted to chemical energy. The membrane-attached FMO protein functions as a “wire” to transfer the excitation energy from the peripheral antenna chlorosome to the reaction center. The isolated FMO protein has long been a model system to understand energy transfer

mechanisms and has been investigated by a large variety of spectroscopic and theoretical studies.

In the thesis, the structural and functional properties of the FMO protein were further investigated by studying the protein isolated from different species and also a genetically modified version. In addition, the interaction network in vivo centered on the FMO protein was elucidated.

The structure of the FMO protein from *P. aestuarii* 2K was solved to 1.3 Å resolutions, and an 8th pigment was discovered. The nature and stoichiometry of the 8th pigment in the protein was studied by native electrospray mass spectrometry (MS) coupled to HPLC pigment analysis. The structure of the FMO protein from *P. phaeum* was also determined. The first FMO mutant generated by replacing the phytyl tail of the BChl *a* to geranylgeranyl in *Chlorobaculum tepidum* was characterized. Spectral and structural insights into the FMO protein were further gained from the comparative study of the FMO protein purified from a newly discovered sixth group of photosynthetic bacteria called *Candidatus Chloracidobacterium thermophilum*. The collection and study of the various FMO proteins have deepened our understanding of this antenna complex.

The orientation of the FMO protein on the cytoplasmic membrane in vivo was determined by combining a specific chemical labeling method with MS analysis. The results gave the first experimental evidence that the BChl *a* #3 side of the protein is in close contact with the membrane. This MS-based specific protein surface mapping method was further developed to study protein-ligand interactions. Furthermore, the detailed interaction between the FMO protein and the chlorosome, specifically the baseplate protein at the bottom of the chlorosome, was investigated using hydrogen/deuterium exchange coupled with MS analysis.

The high excitation energy transfer efficiency observed in photosynthetic organisms relies on the optimal pigment-protein binding geometry in the individual protein complexes and also on the overall architecture of the photosystems. On the basis of this work, a general picture of the photosystem from GSB can be constructed.

KEYWORDS:

FMO protein; Energy transfer; Green sulfur bacteria; Native spray mass spectrometry; Protein surface mapping; Renewable energy

ACKNOWLEDGEMENTS

There are so many people who have made their contributions to my pleasant and successful experience at Wash U. I feel so sorry for being unable to list everyone whom I wish to thank.

I would like to give my deep appreciation and thanks to my research advisor and also the chair of my committee, Dr. Robert E. Blankenship. Bob, I thank you! First of all, your wisdom, generosity and knowledge have stimulated and guided me to do my best throughout my doctoral studies. Thank you for showing faith in me; for giving me the freedom to find my way in the scientific labyrinth; for the continuous support and encouragement, and for the things I learned from you.

I would like to thank the lab members in the Blankenship Lab. Thanks to past member Dr. Yueyong Xin for advices on protein purification. Thanks to Dr. Joseph Tang for bringing me the technique of small angle neutron scattering. Thanks to Dr. Connie Kang for teaching me molecular biology and genetics. I especially want to thank Dr. Aaron Collins for being my big brother. We worked together, played together, and grew together. You taught me everything from English to the American Way. It is my great pleasure and fortune to have you as my lab mate. Thanks to Xinliu Gao, Hai Yue, Xianglu Li, Dr. Dariusz Niedzwiedzki, Patrick Bell, Barbara Honchak, Jeanne Sheffield, the new members Jing He, Qian Liu, and the past members Dr. W. Matthew Sattley, Dr. Brad Postier, Dr. Surobhi Lahiri, Dr. Su Lin, Dr. Yi-kuang Lu, Dr. Tien Olson, Dr. Martin Hohmann-Marriott, Dr. Wes Swingley and Heather Matthews. I won't even try to express

my feelings about being a member of this scientific community. The group has been almost a second family to me. The experience in the lab will be invaluable for my future career.

Prof. Michael Gross, thank you very much for your continuous support and enthusiasm on my projects. I will always remember your words “KISS”. :) A fancy technique I learned in my graduate life is MS. Without you and the MS center, this wouldn't have been possible. I want to say thanks to several of your students and staff members. First I want to thank Hao Zhang who worked with me in developing the specific D/E surface mapping method and also the native spray. I still remember the excitement when we saw the first native spray spectrum of the FMO protein. Thanks to Richard Huang who taught me H/D exchange. Thanks to Drs. Henry Rohrs, Weidong Cui, Ilan Geerlof Vidavsky, Don Rempel, Adam Brustkern and Dian Su for all kinds of help when I was running experiments in your lab.

Thanks to Prof. Don Bryant and his postdoc Dr. Yusuke Tsukatani for sharing the new FMO protein and bringing a great collaboration. Thanks to Prof. Jiro Harada, Prof. Hitoshi Tamiaki and Prof. Hirozo Oh-oka for bringing me the mutant. Thanks to Prof. Graham Fleming and Prof. Greg Engel for your interest in FMO and the great work you have done on the FMO protein. Thanks to Dr. Dale Tronrud for the great collaboration on the structure of the FMO protein from *P. aestuarii*, which raised a lot of great questions. Thanks to Prof. James Allen for the collaboration in solving the structure of FMO from *P. phaeum*. Thanks to Prof. W. E. Moerner and his postdoc Dr. Randy Howard Goldsmith

for the interest of single molecule study of the FMO protein using anti-Brownian electrokinetic trap. Thanks to Prof. Ryszard Jankowiak and his student Khem Acharya for the interest of the spectral hole-burning study of the FMO protein. Thanks to Prof. Cynthia Lo and her student Sándor Kovács for the interest of molecule docking and simulation of the FMO/baseplate interaction. Thanks to Prof. Pratim Biswas and his student Luis Modesto-Lopez for the interest of using FMO to make bio-hybrid devices. Thanks to Bob again for bringing me so many great and productive collaborations.

Thanks to Prof. Richard Loomis and his student Kenneth Buyle for the help in running TCSPC experiments. Thanks to Dr. Min Chen for the discussion of chlorophyll *d* and phycocyanin from *A. marina*. Thanks to Prof. Timothy Lohman and his postdoc Dr. Binh Nguyen for the help in running analytical ultracentrifugation. Thanks to Prof. Yan-mei Wang for teaching me single molecule detection using TIRF and being on my committee. Thanks to Prof. Dewey Holten and Prof. John Taylor for being on my committee. You are great mentors. It has been always great discussions in my committee meetings.

My very special thanks go to my family. Thanks to my parents and older brother, Jianming, for their unconditional love, firm support and full confidence in me, for important values of life they taught me by their examples in my childhood such as responsibility, self-confidence and never give up. It is you who shaped me what I am now. My lovely wife, Lina, thank you! Without your love and understanding, I won't be able to go far as a scientific researcher.

TABLE OF CONTENTS

	Page
LIST OF TABLES.....	xii
LIST OF FIGURES.....	xiii
Abstract.....	iii
Acknowledgements.....	vi
Chapter 1. Introduction to the energy transfer mechanism and regulation in photosynthetic light harvesting antenna	1
1.1 Energy transfer mechanism.....	4
1.2 Mechanism of energy-transfer regulation.....	15
1.3 Statement of thesis.....	20
1.4 References.....	23
Chapter 2. Structure of the FMO protein and the nature of the 8th pigment by native spray mass spectrometry.....	36
2.1 Abstract.....	37
2.2 Introduction.....	38
2.3 Results and Discussion.....	45
2.3.1 Nature and stoichiometry of the 8th pigment.....	45
2.3.2 Function of the 8th pigment.....	55
2.3.3 Structural mass spectrometry by native spray.....	56
2.4 Materials and Methods.....	57
2.4.1 FMO purification.....	57
2.4.2 Absorbance.....	58
2.4.3 MS measurement.....	58
2.4.4 Pigment analysis by HPLC.....	59
2.5 References.....	60

Chapter 3. Pigment mutants of the FMO antenna protein

	from green photosynthetic bacteria.....	64
3.1	Abstract.....	65
3.2	Introduction.....	66
3.3	Results.....	70
3.3.1	Cell absorption and biochemical purification indicate less FMO in the mutant cells.	70
3.3.2	Pigment analysis of the FMO_BchP.....	73
3.3.3	Steady-state spectra of FMO_BchP.....	76
3.3.4	Fluorescence dynamics.....	82
3.3.5	Thermal stability of FMO_BchP.....	85
3.3.6	Gene expression profiles.....	87
3.4	Discussion.....	89
3.4.1	FMO assembly.....	89
3.4.2	Optical property and thermal stability.....	93
3.4.3	Membrane topology.....	94
3.5	Materials and Methods.....	95
3.5.1	<i>C. tepidum</i> mutagenesis, culture conditions and FMO purification.....	95
3.5.2	Pigment analysis by HPLC.....	96
3.5.3	Pigment analysis by MALDI-TOF.....	96
3.5.4	Steady-state spectra.....	97
3.5.5	Fluorescence lifetime.....	97
3.5.6	Thermal stability by UV.....	98
3.5.7	RNA purification and quantitative real-time PCR (qRT-PCR).	99
3.6	References.....	102

Chapter 4. Membrane Orientation of the FMO Antenna Protein

	from <i>Chlorobaculum tepidum</i> as Determined by Mass Spectrometry-Based Footprinting.....	108
4.1	Abstract.....	109
4.2	Introduction.....	110
4.3	Results.....	115
4.4	Discussion.....	131
4.4.1	Membrane orientation of FMO protein.....	131
4.4.2	Packing of the chlorosome, FMO and cytoplasmic membrane layers.	131
4.4.3	Packing of FMO on the cytoplasmic membrane.....	134
4.5	Conclusion.....	135
4.6	Materials and Methods.....	135
4.6.1	Native membrane preparation.....	135
4.6.2	FMO protein purification.....	136
4.6.3	Chlorosome-depleted membrane preparation.....	136
4.6.4	Carboxyl group modification.....	137
4.6.5	LC-MS/MS analysis.....	137
4.7	References.....	139
Chapter 5.	Conclusions and Future directions.....	143

APPENDICES

Appendix A	Publications
Appendix B	Awards
Appendix C	Curriculum Vitae

LIST OF TABLES

Table		Page
1	88
2	91
3	101

LIST OF FIGURES

	Page
Chapter 1	
Fig. 1	3
Fig. 2	5
Fig. 3	6
Fig. 4	7
Fig. 5	17
Fig. 6	22
Chapter 2	
Fig. 1	39
Fig. 2	40
Fig. 3	44
Fig. 4	47
Fig. 5	48
Fig. 6	50
Fig. 7	52
Fig. 8	54
Chapter 3	
Fig. 1	67

Fig. 2	71
Fig. 3	74
Fig. 4	75
Fig. 5	77
Fig. 6	79
Fig. 7	81
Fig. 8	83
Fig. 9	84
Fig. 10.....	86
Fig. 11.....	90

Chapter 4

Fig. 1	111
Fig. 2	114
Fig. 3	116
Fig. 4	118
Fig. 5	119
Fig. 6	120
Fig. 7	122
Fig. 8	123
Fig. 9	126

Fig. 10..... 128

Fig. 11..... 129

Fig. 12..... 130

Chapter 5

Fig. 1 147

Chapter 1

Introduction to the energy transfer mechanism and regulation in photosynthetic light harvesting antenna

Photosynthesis is a central biological process that has produced all our food and the majority of energy used by human beings (1). Intense attention has been focused on using photosynthetic organisms or mechanisms adapted from photosynthesis as sources to produce cheap, clean and renewable energy. A critical step along the road is to understand deeply the basic molecular mechanism of the photosynthetic process, which includes the mechanism of the energy capture and storage and the molecular structures of the complexes that mediate this process.

An essential group of molecules in the whole photosynthetic process is pigments, which also makes the world so colorful. The library of pigment molecules nature has produced includes (bacterio)chlorophylls, which are porphyrin-based pigments (2), bilins, which are open-chain tetrapyrrol molecules (3), and all kinds of carotenoids (4) (Fig. 1). By slightly modifying the structure of the pigments, nature has obtained the ability to tune the absorption wavelength of different pigments so that they cover almost the entire UV/Vis/NIR spectrum of solar radiation. In a single species, where limited types of pigments are synthesized, cells have extended their absorption cross section by tuning the absorption properties of the pigment through coupling to other nearby pigments and the surrounding protein environments. To do this, cells build specific pigment-protein complexes called light harvesting complexes (5-21, Fig. 2) whose functions are to absorb the photon energy and to transfer efficiently the energy to a complex called a reaction center (22-26, Fig. 3) where the light energy is converted into chemical energy that can be utilized by cellular processes. Surprisingly, nature has built a quite diverse group of light-harvesting complexes, and almost every group of photosynthetic species has their unique light-harvesting complexes (3, 5-21). However, no matter how different they are

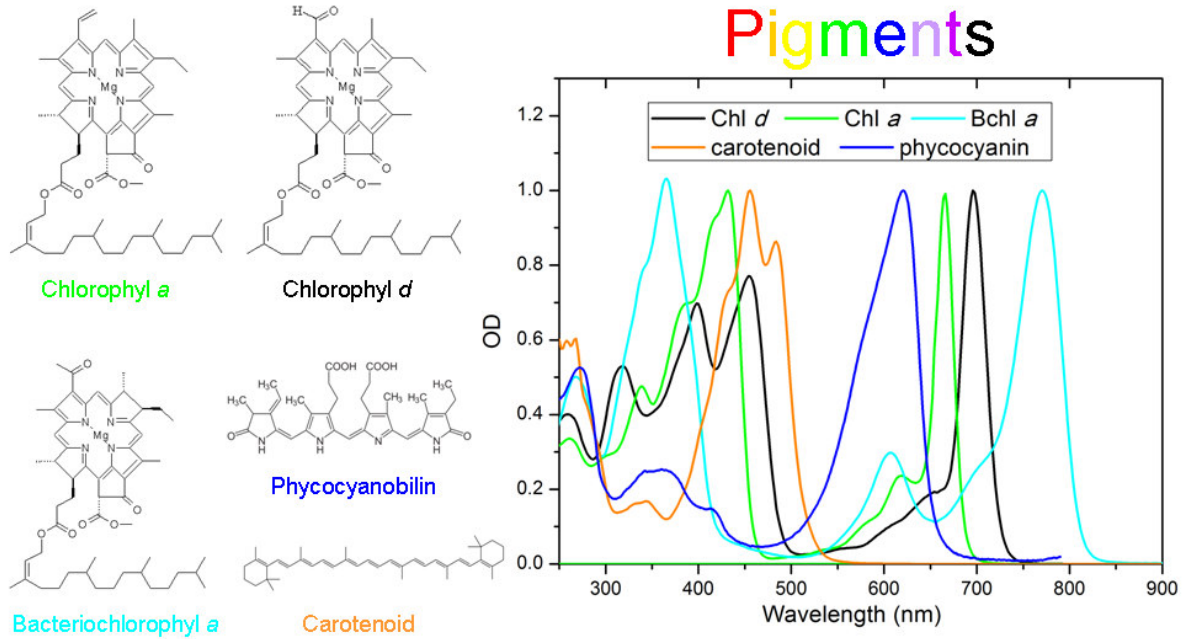


Fig. 1 Certain pigments and their absorption. Bacteriochlorophyll *a*, chlorophyll *d* and chlorophyll *a* are porphyrin-based pigments with sequential blue-shifted Q_y absorption peaks. Phycocyanobilin is shown as an example of bilins which are tetrapyrrol porphyrin molecules covering the green region of the spectra. An example of carotenoid (beta-caratene) is shown.

structurally, their main function is to harvest sunlight and to transfer the light energy efficiently to the reaction center (Fig. 4). The quantum yield of the transfer is very high; nearly every photon absorbed reaches the reaction center and initiates a charge separation under favorable conditions.

It has been an interdisciplinary research effort to understand fully the energy transfer mechanism in photosynthesis. Biochemists provide natural or genetically modified protein samples (5, 6, 8, 11-13, 16-18, 27-30); crystallographers determine atomic resolution structures of these protein complexes (7, 9, 10, 14, 15, 19, 20, 26, 31, 32); spectroscopists develop and adopt very sophisticated techniques to probe experimentally the transfer process (33-39); and theoretists develop physical models to connect the structural information with the experimental results (40-51). Although there is not yet a generalized mechanism to describe all the excitation energy transfer processes, our understanding of this process has deepened in the past years (52-57).

Energy transfer mechanism

The appropriate theory for a given system depends on the relative strength of pigment-pigment and pigment-protein coupling. Before we move on, we want to mention one very important parameter in understanding the spectroscopic properties of light harvesting complexes - the site energy of a pigment or transition energy (41, 44, 51). For the same kind of pigment in a protein complex, it will have different site energies owing to the interactions with the different local protein environments. Such pigment-protein interactions include: electrostatic interaction with surrounding charged amino acids (58,

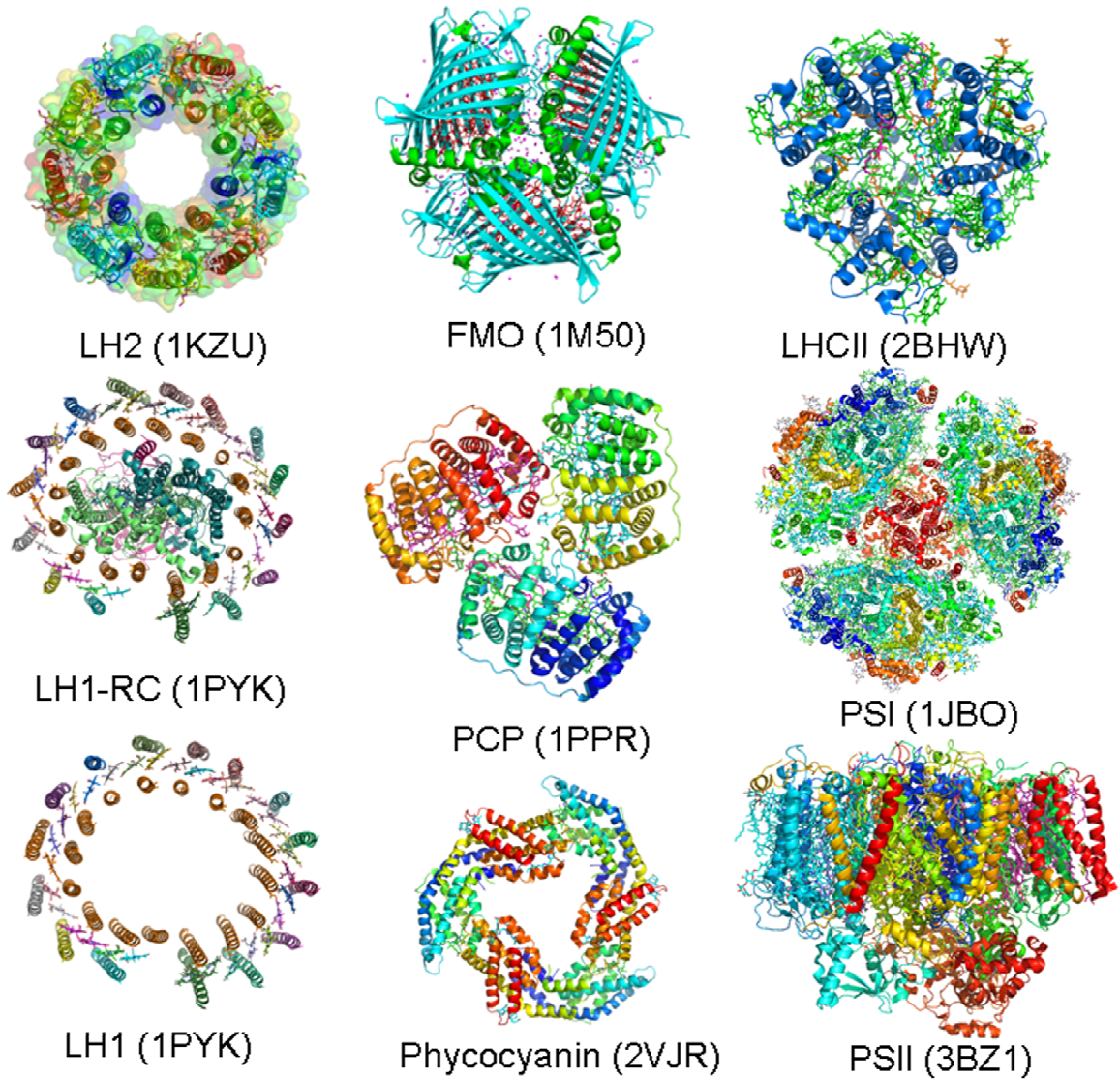


Fig. 2 Structures of certain light harvesting antenna complexes. They are extremely structurally diverse, which indicates that they have multiple independent evolutionary origins.

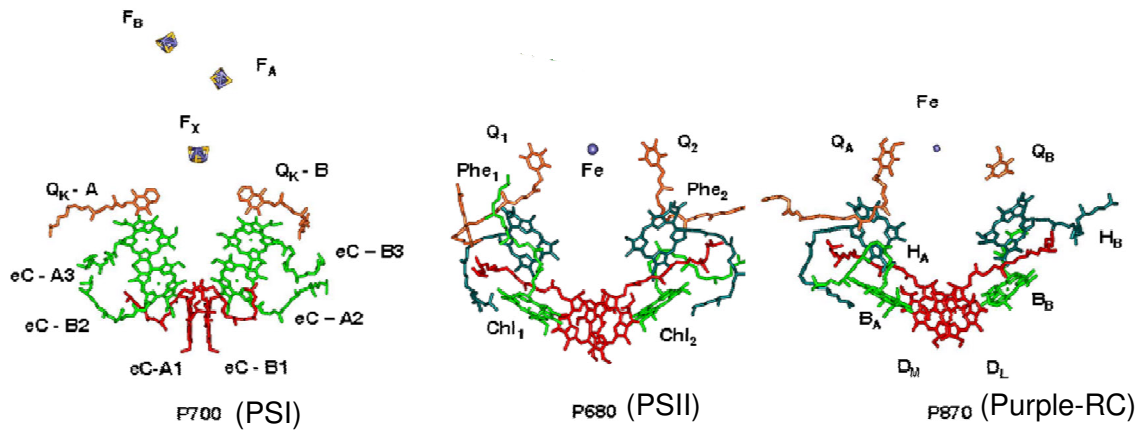


Fig. 3 The electron transfer chain of PSI, PSII and RC from purple bacteria. They show very similar pseudosymmetry suggesting a common ancestor.

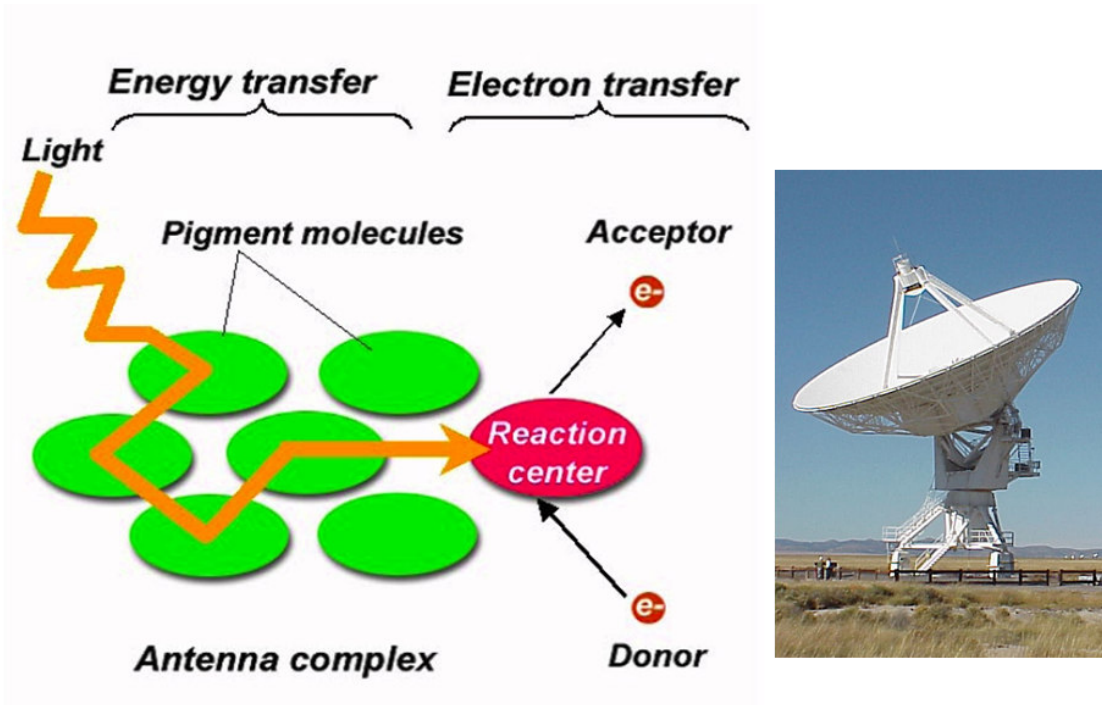


Fig. 4 The photosynthetic energy capture and storage process includes the initial energy transfer and later electron transfer processes. Nature has built a variety of light harvesting complexes in different species to harvest the photon energy and efficiently transfer the excitation energy to the reaction center where photochemistry happens. The extracted electrons at the RC then join the metabolic pathways to fix carbon and are involved in other cellular activities. The whole working principle is similar as that of the radio telescope. (Figure adapted from ref. 145, Fig. 7.10)

59); hydrogen bonding between the pigment and the protein (28, 60); distortion of the pigment macrocycle (61); the axial ligation to the central magnesium (29); electrostatic interaction with the protein backbone, etc (48, 62, 63). Such energetic tuning can shift the site energy by up to tens of nanometers. Besides the above static shift of the site energy, there is also a dynamic regulation of the site energy induced by the coupling of the electronic transition with the protein vibrations (64, 65).

The fundamental theory of excitation energy transfer between molecular electronic transition dipoles is that of Förster resonance energy transfer (66). This mechanism applies when the excitonic coupling between two pigments is small compared to the difference of their site energies. Normally this requires that the two pigments are well separated in space. Excitation energy is basically localized on an individual pigment and non-radiatively transfers between them through incoherent hopping. Under this situation, the coupling energy between the two pigments 1 and 2 can be described using a point-dipole approximation (44, 67, 68).

$$V_{12} = \frac{1}{4\pi\epsilon_0\epsilon_r} \bullet \left[\frac{\bar{\mu}_1 \cdot \bar{\mu}_2}{R_{12}^3} - \frac{3(\bar{\mu}_1 \cdot \bar{R}_{12})(\bar{\mu}_2 \cdot \bar{R}_{12})}{R_{12}^5} \right] \quad (1)$$

All the protein environment effects are taken into account by the dielectric constant ϵ_r .

$\bar{\mu}_1$ and $\bar{\mu}_2$ are the optical transition dipoles of pigments 1 and 2, and \bar{R}_{12} is the center to center spatial vector from 1 to 2.

The energy transfer rate can be described by:

$$k = \frac{8.79 \times 10^{-5} k_f K^2}{(R_{12}^6 n^4)} \bullet \int \epsilon(\lambda) F_D(\lambda) \lambda^4 d\lambda \quad (2)$$

where k_f is the fluorescence decay rate of the energy donor; $\kappa^2 = (\cos \alpha - 3 \cos \beta_1 \cos \beta_2)^2$ is an orientation factor where α is the angle between transition dipoles $\bar{\mu}_1$ and $\bar{\mu}_2$ and β s are the angles between $\bar{\mu}_1$ and \bar{R}_{12} , $\bar{\mu}_2$ and \bar{R}_{12} ; n is the refractive index; the rate k depends on the sixth-order distance between the donor and acceptor R_{12}^6 ; $\int \varepsilon(\lambda) F_D(\lambda) \lambda^4 d\lambda$ is the spectral overlap of the donor emission spectrum and the acceptor absorption spectrum where $\varepsilon(\lambda)$ is the molar absorptivity of the acceptor on a wavelength scale and $F_D(\lambda)$ is the normalized emission spectrum of the donor.

This mechanism is used to describe successfully the energy transfer process in the Peridinin-chlorophyll *a*-protein (PCP) complex found in dinoflagellates (69, 70), but often does not give satisfactory results in elucidating the observed energy transfer phenomena in other photosynthetic complexes (44, 52). The chlorophyll molecules in the PCP complex are separated by approximately 18 nm (21, 70) falling into the range of Förster's assumption, while the pigment molecules in most of the other known light-harvesting complexes are densely packed, and the excitonic coupling between them is strong. The excitation is instead delocalized on multiple pigments simultaneously and the overall excitation wave function can be viewed as coherent superpositions of the monomeric excited states. Nevertheless, the classical description of the Förster energy transfer is easy to understand and can provide a qualitative description of the light-harvesting process in the photosystems. The basic concept used to describe the electronic-vibrational coupling provides the foundation of advanced theories developed using quantum mechanics to describe the energy transfer mechanism under the strong coupling cases.

For the strong excitonic coupling but weak excitation-vibrational coupling case, the wave function of the exciton states is viewed as the coherent superposition of localized excited states. The relaxation of the delocalized excitation states (under this condition, the traditional point-dipole approximation in the Förster mechanism is not valid owing to the short distance between the coupling pigments) can be described by several theories among which the Redfield relaxation theory is widely applied (65, 71, 72). According to Redfield relaxation theory, weak exciton-vibrational interaction is treated as a perturbation in contrast to the Förster mechanism where the weak excitonic coupling is treated as a perturbation (73). The rate of the exciton relaxation derived is dependent on the energy difference between the two exciton states, the overlap of the two exciton wavefunctions, the correlation of the protein vibrations (uncorrelated vibrations lead to fast exciton relaxation), and the ability of the vibrational environment to dissipate the excess energy during exciton relaxation (74-76).

Versions of modified Redfield theory (65, 77-80) were also developed to treat the strong excitonic coupling and strong exciton-vibrational coupling systems in which the nuclear reorganization was also taken into account non-perturbatively. In the Redfield theory, the nuclear relaxation is assumed to be fast compared to the energy transfer between different exciton states and only a single phonon is considered in the exciton-nuclear interaction. This limitation breaks down in the modified Redfield equation where the nuclei relax into different equilibrium states in the strong exciton-vibrational coupling conditions (65, 73).

In the photosynthetic light-harvesting process, an energy gradient is almost always

formed in the individual light harvesting complexes by different excitonic coupling or environment tuning of the site energies of different pigments, or by building different structures (30, 81). This energy gradient on one hand guides the energy flow to the reaction center. On the other hand, the excess energy generated must be dissipated into the environment. The uncontrollable environmental fluctuations are usually assumed to be destructive in the energy transfer process especially when the system is fundamentally quantum mechanical. However, it was recently found that the fluctuations can dynamically manipulate the site energies which can increase the overlap of different energy levels and may actually aid transport through a dissipative network by opening up additional energy transfer pathways. This noise-assisted transport has been proposed to enhance both the rate and yield of energy transfer, especially in the quantum coherence energy evolution that will be mentioned later (82-85).

As discussed before, the Förster theory has proved successful to predict the energy transfer rate between two weakly coupled donor and acceptor molecules, but it can not be employed to describe the energy transfer in a confined geometry with multi-chromophores in which the exciton relaxation theory should be considered. In the past decade, a generalized Förster energy transfer mechanism (86-91) has been developed to explore and quantify the energy transfer dynamics in large light-harvesting complexes in which not all the pigments are coupled strongly with each other, but rather they form certain domains (92-94). Within each domain, the pigments are tightly coupled and share the excitation. The interaction between different domains is weak. Redfield or modified Redfield theory can be used to describe the exciton relaxation within the domains. The

generalized Förster theory can be used to describe the energy transfer between the domains. Here each domain is viewed as a supermolecule with collective exciton states.

It is exciting to see the great breakthroughs of understanding the energy transfer process in the individual light harvesting complexes (57). However, in large scale, it is still not well understood how the long range energy-transfer process in a native photosynthetic membrane is achieved so efficiently especially when the photon energy needs to migrate a long distance from the peripheral light-harvesting complex to the reaction center. On the microscopic scale, the detailed exciton-bath interaction, such as the tuning of the site energy by the protein environment, the effect of environmental fluctuation on the transfer efficiency, is still not clearly understood.

Free (bacterio)chlorophylls in organic solvents and the isolated light harvesting complexes in most cases have an excited state lifetime of approximately several nanoseconds. The light energy captured by these protein complexes in the native membrane must migrate rapidly to be utilized for photosynthesis by non-radiative processes which normally occur in a few hundred picoseconds to sub-picoseconds to compete with the fluorescence and other decay processes. The developments of advanced laser and optical spectroscopy techniques in the past decades have made observing these ultrafast process possible (37). Techniques such as pump-probe (34-36), hole burning (95, 96), single-molecule spectroscopy (97, 98), photon echo, etc, have been applied to or developed through studying the light harvesting complexes and have already generated

tremendous amounts of experimental results, which are used to support the development of theories.

Recently, a new ultrafast nonlinear spectroscopy technique called two dimensional electronic spectroscopy (38, 39, 99-101) pioneered by the Fleming group has been used to probe energy transfer dynamics in several light harvesting complexes (102-105), like the FMO complex, a crucial part of the photosynthetic system of green sulfur bacteria. This new technique has the ability to record both the population and phase information. The excitonic coupling and dynamics can be directly viewed in the off-diagonal peaks. Experiments using this technique have demonstrated the existence of strong and long-lived quantum coherences at liquid nitrogen temperature (103, 106) and also physiological temperature in several light harvesting complexes (107-109). Such long-lived coherences were proposed to improve energy transfer efficiency in photosynthetic systems by allowing an excitation to follow a quantum random walk as it approaches the reaction center. These observations have generated considerable interest in understanding the possible role of quantum coherence effects in the remarkably efficient excitation energy transfer in FMO and other pigment binding protein complexes.

Overall, photosynthetic species have developed a large variety of antenna complexes. On one hand, these light-harvesting complexes increase the spectral and spatial absorption cross section of the surrounding reaction center, and let the cells make full use of the solar radiation. On the other hand, the increase of the size and/or population of the antennas around the reaction center introduce the challenge of efficient excitation energy

transfer by increasing the distance, introducing possible complex transfer pathways and more uncontrollable dynamic fluctuations. Remarkably, nature seems to be able to circumvent the difficulty through billions of years of evolutionary pressure and reach a quantum efficiency of almost unity during the energy-transfer process. Not only will a deep understanding of the mechanism behind this natural process revolutionize our knowledge of the light-harvesting complexes, but also the techniques and theory developed by studying these wonderful model systems may also shine light on the other light-matter interactions, e.g., nano-materials and semi-conductors (*110*), on the applications of solar energy conversions (*111*), artificial photosynthesis, and quantum information (*112, 113*).

The light absorbed is finally utilized to generate a charge separation at the reaction center from where electrons are extracted to join the metabolic pathways to fix carbon or be involved in other cellular processes. Compared to the ultrafast energy transfer in the light reactions, the rates of the subsequent dark reactions are slow, and this forms the bottleneck of the whole light-driven energy storage process. It is extremely dangerous when the cells generate too much reducing power by transferring too much photon energy to the reaction center, which can easily happen under full sunshine. In addition, the quantity and quality of the light in natural environments can vary over several orders of magnitude on a time scale of seconds to seasons. To avoid the deadly situations and adapt to the environmental fluctuations, cells have generated the ability to control dynamically the energy transfer process to prevent photodamage, although different groups of photosynthetic species sometimes use different regulation methods as described

below.

Mechanism of energy-transfer regulation

In plants, algae and cyanobacteria, photosystem I (PSI) and photosystem II (PSII) work together to split water and evolve oxygen. Electrons extracted from water by PSII are transferred to PSI, and their serial connection means that the rate of electron transport between the two photosystems must be similar. Thus, the light energy received by both photosystems should also be similar to achieve maximum efficiency (114). “State transitions” are a phenomenon generally adapted by oxygenic species to balance the energy input to PSI and PSII under low light conditions.

State transitions are a short-term adaption mediated mainly by the reversible phosphorylation of the main light-harvesting complex protein (LHCII) in plants and green algae and its migration between photosystem I (PSI) and photosystem II (PSII), which is mainly controlled by the redox state of plastoquinone pool and cytochrome *b_f* complex (115-117). When the illumination is favouring PSII, LHCII is phosphorylated, detached from PSII and migrates to PSI. The absorption cross section of PSI is thus increased. This is called State II. If PSI is preferentially excited, LHCII is dephosphorylated and migrates back to PSII to redistribute the excitation energy. This is called State I. Through state transitions, the system distributes the excitation such that the light-limited photosystem receives more energy. In cyanobacteria, a similar transition is achieved by the migration of phycobilisome between PSI and PSII to balance the distribution of excitation energy (118).

Under high light or saturated light conditions, plants and algae have evolved ways to get rid of excess energy that has already been absorbed. This is mainly achieved by a thermal dissipation process called non-photochemical quenching (NPQ) in PSII, measured as the quenching of chlorophyll fluorescence (*119, 120*). The regulatory mechanism of energy dependent NPQ is induced by a decrease of the pH of lumen of the thylakoid that is generated by over reducing the photosynthetic electron transport chain. The low pH of the lumen allows certain PSII proteins to be protonated and to activate a xanthophyll cycle (Fig. 5). A lumen-located violaxanthin de-epoxidase enzyme catalyzes the conversion of violaxanthin to zeaxanthin via the intermediate antheraxanthin at low pH (*121*). Violaxanthin has nine conjugated double bonds, while antheraxanthin and zeaxanthin have ten and eleven, respectively. The increased conjugation will lower the excitation energy level of the carotenoid and facilitate the de-excitation of chlorophyll either directly through triplet formation or indirectly through structural changes. In limiting light, a reversal of the cycle is mediated by the enzyme zeaxanthin epoxidase. In addition, mutants produced by deleting a component of PSII called PsbS protein confirmed that this protein is also an essential component for NPQ and is a sensor of the lumen pH (*122, 123*). While the understanding of the energy dependent NPQ has deepened in the past several years, the most fundamental question that the physical mechanism of chlorophyll deactivation is still not very clear. The identity of the quenching species, in terms of both pigment composition and location, and the means by which the quencher(s) dissipates the excess energy are still under debate (*124-126*).

If excess energy is not quenched in a timely manner, reactive oxygen species are

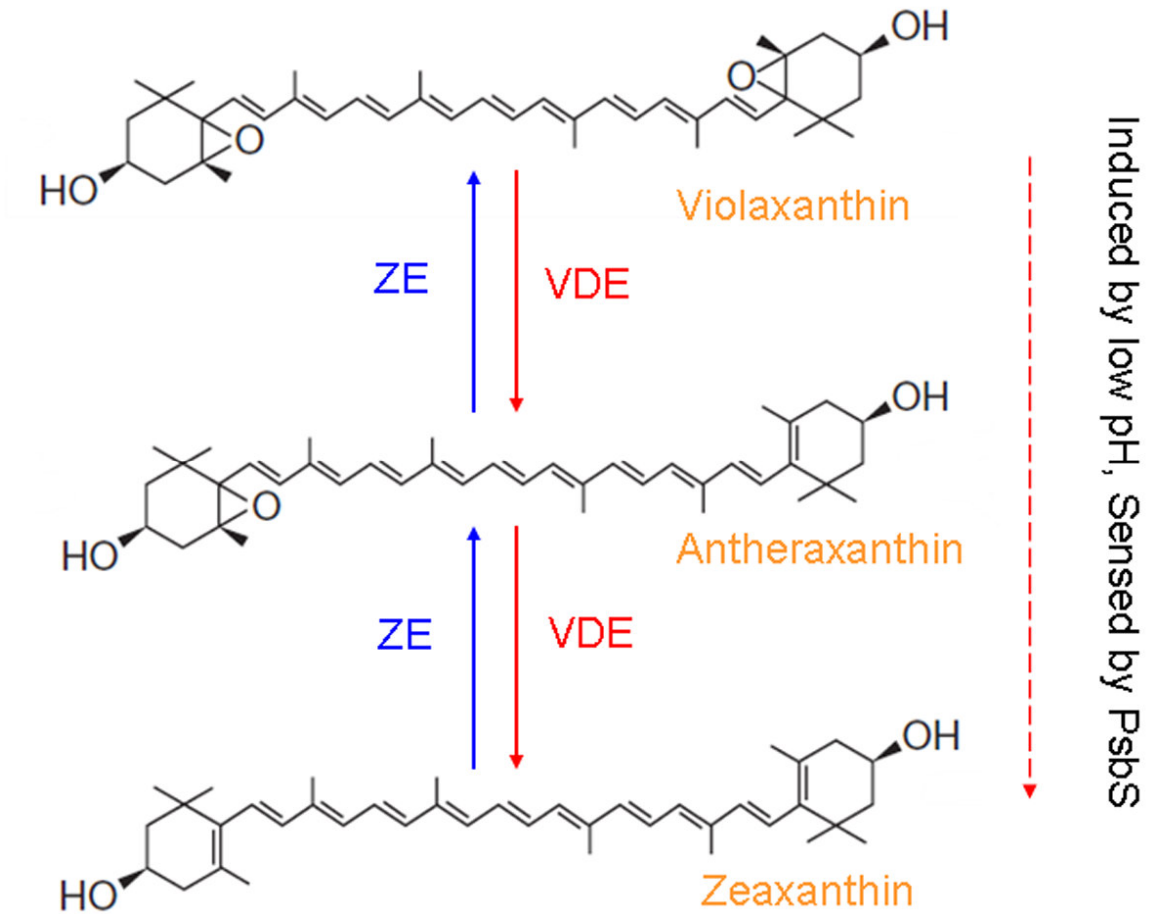


Fig. 5 Xanthophyll cycles. Excess light induces the decrease of lumen pH which is sensed by the PsbS protein through protonation. The de-epoxidation reaction of violaxanthin through antheraxanthin to zeaxanthin is activated by the violaxanthin de-epoxidase (VDE). Once the high light stress is released, a reverse cycle is catalyzed by zeaxanthin epoxidase (ZE).

produced and photodamage happens. Cells have evolved different mechanisms to repair the damaged protein. For example, the D1 protein from the PSII core turnovers very rapidly in a light-dependent manner (127). Damaged D1 is digested by proteases, and new D1 protein is synthesized to repair the PSII. During the repair process, there seems to be a migration of PSII between the grana and stromal lamellae (128). So far intense attention has been focused on understanding the recognition of damaged D1 protein by protease and the mechanism of the disassembly and assembly of PSII in the repair cycle (129). It is hypothesized that the rapid turnover of D1 protein prevents the damage of the entire PSII.

Compared to oxygenic photosynthetic species, the regulation of energy transfer in the anoxygenic prokaryotes including green sulfur bacteria, filamentous anoxygenic phototrophs, purple bacteria, heliobacteria and the newly discovered photosynthetic acidobacteria, is not well studied.

In green sulfur bacteria, a variety of lines of evidence suggest that a redox dependent regulation of energy transfer occurs in the chlorosome and FMO antenna protein (130). When the chlorosome is under oxidizing conditions, the fluorescence emission intensity will dramatically decrease owing to induction of quenchers. Such an effect was observed in the isolated chlorosome, native membrane and whole cells, and could be a possible method to protect the cell from transient exposure to oxidizing conditions by efficiently quenching the excitation (131). A redox species like chlorobiumquinone was proposed to be involved in the quenching (132). The photon energy harvested by the chlorosome is

transferred through FMO to the reaction center. A similar quenching phenomenon was also found in the FMO protein, but the molecular mechanism is still unclear (133). The newly discovered *Candidatus Chloracidobacterium thermophilum*, which belongs to the phylum Acidobacteria also exhibits a similar redox regulation at least in the FMO level as found in green sulfur bacteria (134). It was also observed that chlorosomes from green sulfur bacteria and filamentous anoxygenic bacteria modify the composition and morphology along the growth environment to regulate the energy transfer (135-137). Several species also synthesize different bacteriochlorophylls (*c*, *d* or *e*) to assemble the chlorosomes, which show different internal structures and optical properties. Savikhin and co-workers (138) also proposed the formation of triplet excitons in chlorosomes owing to triplet-triplet interaction between the closely packed BChls and predict that the energy of these triplet excitons may fall below that of singlet oxygen and triplet carotenoids, thus preventing energy transfer from triplet BChl and serves as an alternative photoprotection mechanism.

Cells of purple photosynthetic bacteria when exposed to elevated levels of oxygen will reduce the amount of synthesized LH complexes. Under low light condition, more antenna complexes are made, and a higher LH2:LH1 ratio is observed. Certain species will synthesize modified antenna complexes, changing the spectral properties according to the light intensity and quality (30). For example, the *Rps. palustris* genome contains at least four different gene pairs that encode putative LH2 $\alpha\beta$ -apoproteins, and different genes are expressed depending on the growth conditions, which could even make some complexes having mixed apoprotein types within single complete rings and produce

different spectral types (139, 140).

To prevent effectively the production of reactive oxygen species, a common strategy used by almost all the photosynthetic species is to synthesize carotenoids and embed them into the light harvesting and reaction center complexes (141). Multiple functions are performed by carotenoids in photosynthesis (4). They serve as accessory light harvesting pigments, extending the range of wavelengths over which light can drive photosynthesis, and they also build blocks of various light harvesting and RC complexes and help assemble and stabilize proteins (142, 143). One additional unique property is to protect the chlorophyllous pigments from the harmful photodestructive reaction, which occurs in the presence of oxygen. Carotenoids absorb the green and blue light (which is not covered by the chlorophyllous pigment absorption) for photosynthetic energy conversion by a singlet-singlet energy transfer to neighbouring (bacterio)chlorophylls. The protective role against photo-oxidation is achieved by a triplet-triplet energy transfer. Via the triplet state, carotenoids can quench the (bacterio)chlorophyll triplet states that may be formed from the singlet states by inter-system crossing. In this way, carotenoids will prevent the triplet (bacterio)chlorophylls reacting with the ground state triplet oxygen to form highly reactive singlet oxygen. In addition, carotenoids can directly quench the singlet oxygen via their triplet states owing to their lower energy level of triplet states (144).

Statement of thesis

To understand the molecular mechanism of photosynthesis, we used the photosystem from a group of prokaryotes called green sulfur bacteria (GSB) as a model system (Fig. 6). GSB has a large antenna complex called a chlorosome (17). After photons are

captured by the chlorosome, the photon energy is transferred through two pigment-binding proteins, the baseplate protein (18) and FMO protein (15), to the reaction center, where excitation energy is converted to chemical energy. One of my interests is to understand the structure of individual pigment-binding protein complexes and hope to elucidate the architecture of the whole photosystem. On top of that, we are interested in understanding the long-range energy transfer process, which is how the photons absorbed by the peripheral antenna can be efficiently transferred to the reaction center and also the relevant regulation of the energy transfer.

The goal of my Ph.D thesis was: 1) to investigate the structural and functional relationship of the FMO protein, specifically the pigment/pigment interactions and pigment/protein interactions, and how these interactions facilitate the high energy transfer efficiency; 2) to study the FMO interaction network in vivo and build a detailed overall membrane architecture, specifically to show how the FMO protein interacts with the cytoplasmic membrane and the chlorosomes, and 3) to determine the binding sites, stoichiometry and affinity of the FMO protein with the baseplate protein. To achieve these goals, we employed multi-disciplinary approaches including biochemistry techniques, biophysical techniques and molecular biology.

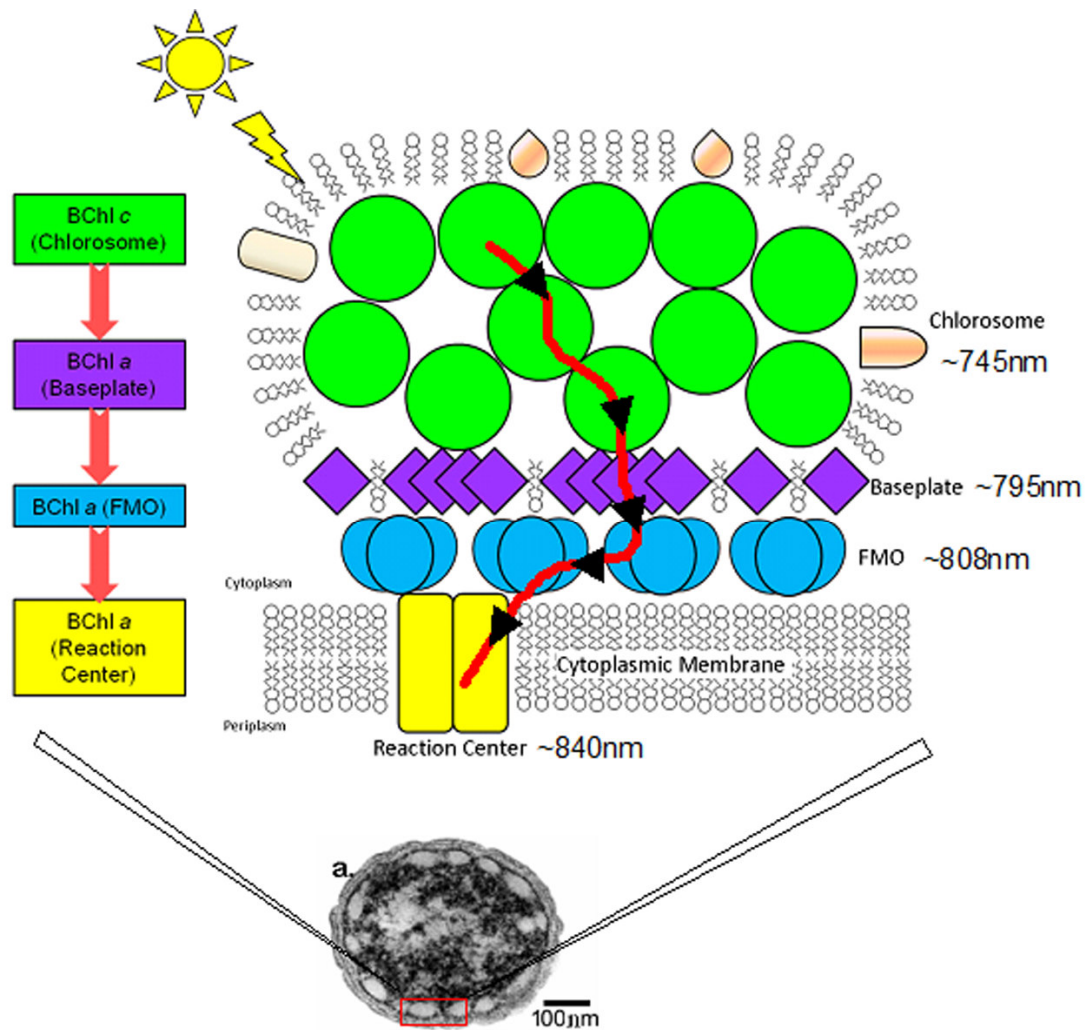


Fig. 6 Schematic picture of photosystem from green sulfur bacteria. Energy collected by the big chlorosome antenna is funneled through the baseplate protein and FMO protein to the RC.

References

1. Blankenship RE. (2002) *Molecular Mechanisms of Photosynthesis*. London: Blackwell Sci.
2. Scheer H (2006) An overview of chlorophylls and bacteriochlorophylls: biochemistry, biophysics, functions and applications. In: Grimm B, Porra RJ, Rüdiger W and Scheer H (eds) *Chlorophylls and Bacteriochlorophylls (Advances in Photosynthesis and Respiration)* pp. 1-26. Springer, Dordrecht, the Netherlands
3. MacColl R (1998) Cyanobacterial phycobilisomes *J. of Structural Biology* 124:311–334
4. Frank HA, Cogdell RJ (1996) Carotenoids in Photosynthesis. *Photochem. Photobiol.* 63:257-264
5. Wientjes E, Oostergetel GT, Jansson S, Boekema EJ, Croce R (2009) The role of Lhca complexes in the supramolecular organization of higher plant photosystem I, *J. Biol. Chem.* 284:7803-7810.
6. Zheleva D, Sharma J, Panico M, Morris HR, Barber J (1998) Isolation and characterization of monomeric and dimeric CP47-reaction center photosystem II complexes. *J. Biol. Chem.* 273:16122-16127.
7. Liu Z, Yan H, Wang K, Kuang T, Zhang J, Gui L, An X, Chang W (2004) Crystal structure of spinach major light-harvesting complex at 2.72 Å resolution. *Nature* 428:287-292.
8. Doust AB, Marai CNJ, Harrop SJ, Wilk KE, Curmi PMG, Scholes GD (2004) Developing a structure-function model for the cryptophyte phycoerythrin 545 using ultrahigh resolution crystallography and ultrafast laser spectroscopy, *J. Mol. Biol.* 344:135-153.
9. Roszak AW, Howard TD, Southall J, Gardiner AT, Law CJ, Isaacs NW, Cogdell RJ (2003) Crystal structure of the RC-LH1 core complex from *Rhodospseudomonas palustris*. *Science* 302:1969-1972.
10. McDermott G, Prince SM, Freer AA, Hawthornthwaite-Lawless AM, Papiz MZ, Cogdell RJ, Isaacs NW (1995) Crystal structure of an integral membrane light-harvesting complex from photosynthetic bacteria. *Nature* 374:517-521.
11. Collins AM, Xin Y, Blankenship RE (2009) Pigment organization in the

- photosynthetic apparatus of *Roseiflexus castenholzii*. *Biochim Biophys Acta* 1787:1050-1056.
12. Xin Y, Lin S, Montaña GA, Blankenship RE (2005) Purification and characterization of the B808-866 light-harvesting complexes from green filamentous bacterium *Chloroflexus aurantiacus*. *Photosyn. Res.* 86:155-163.
 13. Tronrud DE, Wen J, Gay L, Blankenship RE. (2009) The structural basis for the difference in absorbance spectra for the FMO antenna protein from various green sulfur bacteria. *Photosynth Res.* 100:79-87
 14. Fenna RE, Matthews BW(1975) Chlorophyll arrangement in a bacteriochlorophyll protein from *Chlorobium limicola*. *Nature* 258:573–577.
 15. Li Y-F, Zhou W, Blankenship RE, Allen JP (1997) Crystal structure of the bacteriochlorophyll a protein from *Chlorobium tepidum*. *J Mol Biol* 271:456–471.
 16. Tsukatani Y, Wen J, Blankenship RE, and Bryant DA(2010) Characterization of the FMO protein from the aerobic chlorophototroph, *Candidatus Chloracidobacterium thermophilum*. *Photosyn. Res.* 10.1007/s11120-009-9517-0
 17. Ganapathy S, Oostergetel GT, Wawrzyniak PK, Reus M, Gomez Maqueo Chew A, Buda F, Boekema EJ, Bryant DA, Holzwarth AR, de Groot HJ (2009) Alternating syn-anti bacteriochlorophylls form concentric helical nanotubes in chlorosomes. *Proc Natl Acad Sci USA* 106:8525–8530
 18. Pedersen MØ, Pham L, Steensgaard DB, Miller M. (2008) A reconstituted light-harvesting complex from the green sulfur bacterium *Chlorobium tepidum* containing CsmA and bacteriochlorophyll a. *Biochemistry* 47:1435-41.
 19. Contreras-Martel C, Matamala A, Bruna C, Poo-Caamaño G, Almonacid D, Figueroa M, Martínez-Oyanedel J, Bunster M. (2007) The structure at 2 Å resolution of phycocyanin from *Gracilaria chilensis* and the energy transfer network in a PC-PC complex. *Biophys Chem.* 125:388-396.
 20. Nield J, Rizkallah PJ, Barber J, Chayen NE. (2003) The 1.45 Å three-dimensional structure of C-phycocyanin from the thermophilic cyanobacterium *Synechococcus elongatus*. *J Struct Biol.* 141:149-55.
 21. Hofmann E, Wrench PM, Sharples FP, Hiller RG, Welte W, Diederichs K (1996) Structural basis of light harvesting by carotenoids: peridinin–chlorophyll-protein from

- Amphidinium carterae*. *Science* 272:1788–1791.
22. Amunts A, Drory O, Nelson N (2007) The structure of a plant photosystem I supercomplex at 3.4 Å resolution. *Nature* 447:58-63.
 23. Loll B, Kern J, Saenger W, Zouni A, Biesiadka J. (2005) Towards complete cofactor arrangement in the 3.0 Å resolution structure of photosystem II. *Nature* 438:1040-1044.
 24. Ferreira KN, Iverson TM, Maghlaoui K, Barber J, Iwata S. (2004) Architecture of the photosynthetic oxygen-evolving center. *Science* 303:1831-1838
 25. Jordan P, Fromme P, Witt HT, Klukas O, Saenger W, Krauss N. (2001) Three-dimensional structure of cyanobacterial photosystem I at 2.5 Å resolution. *Nature* 411:909-17.
 26. Deisenhofer J, Michel H. (1989) The photosynthetic reaction center from the purple bacterium *Rhodospseudomonas viridis*. *Science*. 245:1463-1473.
 27. Schulte T, Hiller RG, Hofmann E (2010) X-ray structures of the peridinin–chlorophyll-protein reconstituted with different chlorophylls. *FEBS letters* 584:973-978
 28. Fowler GJ, Visschers RW, Grief GG, van Grondelle R, Hunter CN (1992) Genetically modified photosynthetic antenna complexes with blueshifted absorbance bands. *Nature* 355:848–50
 29. Lin S, Jaschke PR, Wang H, Paddock M, Tufts A, Allen JP, Rosell FI, Mauk AG, Woodbury NW, Beatty JT (2009) Electron transfer in the *Rhodobacter sphaeroides* reaction center assembled with zinc bacteriochlorophyll. *Proc Natl Acad Sci USA* 106:8537-8542
 30. Cogdell RJ, Gall A, Köhler J. (2006) The architecture and function of the light-harvesting apparatus of purple bacteria: from single molecules to in vivo membranes. *Q. Rev. Biophys.* 39:227–324
 31. Fromme P, Allen JP (2008) X-ray crystallography of photosynthetic proteins. In: Aartsma TJ, Matysik J (eds) *Biophysical techniques in photosynthesis*, Vol II. Springer, Dordrecht, The Netherlands, pp 97–124
 32. Cogdell RJ, Lindsay JG. (2000) The structure of photosynthetic complexes in bacteria and plants: an illustration of the importance of protein structure to the future

- development of plant science. *New Phytol.* 145:167–96
33. Noomnarm U, Clegg RM (2009) Fluorescence lifetimes: fundamentals and interpretations. *Photosyn. Res.* 101:181-194
 34. Holzwarth AR (1995) Time-resolved fluorescence spectroscopy. *Method Enzymol* 246:334-362.
 35. Vanamerongen H, van Grondelle R (1995) Transient absorption spectroscopy in study of processes and dynamics in biology. *Method Enzymol* 246:201-226
 36. Berera R, van Grondelle R, Kennis JTM (2009) Ultrafast transient absorption spectroscopy: principles and application to photosynthetic systems. *Photosynth Res* 101:105-118
 37. Zigmantas D, Ma YZ, Read EL, Fleming GR (2008) Nonlinear Femtosecond Optical Spectroscopy Techniques in Photosynthesis. In: *Thijs J. Aartsma and Jörg Matysik (eds): Biophysical Techniques in Photosynthesis II, pp. 201–222.*
 38. Mukamel S (2000) Multidimensional femtosecond correlation spectroscopies of electronic and vibrational excitations. *Annu. Rev. Phys. Chem.* 51:691–729
 39. Jonas DM (2003) Two-dimensional femtosecond spectroscopy. *Annu. Rev. Phys. Chem.* 54:425-463
 40. Renger T, May V, Kuhn O (2001) Ultrafast excitation energy transfer dynamics in photosynthetic pigment-protein complexes. *Phys. Rep.* 343:137–254
 41. van Amerongen H, Valkunas L, van Grondelle R. (2000) Photosynthetic Excitons. Singapore:World Sci.
 42. Pearlstein RM. (1982) Exciton migration and trapping in photosynthesis. *Photochem. Photobiol.* 35:835–44
 43. Breuer HP, Petruccione F. (2002) The theory of open quantum systems. Oxford: Oxford Univ. Press
 44. T. Renger (2009) Theory of excitation energy transfer: from structure to function. *Photosyn. Res.* 102:471-485
 45. Alden RG, Johnson E, Nagarajan V, Parson W, Law C, Cogdell RG (1997) Calculations of spectroscopic properties of the LH2 bacteriochlorophyll-protein antenna complex from *Rhodospseudomonas acidophila*. *J. Phys. Chem. B* 101:4667–80

46. Krueger BP, Scholes GD, Fleming GR. (1998) Calculation of couplings and energy-transfer pathways between the pigments of LH2 by the ab initio transition density cube method. *J. Phys. Chem. B* 102:5378–86
47. Madjet MEA, Abdurahman A, Renger T. (2006) Intermolecular Coulomb couplings from ab initio electrostatic potentials: application to optical transitions of strongly coupled pigments in photosynthetic antennae and reaction centers. *J. Phys. Chem. B* 110:17268–81
48. Adolphs J, Renger T. (2006) How proteins trigger excitation energy transfer in the FMO complex of green sulfur bacteria. *Biophys. J.* 91:2778–97
49. Louwe R, Vrieze J, Hoff A, Aartsma TJ. (1997) Toward an integral interpretation of the optical steady-state spectra of the FMO complex of *Prosthecochloris aestuarii*. 2. Exciton simulations. *J. Phys. Chem. B* 101:11280–87
50. Curutchet C, Scholes GD, Mennucci B, Cammi R. (2007) How solvent controls electronic energy transfer and light harvesting: toward a quantum-mechanical description of reaction field and screening effects. *J. Phys. Chem. B* 111:13253–65
51. Adolphs J, Müh F, Madjet MEA, Renger T. (2008) Calculation of pigment transition energies in the FMO protein: from simplicity to complexity and back. *Photosyn. Res.* 95:197–209
52. Scholes GD, Fleming GR. (2005) Energy transfer and photosynthetic light harvesting. *Adv. Chem. Phys.* 132:57–130
53. van Grondelle R, Novoderezhkin VI. (2006) Energy transfer in photosynthesis: experimental insights and quantitative models. *Phys. Chem. Chem. Phys.* 8:793–807
54. Scholes GD. (2003) Long-range resonance energy transfer in molecular systems. *Annu. Rev. Phys. Chem.* 54:57–87
55. Leegwater J. (1996) Coherent versus incoherent energy transfer and trapping in photosynthetic antenna complexes. *J. Phys. Chem.* 100:14403–9
56. A. N. Glazer (1985) Light harvesting by phycobilisomes. *Annu. Rev. Biophys. Biophys. Chem.* 14:47-77.
57. Cheng YC, Fleming GR (2009) Dynamics of Light Harvesting in Photosynthesis. *Annu. Rev. Phys. Chem* 60:241-262
58. Eccles J, Honig B. (1983) Charged amino-acids as spectroscopic determinants for

- chlorophyll in vivo. *Proc. Natl. Acad. Sci. USA* 80:4959-4962.
59. Diner, B. A., E. Schlodder, P. J. Nixon, W. J. Coleman, F. Rappaport, J. Lavergne, W. F. J. Vermaas, and D. A. Chisholm. 2001. Site-directed mutations at D1-HIS198 and D2-HIS197 of Photosystem II in *Synechocystis PCC 6803*: Sites of primary charge separation and cation and triplet stabilization. *Biochemistry* 40:9265-9281.
 60. Witt, H, Schlodder E, Teutloff C, Niklas J, Bordignon E, Carbonera D, Kohler S, Labahn A, Lubitz W (2002) Hydrogen bonding to P700: Site-directed mutagenesis of threonine A739 of Photosystem I in *Chlamydomonas reinhardtii*. *Biochemistry* 41:8557-8569.
 61. Lapouge K, Naveke A, Gall A, Ivancich A, Seguin J, Scheer H, Sturgis JN, Mattioli TA, Robert B (1999). Conformation of bacteriochlorophyll molecules in photosynthetic proteins from purple bacteria. *Biochemistry* 38:11115–11121.
 62. Gudowska-Nowak, E., M. D. Newton, and J. Fajer. (1990) Conformational and environmental effects on bacteriochlorophyll optical spectra: Correlations of calculated spectra with structural results. *J. Phys. Chem.* 94:5795-5801.
 63. Madjet MEA, Adolphs J, Abdurahman A, Rabenstein B, Ishikita H, Knapp EW, Renger T (2007) alpha-Helices direct excitation energy flow in the Fenna-Matthews-Olson protein. *Proc. Natl. Acad. Sci. USA* 104:16862-16867.
 64. Novoderezhkin VI, van Grondelle R (2002) Exciton-vibrational relaxation and transient absorption dynamics in LH1 of *Rhodospseudomonas viridis*: a redfield theory approach. *J Phys Chem B* 106:6025–6037
 65. Yang M, Fleming GR (2002) Influence of phonons on exciton transfer dynamics: comparison of the Redfield, Förster, and modified Redfield equations. *Chem Phys* 275:355–372
 66. Förster T. (1948) Zwischenmolekulare energiewanderung und fluoreszenz. *Ann. Phys. (Berlin)* 437:55–75
 67. Krueger BP, Scholes GD, Fleming GR (1998) Calculation of couplings and energy-transfer pathways between the pigments of LH2 by the ab initio transition density cube method. *J Phys Chem B* 102:5378–5386
 68. Madjet ME, Abdurahman A, Renger T (2006) Intermolecular Coulomb couplings from ab initio electrostatic potentials: application to optical transitions of strongly

- coupled pigments in photosynthetic antennae and reaction centers. *J Phys Chem B* 110:17268–17281
69. Kleima FJ, Hofmann E, Gobets B, van Stokkum IHM, van Grondelle R, Diederichs K, van Amerongen H (2000) Förster excitation energy transfer in peridinin-chlorophyll-a-protein. *Biophys J* 78:344–353
70. Polivka, T, Hiller RG, Frank HA (2007) Spectroscopy of the peridinin-chlorophyll-a protein: Insight into light-harvesting strategy of marine algae. *Archives of Biochemistry and Biophysics* 458(2): 111-120.
71. Redfield AG. (1957) On the theory of relaxation processes. *IBM J. Res. Dev.* 1:19–31
72. Renger T, May V, Kühn O (2001) Ultrafast excitation energy transfer dynamics in photosynthetic pigment–protein complexes. *Phys Rep* 343:138–254
73. Cheng YC, Silbey RJ (2005) Markovian approximation in the relaxation of open quantum systems. *J. Phys. Chem. B* 109:21399–405
74. Kuhn O, Sundström V, Pullerits T. (2002) Fluorescence depolarization dynamics in the B850 complex of purple bacteria. *Chem. Phys.* 275:15–30
75. Novoderezhkin VI, van Grondelle R (2002) Exciton-vibrational relaxation and transient absorption dynamics in LH1 of *Rhodospseudomonas viridis*: a redfield theory approach. *J Phys Chem B* 106:6025–6037
76. Novoderezhkin VI, Salverda JM, van Amerongen H, van Grondelle R (2003) Exciton modeling of energy-transfer dynamics in the LHCII complex of higher plants: a Redfield theory approach. *J Phys Chem B* 107:1893–1912
77. Zhang W, Meier T, Chernyak V, Mukamel S. (1998) Exciton-migration and three-pulse femtosecond optical spectroscopies of photosynthetic antenna complexes. *J. Chem. Phys.* 108:7763–74
78. Novoderezhkin VI, Palacios MA, van Amerongen H, van Grondelle R. (2004) Energy-transfer dynamics in the LHCII complex of higher plants: modified Redfield approach. *J. Phys. Chem. B* 108:10363–75
79. Novoderezhkin VI, Rutkauskas D, van Grondelle R. (2006) Dynamics of the emission spectrum of a single LH2 complex: interplay of slow and fast nuclear motions. *Biophys. J.* 90:2890–902
80. Schröder M, Kleinekathöfer U, Schreiber M. (2006) Calculation of absorption spectra

- for light-harvesting systems using non-Markovian approaches as well as modified Redfield theory. *J. Chem. Phys.* 124:084903
81. Wen JZ, Zhang H, Gross ML, Blankenship RE (2009) Membrane orientation of the FMO antenna protein from *Chlorobaculum tepidum* as determined by mass spectrometry-based footprinting. *Proc. Natl. Acad. Sci. USA* 106:6134-6139.
 82. Mohseni M, Rebentrost P, Lloyd S, Aspuru-Guzik A (2008) Environment-assisted quantum walks in photosynthetic energy transfer. *J. Chem. Phys.* 129:174106
 83. Chin AW, Datta A, Caruso F, Huelga SF, Plenio MB (2009) Noise-assisted energy transfer in quantum networks and light-harvesting complexes. arXiv:0910.4153v1
 84. Scholak T, de Melo F, Wellens T, Mintert F, Buchleitner A (2009) Entanglement-enhanced efficient energy transport. arXiv:0912.3560v1
 85. Caruso F, Chin AW, Datta A, Huelga SF, Plenio MB (2009) Highly efficient energy excitation transfer in light-harvesting complexes: The fundamental role of noise-assisted transport. *J. Chem. Phys.* 131:105106
 86. Scholes GD, Jordanides X, Fleming GR. (2001) Adapting the Förster theory of energy transfer for modeling dynamics in aggregated molecular assemblies. *J. Phys. Chem. B* 105:1640–51
 87. Sumi H. 1999. Theory on rates of excitation energy transfer between molecular aggregates through distributed transition dipoles with application to the antenna system in bacterial photosynthesis. *J. Phys. Chem. B* 103:252–60
 88. Jang S, Newton MD, Silbey RJ. (2004) Multichromophoric Förster resonance energy transfer. *Phys. Rev. Lett.* 92:218301
 89. Jang S. (2007) Generalization of the Förster resonance energy transfer theory for quantum mechanical modulation of the donor-acceptor coupling. *J. Chem. Phys.* 127:174710
 90. Scholes GD, Fleming GR. 2000. On the mechanism of light harvesting in photosynthetic purple bacteria: B800 to B850 energy transfer. *J. Phys. Chem. B* 104:1854–68
 91. Beljonne D, Curutchet C, Scholes GD, Silbey RJ (2009) Beyond forster resonance energy transfer in biological and nanoscale systems. *J. Phys. Chem. B* 113:6583-6599.
 92. Mukai K, Abe S, Sumi H (1999) Theory of rapid excitation energy transfer from

- B800 to optically forbidden exciton states of B850 in the antenna system LH2 of photosynthetic purple bacteria. *J Phys Chem B* 103:6096–6102
93. Fetisova Z, Freiberg A, Muring K, Novoderezhkin V, Taisova A, Timpmann K (1996) Excitation energy transfer in chlorosomes of green bacteria: theoretical and experimental studies. *Biophys J* 71:995–1010
94. Jordanides XJ, Scholes GD, Fleming GR (2001) The mechanism of energy transfer in the bacterial photosynthetic reaction center. *J Phys Chem B* 105:1652–1669
95. Volker S. (1989) Hole-burning spectroscopy. *Annu. Rev. Phys. Chem* 40:499-530.
96. Purchase R, Volker S (2009) Spectral hole burning: examples from photosynthesis. *Photosyn. Res.* 101:245-266.
97. Cogdell RJ, Kohler J (2009) Use of single-molecule spectroscopy to tackle fundamental problems in biochemistry: using studies on purple bacterial antenna complexes as an example. *Biochemical Journal* 422: 193-205.
98. Saga Y, Tamiaki H (2004) Fluorescence spectroscopy of single photosynthetic light-harvesting supramolecular systems. *Cell Biochemistry and Biophysics* 40:149-165.
99. Cho M. (2008) Coherent two-dimensional optical spectroscopy. *Chem. Rev.* 108:1331–418
100. Milota F, Sperling J, Nemeth A, Mančal T, Kauffmann HF (2009) Two-dimensional electronic spectroscopy of molecular excitons. *Acc. Chem. Res.* 42:1364–1374
101. Ginsberg NS, Cheng YC, Fleming GR (2009) Two-dimensional electronic spectroscopy of molecular aggregates. *Acc. Chem. Res* 42:1352–1363
102. Brixner T, Stenger J, Vaswani HM, Cho M, Blankenship RE, Fleming GR (2005) Two-dimensional spectroscopy of electronic couplings in photosynthesis. *Nature* 434:625–28
103. Engel GS, Calhoun TR, Read EL, Ahn TK, Mancal T, Cheng YC, Blankenship RE, Fleming GR (2007) Evidence for wavelike energy transfer through quantum coherence in photosynthetic systems. *Nature* 446:782–86
104. Zigmantas D, Read EL, Mancal T, Brixner T, Gardiner AT, Cogdell RJ, Fleming GR (2006) Two-dimensional electronic spectroscopy of the B800–B820 light-harvesting complex. *Proc. Natl. Acad. Sci. USA* 103:12672–77
105. Read E, Schlau-Cohen G, Engel GS, Wen J, Blankenship RE, Fleming GR

- (2008) Visualization of excitonic structure in the Fenna-Matthews-Olson photosynthetic complex by polarization-dependent two-dimensional electronic spectroscopy. *Biophys. J.* 95:847–56
106. Lee, H., Y. C. Cheng, Fleming GR (2007) Coherence dynamics in photosynthesis: Protein protection of excitonic coherence. *Science* 316:1462-1465.
107. Collini E, Wong CY, Wilk KE, Curmi PMG, Brumer P, Scholes GD (2010) Coherently wired light-harvesting in photosynthetic marine algae at ambient temperature. *Nature* 463:644-648
108. Ishizaki A, Fleming GR (2009) Theoretical examination of quantum coherence in a photosynthetic system at physiological temperature. *Proc. Natl. Acad. Sci. USA* 106:17255-17260.
109. Panitchayangkoon G, Hayes G, Fransted KA, Caram JR, Harel E, Wen J, Blankenship RE, Engel GS (2010) Long-lived quantum coherence in photosynthetic complexes at physiological temperature. arXiv:1001.5108v1
110. Scholes GD, Rumbles G (2006) Excitons in nanoscale systems. *Nature Materials* 5:920-920.
111. Lewis NS, Nocera DG (2006) Powering the planet: Chemical challenges in solar energy utilization. *Proc. Natl. Acad. Sci. USA* 103:15729-15735.
112. Coecke, B. (2010) Quantum pictorialism. *Contemporary Physics* 51:59-83.
113. Dowling JP, Milburn GJ (2003) Quantum technology: the second quantum revolution. *Phil. Trans. R. Soc. Lond. A* 361:1655-1674.
114. Allen JF (2003) State transitions – a question of balance. *Science* 299:1530-1531
115. Allen JF. (1992) Protein phosphorylation in regulation of photosynthesis. *Biochim Biophys Acta* 1098:275-335
116. Rintamaki E, Salonen M, Suoranta UM, Carlberg I, Andersson B, Aro EM. (1997) Phosphorylation of light-harvesting complex II and photosystem II core proteins shows different irradiance-dependent regulation in vivo. Application of phosphothreonine antibodies to analysis of thylakoid phosphoproteins. *J Biol Chem* 272:30476-30482
117. Wollman FA (2001) State transitions reveal the dynamics and flexibility of the photosynthetic apparatus. *EMBO J* 20:3623-3630

118. Allen J, Mullineaux C, Sanders C, Melis A (1989) State transitions, photosystem stoichiometry adjustment and non-photochemical quenching in cyanobacterial cells acclimated to light absorbed by photosystem I or photosystem II. *Photosyn. Res.* 22:157-166
119. Horton P, Ruban AV, Walters RG (1994) Regulation of light harvesting in green plants: indication by non-photochemical quenching of chlorophyll fluorescence. *Plant Physiol.* 106:415-420
120. Müller P, Li XP, Niyogi KK (2001) Non-photochemical quenching. A response to excess light energy. *Plant Physiol.* 125:1558-1566
121. Demmig-Adams B, Adams III WW. (1996) The role of xanthophyll cycle carotenoids in the protection of photosynthesis. *Trends in Plant Science* 1:21–26.
122. Li X-P, Gilmore AM, Caffarri S, Bassi R, Golan T, Kramer D, Niyogi KK. 2004. Regulation of photosynthetic light harvesting involves intrathylakoid lumen pH sensing by the PsbS protein. *Journal of Biological Chemistry* 279, 22866–22874.
123. Niyogi KK, Li XP, Rosenberg V, Jung HS (2004) Is PsbS the site of non-photochemical quenching in photosynthesis? *J Exp. Bot* 56:375-382
124. Holt NE, Zigmantas D, Valkunas L, Li XP, Niyogi KK, Fleming GR (2004) Carotenoid cation formation and the regulation of photosynthetic light harvesting. *Science* 307:433-436
125. Pascal AA, Liu ZF, Broess K, van Oort B, van Amerongen H, Wang C, Horton P, Robert B, Chang W, Ruban A (2005) Molecular basis of photoprotection and control of photosynthetic light-harvesting. *Nature* 436, 134–137.
126. Ruban AV, Berera R, Iliaia C, van Stokkum IHM., Kennis JTM, Pascal AA, van Amerongen H, Robert B, Horton P, van Grondelle R (2007) Identification of a mechanism of photoprotective energy dissipation in higher plants. *Nature* 450:575-578
127. Shipton CA, Barber J(1991) Photoinduced degradation of the D1 polypeptide in isolated reaction centers of photosystem II: Evidence for an autoproteolytic process triggered by the oxidizing side of the photosystem. *Proc. Natl. Acad. Sci. USA* 88:6691-6695
128. Marvin Edelman, Autar K. Mattoo (2008) D1-protein dynamics in photosystem II:

- the lingering enigma. *Photosynth Res* 98:609–620
129. Yusuke Kato and Wataru Sakamoto (2009) Protein quality control in chloroplasts: A current model of D1 protein degradation in the photosystem II repair cycle. *J. Biochem.* 146:463–469
 130. Blankenship RE, Matsuura K (2003) Antenna Complexes from Green Photosynthetic Bacteria. In Beverley R. Green and William W. Parson (eds): Light-Harvesting Antennas, pp. 195–217. Kluwer Academic Publishers, Dordrecht
 131. Blankenship RE, Cheng PL, Causgrove TP, Brune DC, Wang SHH, Choh JU, Wang J (1993) Redox regulation of energy transfer efficiency in antennas of green photosynthetic bacteria. *Photochem Photobiol* 57: 103–107
 132. Frigaard NU, Takaichi S, Hirota M, Shimada K, Matsuura K (1997) Quinones in chlorosomes of green sulfur bacteria and their role in the redox-dependent fluorescence studied in chlorosome-like bacteriochlorophyll c aggregates. *Arch Microbiol* 167: 343–349
 133. Zhou W, LoBrutto R, Lin S and Blankenship RE (1994) Redox effects on the bacteriochlorophyll a-containing Fenna-Matthews-Olson protein from *Chlorobium tepidum*. *Photosynth Res* 41: 89–96
 134. Tsukatani Y, Wen J, Blankenship RE, Bryant DA. Characterization of the FMO protein from the aerobic chlorophototroph, *Candidatus Chloracidobacterium thermophilum*. *Photosynth Res.* 10.1007/s11120-009-9517-0
 135. Morgan-Kiss RM, Chan LK, Modla S, Weber TS, Warner M, Czymbek KJ, Hanson TE (2009) *Chlorobaculum tepidum* regulates chlorosome structure and function in response to temperature and electron donor availability. *Photosynth Res* 99:11–21
 136. Yakovlev AG, Taisova AS, Fetisova ZG (2002) Light control over the size of an antenna unit building block as an efficient strategy for light harvesting in photosynthesis. *FEBS Letters* 512:129-132
 137. Pšenčík J, Collins AM, Liljeroos L, Torkkeli M, Laurinmäki P, Ansink HM, Ikonen TP, Serimaa RE, Blankenship RE, Tuma R, Butcher SJ (2009) Structure of Chlorosomes from the Green Filamentous Bacterium *Chloroflexus aurantiacus*. *J Bactiol.* 191:6701–6708
 138. Kim H, Li H, Maresca JA, Bryant DA, Savikhin S (2007) Triplet exciton formation

as a novel photoprotection mechanism in chlorosomes of *Chlorobium tepidum*.
Biophys. J 93:192 - 201

139. Evans MB, Hawthornthwaite AM, Cogdell RJ (1990). Isolation and characterization of the different B800-850 light-harvesting complexes from low- and high-light grown cells of *Rhodospseudomonas palustris*, strain 2.1.6. *Biochimica Biophysica Acta* 1016:71 - 76.
140. Moulisová V, Luer L, Hoseinkhani S, Brotosudarmo TH, Collins AM, Lanzani G, Blankenship RE, Cogdell RJ (2009) Low light adaptation: energy transfer processes in different types of light harvesting complexes from *Rhodospseudomonas palustris*. *Biophys J*. 97:3019-2028.
141. Koyama Yasushi (1991) New trends in photobiology: Structures and functions of carotenoids in photosynthetic systems. *J. Photochem. Photobiol. B: Biol.* 9:265-280
142. Hunter CN., Hundle BS, Hearst JE, Lang HP, Gardiner AT, Takaichi S, Cogdell RJ (1994). Introduction of new carotenoids into the bacterial photosynthetic apparatus by combining the carotenoid biosynthetic pathways of *Erwinia herbicola* and *Rhodobacter sphaeroides*. *J Bacteriol* 176:3692-3697.
143. Lang HP, Hunter CN (1994). The relationship between carotenoid biosynthesis and the assembly of the light-harvesting LH2 complex in *Rhodobacter sphaeroides*. *Biochem. J* 298:197-205.
144. Young AJ, Frank HA (1996) Energy transfer reactions involving carotenoids: quenching of chlorophyll fluorescence. *J. Photochem. Photobiol. B: Biol* 36:3-15
145. Blankenship RE (2006) Photosynthesis: The Light Reactions. Chapter 7 in *Plant Physiology*, 4th Ed, Taiz L and Zeiger E (eds), Sinauer Publishing, 125-158.

Chapter 2.

**Structure of the FMO protein and the nature of the 8th pigment by
native spray mass spectrometry**

Abstract:

As the first (bacterio)chlorophyll-containing light harvesting antenna that had its X-ray crystal structure determined, the FMO protein has drawn intense structural, spectroscopic and theoretical attention. Surprisingly, in the newly refined FMO structure from *Prosthecochloris aestuarii*, strain 2K (*P. aestuarii*) at 1.3 Å resolution, a new pigment was discovered at the FMO monomer connection region with occupancy of the electron density being 34%. The refined FMO structure from *Chlorobaculum tepidum* (*C. tepidum*) and the recently finished FMO structure from *Pelodictyon phaeum* (*P. phaeum*) all indicate the existence of this not fully occupied site. In this chapter, the structures of the FMO protein from *C.tepidum*, *P. aestuarii* and *P. phaeum* are briefly described with emphasis on the newly resolved 8th pigment. The stoichiometry and nature of the 8th pigment were investigated by measuring the mass of the whole protein complex using native electrospray mass spectrometry.

Introduction

The anoxygenic photosynthetic green sulfur bacteria (GSB) are obligate photoautotrophs that contain a specialized light-harvesting antenna complex known as the chlorosome, which primarily consists of highly aggregated bacteriochlorophyll *c/d/e* surrounded by a lipid-protein envelope (1). After light energy is collected by the chlorosome, it is funneled down through the baseplate attachment site and the bacteriochlorophyll *a* protein, also known as the Fenna-Matthews-Olson (FMO) protein, into the reaction center (RC) where charge separation takes place (Fig. 1).

The FMO protein was the first photosynthetic antenna complex containing any type of chlorophyll to have its atomic structure known. It was first discovered and isolated from *Prosthecochloris aestuarii* by Olson and coworkers (2), and the structure was determined to a resolution of 2.8 Å in 1975 (3). Subsequently, the structure was refined to 1.9 Å (4).

The FMO protein consists of three identical subunits related by a 3-fold axis of symmetry (Fig. 2A). In each subunit the polypeptide backbone (~ 40 kDa) forms a fold that consists mainly of beta sheet secondary structure enclosing a central core of seven BChl *a* molecules (Fig. 2C, 2D). The BChl *a* molecules are electronically coupled to each other and also interact with the protein environment to give the FMO protein its specific absorption properties (Fig. 2B). The three-dimensional structure of the FMO protein from *Chlorobaculum tepidum* (previously called *Chlorobium tepidum*) was determined by Allen and co-workers in 1997, and this provides a comparative system (5). These high-resolution structures have provided the basis for detailed analysis of the optical spectra of

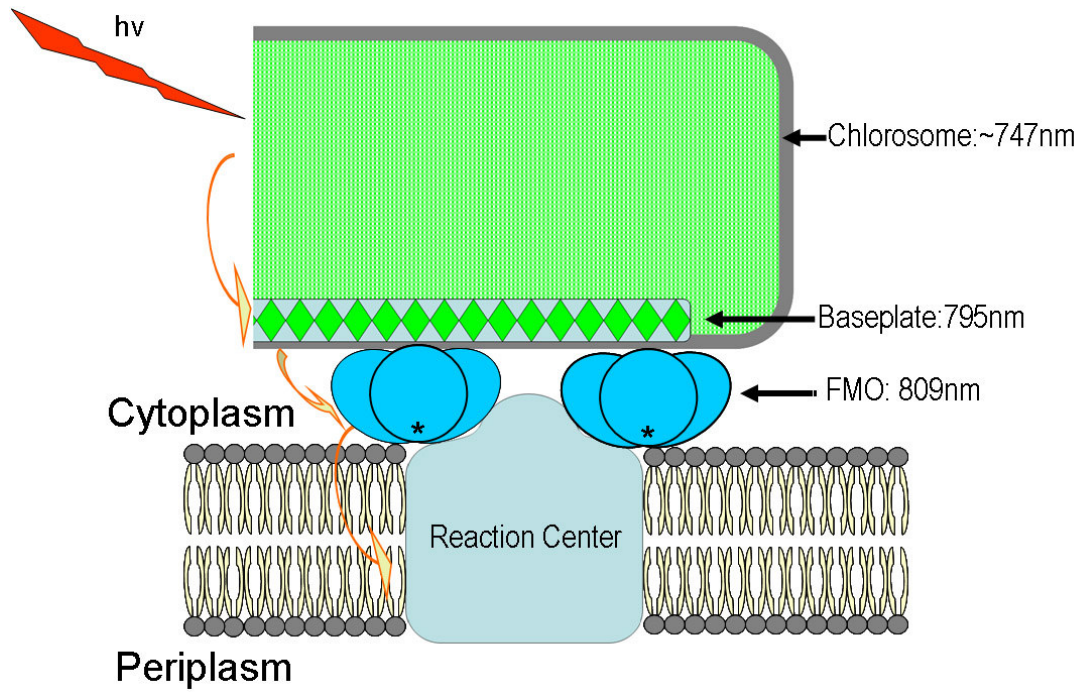


Fig. 1 Schematic representation of the photosystem from green sulfur bacteria. The FMO protein is attached to the cytoplasmic membrane and transfers the excitation energy from the chlorosome to the reaction center.

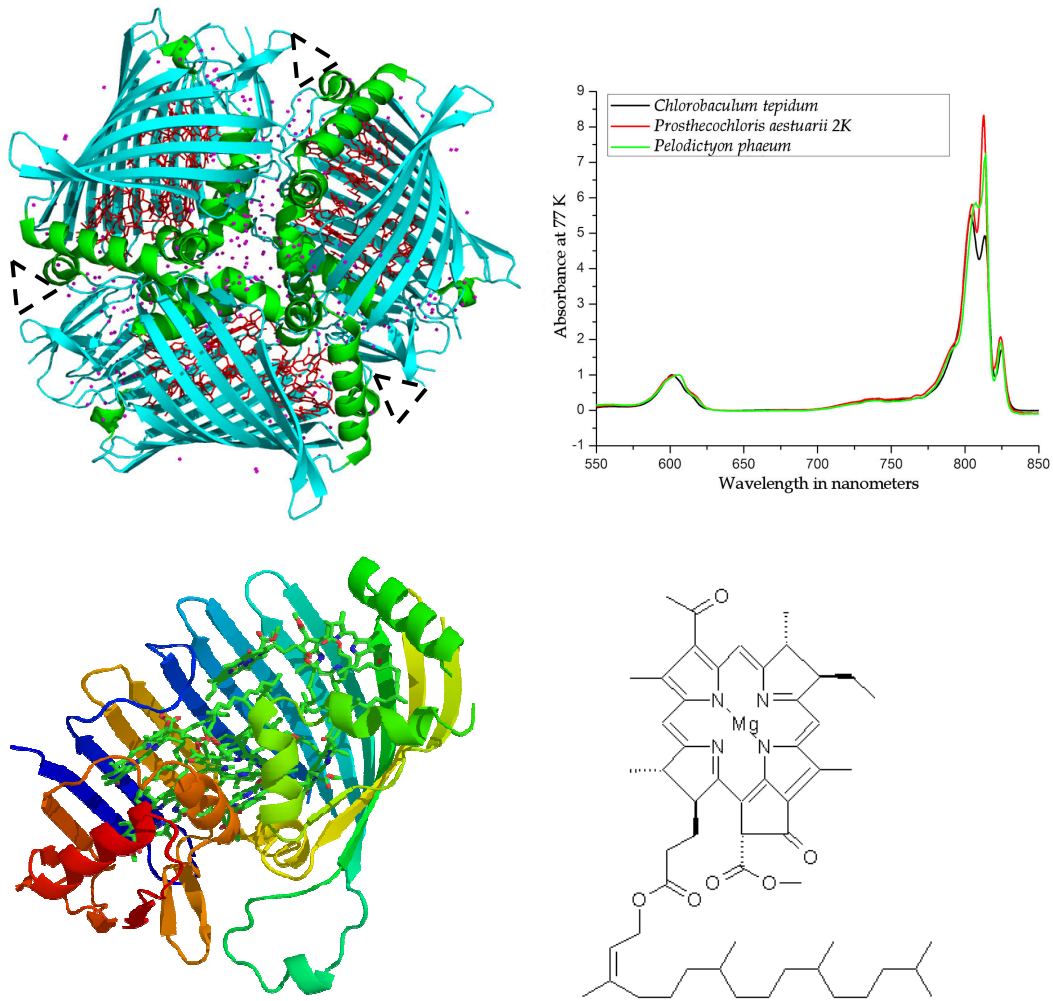


Fig. 2 (A) FMO trimer structure from *Chlorobaculum tepidum* (PDB: 3ENI). Blue: β sheets; Green: α helices; Red: BChl *a*; Pink: water; Dashed triangle: unresolved region of electron density. (B) 77K absorption of the FMO protein from three species of green sulfur bacteria. (C) FMO monomer with pigments shown by sticks and the polypeptide shown by ribbons. (D) Bacteriochlorophyll *a*.

the protein and for understanding the pigment/protein interactions (1, 6).

Although the FMO proteins from different species of GSB are quite highly conserved, with amino acid sequence identities typically on the order of 80%, it was observed that the absorbance and CD spectra for the FMO proteins from different species of GSB can be grouped into two types when measured at 77 K or lower (7). As can be seen in the 77 K absorption spectra (Fig. 2B), the FMO from *P. aestuarii* and *P. phaeum* have higher 813 nm peak, whereas the 805 nm band of FMO from *C. tepidum* is stronger. The overall structures of FMO from *P. aestuarii* and *C. tepidum* show almost no differences. If one superimposes the two, using just the central atoms of the seven BChl *a* rings as a guide, the two structures are nearly identical. Extensive theoretical calculations (8-12) were carried out to describe the origin of the tuning of the electronic structure in these two proteins.

The FMO protein functions both as a photosynthetic antenna harvesting light energy and an energy mediator governing the energy transfer from chlorosome to the reaction centers. As a photosynthetic antenna, the energy delocalization process within this protein has been well described by the recent advances of multidimensional coherent spectroscopies (13, 14), and the electronic structure was recently reviewed by Milder *et al* (6). As an energy mediator, strong fluorescence quenching was reported in the FMO protein depending on either the redox conditions or thermal effects (15). The quantum yield of the FMO fluorescence increases dramatically after the protein is reduced by a strong reducing agent like sodium dithionite. The molecular mechanism of the fluorescence

quenching is still unknown, but the quenching itself is proposed to be an essential excitation modulation by the cells to prevent photo-damage under over-exposed light conditions. A redox-active group or molecule that either tightly binds to the FMO protein or is part of the protein is proposed to be sensitive to the local redox environment and regulate the amount of energy transferred to reaction centers by serving as an excited state quencher when in the oxidized state. However, a search for a non-covalently bound small molecule by HPLC analysis of the FMO protein was unsuccessful. No such molecules were detected by monitoring the UV/Vis absorption of the elution. The measured protein mass matches the protein sequence quite well and no apparent post-translational modifications are indicated.

It is known to crystallographers that there are unresolved electron densities in the FMO structure between the subunits (4), as indicated in Fig. 2A. In addition, Nelson *et al* (16) provided a preliminary structural model with a BChl *a* built at that region. To investigate better this binding site and understand the nature of the extra electron density, Tronrud and co-workers (17) grew new FMO crystals that were supplied by our group and determined an ultra-high resolution structure (1.3 Å) of the FMO protein from *P. aestuarii*. While the new model confirms that a BChl *a* molecule binds at the “eighth site” in both the *P. aestuarii* and *C. tepidum* variants of FMO, they show significantly different details of the binding interaction. In both variants, the carbonyl backbone oxygen of residue 123Y binds to the central magnesium atom on one side of the BChl *a* ring while an α -helix (residues 155–172) covers the other side (Fig. 3A, 3B). The new structure for *P. aestuarii* shows a unique, bidentate interaction between the protein and

this BChl *a* molecule. The additional link is between the central magnesium atom and the side chain oxygen atom of Serine 168 (Fig. 3A). The two links to this BChl *a* molecule originate from two different monomers within the biological trimer (Fig. 3D). However, the FMO from *C. tepidum* does not form this extra ligation, and the Mg is pentacoordinate, as is found in essentially all protein-bound chlorophyll-type pigments (Fig. 3B). The physiological function of two axial ligands of pigments is not clear. A recent mutagenesis study of the RC from purple bacteria that generated six ligands to the B_B BChl *a* shows almost no effect on the electron transfer process (18).

The discovery of the eighth pigment in the FMO protein was a surprise to the field. The two axial ligands to the central magnesium of BChl *a* is the first experimental evidence to show its existence in a natural antenna system. The structure that was reported by Tronrud *et al.* (17) indicates the electron density occupancy of this extra BChl *a* is only 34% that of the other BChl *a* molecules in the complex. The immediate question that arises is the stoichiometry of the 8th pigment in the protein *in vivo*. For example, it is possible that each FMO trimer only has one 8th BChl *a*, which breaks the threefold symmetry and might have specific roles in directing the energy flow. It is, however, also possible that the 8th BChl *a* was partially lost during the purification process as it is bound between two subunits and is relatively exposed to solvent compared to the other seven BChl. A heterogeneous sample with three, two, one and zero of the 8th BChl *a* in a trimer might give the average of 34% occupancy by coincidence.

In addition, the tail of the 8th BChl *a* could not be resolved in the 1.3 Å structure. It looks

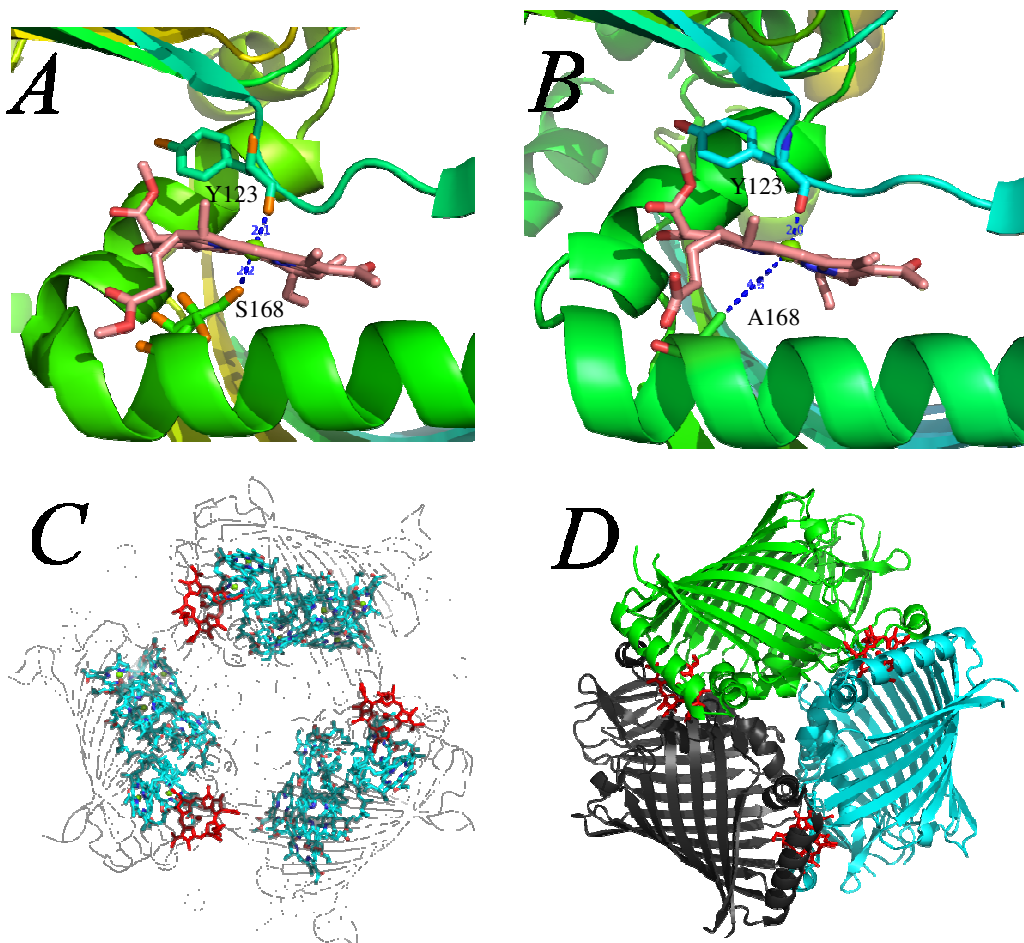


Fig. 3 Nature of the axial ligation of the 8th pigment in FMO from *P. aestuarii* (PDB code: 3EOJ) (A) and *C. tepidum* (PDB code: 3ENI) (B). In the FMO from *P. aestuarii*, one axial-ligation is from the carbonyl O of Y123 and the other is from the side chain O of S168 (A). These two residues are from two protein subunits. In the FMO from *C. tep*, the carbonyl O of Y123 from one subunit forms one axial-ligation. The S168 is replaced by A168 which could not form the 2nd axial-ligation (B). The 8th pigment is located in a cleft on the protein surface at the monomer connection region (C). (D) The 8th pigment sandwiched by two protein subunits, which is clearly shown by highlighting the different protein subunits using different colors.

like a bacteriochlorophyllide *a* (BChlide *a*), BChl *a* without the tail. However, this may be due to the flexibility of the tail in the crystal which is disordered and could not be well resolved.

To understand the stoichiometry and nature of the 8th pigment in the FMO trimer, we employed a recently developed technique, native electrospray mass spectrometry (MS), to measure the mass of the whole protein complex. Mass spectrometry not only plays a crucial role in the identification of proteins involved in the intricate interaction networks of the cell, their expression levels and modifications (19-21), but also is increasingly involved in the characterization of the non-covalent complexes formed by interacting partners (22-27).

In this study, the FMO protein from *C. tepidum* was prepared by two different methods. In one method, it was extracted by washing the membrane with Na₂CO₃ solution. The other method involves detergent extraction. The purified intact FMO protein complexes were introduced into a mass spectrometer under native condition as described in the method section. The molecular weight of the whole complex including noncovalently bound cofactors was recorded, and, thus the stoichiometry of the interacting components was defined unambiguously to provide some insights into the nature and stoichiometry of the 8th pigment.

Results and Discussion

Nature and stoichiometry of the 8th pigment

The MS of the denatured FMO protein shows a series of charge states at low m/z range. For the FMO protein extracted by Na_2CO_3 , all the charge states are located between 650 Da and 1300 Da with the most abundant ion carrying 48 charges (Fig. 4A). Besides the dominant charge-state distribution, there are two weaker distributions labeled with red and blue arrows. The deconvoluted FMO polypeptide mass from the main charge state is 40163 ± 2 Da (Fig. 4B), which is the mass deduced from the protein sequence without the N-terminal methionine residue (theoretical mass: 40163 Da). The two weaker charge distributions gave deconvoluted protein mass of 39831 Da (red arrow) and 39979 Da (blue arrow), which are corresponding to the protein sequence without the N-terminal MALF (theoretical mass: 39831.9 Da) and MAL (theoretical mass: 39979 Da) residues. For the FMO protein extracted by detergent, the deconvoluted molecular weight is 39979 Da, which is very homogeneous.

Under native conditions, the protein shows only four or five main charge states (+21, +22, +23, +24, +25) at high m/z range, no matter how the protein was purified (Fig. 5). For the detergent extracted FMO protein, the deconvoluted molecular weight using the main charge states is 141161 Da, where a simulation of the theoretical charge distribution of a 141161 Da protein is shown by vertical lines (Fig. 5A). The $m/z = 6139$ ion carries 23 positive charges. Similarly, the deconvoluted molecular weight of the FMO protein extracted by Na_2CO_3 is 142009 Da (Fig. 5B). The +23 charge state shifts to $m/z = 6176$. Surprisingly, clear shoulders at the low m/z side of each charge state can be seen (Fig. 5). The shoulders in the spectrum of the FMO extracted from Na_2CO_3 are more apparent and more intense. A similar deconvolution process indicates the molecular weight of one

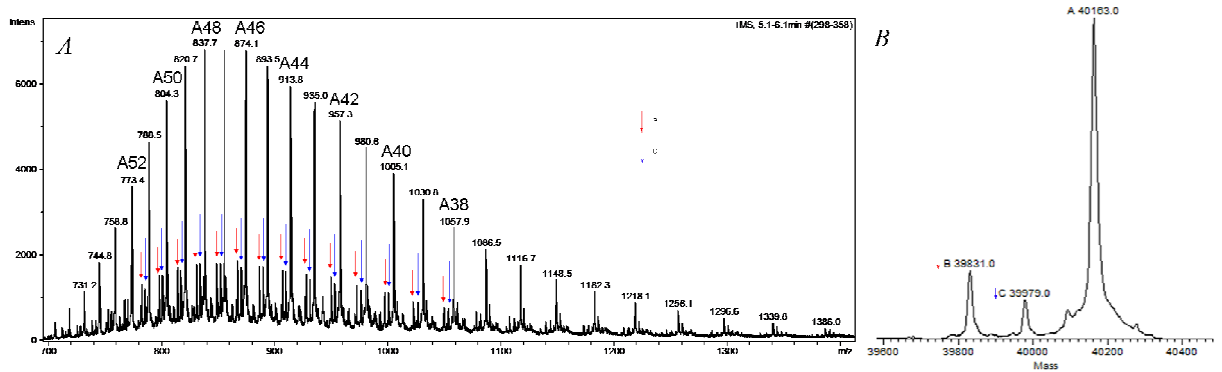


Fig. 4 (A) Mass spectrum of denatured FMO polypeptide by electrospray, which shows a series of charge states at low m/z range. Certain charge states are labeled. Besides the dominant charge states, there are two weaker charge-state distributions labeled with red and blue arrows. (B) Deconvoluted protein mass using the charge states in panel A.

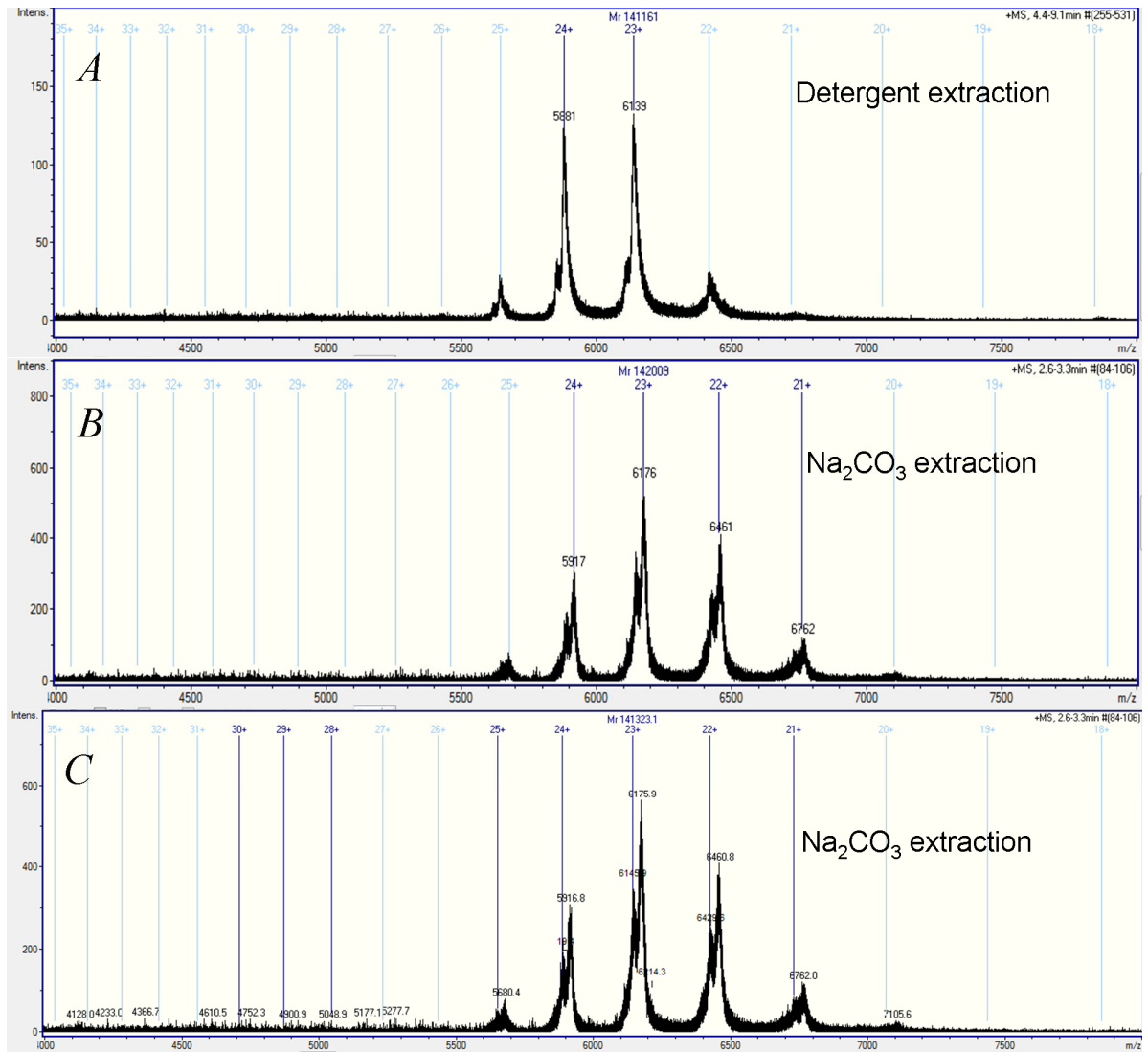


Fig. 5 Mass spectra of the FMO complex by native spray. (A) The FMO protein was extracted by detergent. (B) The FMO protein was extracted by Na₂CO₃. Vertical lines are the simulated charge-state positions using ions having molecular weight of 141161, 142009 and 141323 Da.

shoulder ion is 141323 Da (Fig. 5C). The mass accuracy of the deconvoluted molecular weight is roughly estimated to be 50 – 100 Da on the basis of the full width at half maxima of the ion peaks.

For the detergent-extracted FMO protein, the theoretical mass of the protein complex with 21 BChl *a* is 139,631 Da ($40163 \times 3 + 911.5 \times 21$). This will give a mass difference between the measured mass and the theoretical mass of 1530 Da ($141161 - 139631$ Da), which indicates more pigments binding in the protein, although there may be some solvent or buffer molecules attached to the protein, increasing the measured value. Similarly, the mass difference of the Na₂CO₃-extracted FMO protein between measured and theoretical values is 2378 Da.

More striking evidence that additional pigments exist in a timer, as described in the recent crystal structures discussed in the introduction, comes from the clear shoulders on the lower *m/z* side of the peaks (Fig. 6A, 6B) that we interpret as complexes with fewer copies of the 8th pigment. Surprisingly, the mass difference is ~ 30 Da between the shoulder and the dominant ion peak, for example, for the + 23 charge state of the Na₂CO₃ extracted FMO (Fig. 6B), which means the difference of molecular weight between the two ion species is ~ $30 \times 23 = 690$ Da. Analysis of all the charge states in the spectra of the two FMO complexes shows that the mass differences between the shoulder and the dominant ion peaks are all in the range of 600 – 700 Da. This value is close to the molecular weight of BChlide *a* (632 Da).

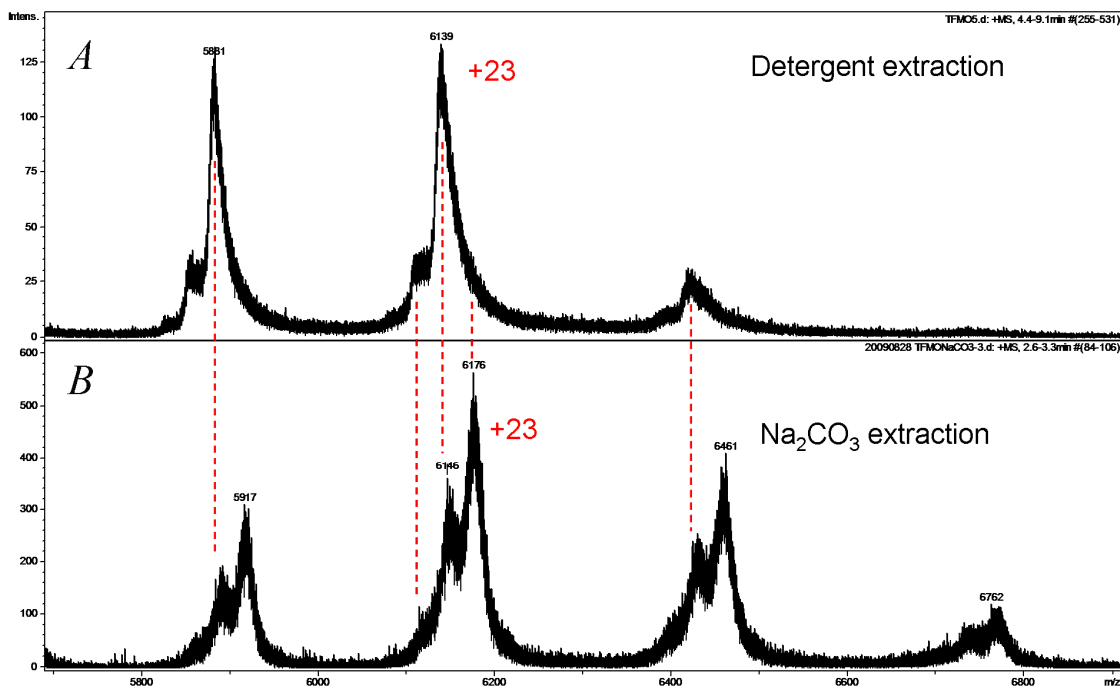


Fig. 6 Expansion of the charge states from native spray MS of the FMO protein extracted by detergent (A) and Na_2CO_3 (B). Shoulders at the low m/z side of the main peak can be clearly visualized. The vertical lines indicate the correspondence of certain ion species.

Another observation is that the dominant ion species in the detergent-extracted FMO is corresponding to the first shoulder ion on the low m/z side of the charge states of the Na_2CO_3 -extracted FMO, as indicated by the vertical lines in Fig. 6. The first shoulder ion on the low m/z side of the charge states of the detergent-extracted FMO corresponds to the 2nd shoulder ions on the low m/z side of the charge states of the Na_2CO_3 -extracted FMO. The dominant ion species in the Na_2CO_3 -extracted FMO is corresponding to the shoulder ion on the high m/z side of the charge states of the detergent-extracted FMO, the shoulder of which can be barely seen owing to the solvent adducts. Thus successful ion assignments of the observed ion peaks and shoulders are that the dominant charge states in the spectrum of the Na_2CO_3 -extracted FMO corresponds to FMO trimer with 21 BChl *a* plus additional 3 BChlide *a*. Under such assignment, the mass difference between the measured and theoretical values is $2378 - 632 \times 3 = 482$ Da. The two shoulders on the low m/z side of the charge states in the Na_2CO_3 -extracted FMO correspond to FMO complex plus 2 and 1 extra BChlide *a*, respectively. Using the intensity of these ion species, the occupancy of the 8th site in the Na_2CO_3 -extracted FMO trimer is estimated to be ~80%. The dominant charge states in the spectrum of the detergent-extracted FMO corresponds to FMO trimer with 21 BChl *a* plus additional 2 BChlide *a*, and the mass difference between the measured and theoretical values is $1530 - 632 \times 2 = 266$ Da. The two shoulders on the low m/z side of the charge states in the detergent-extracted FMO correspond to FMO complex plus 1 and 0 extra BChlide *a*, respectively. The estimated occupancy of the 8th site in the detergent-extracted FMO trimer is ~65%.

Therefore, the above MS analysis especially the clear shoulders in the charge states

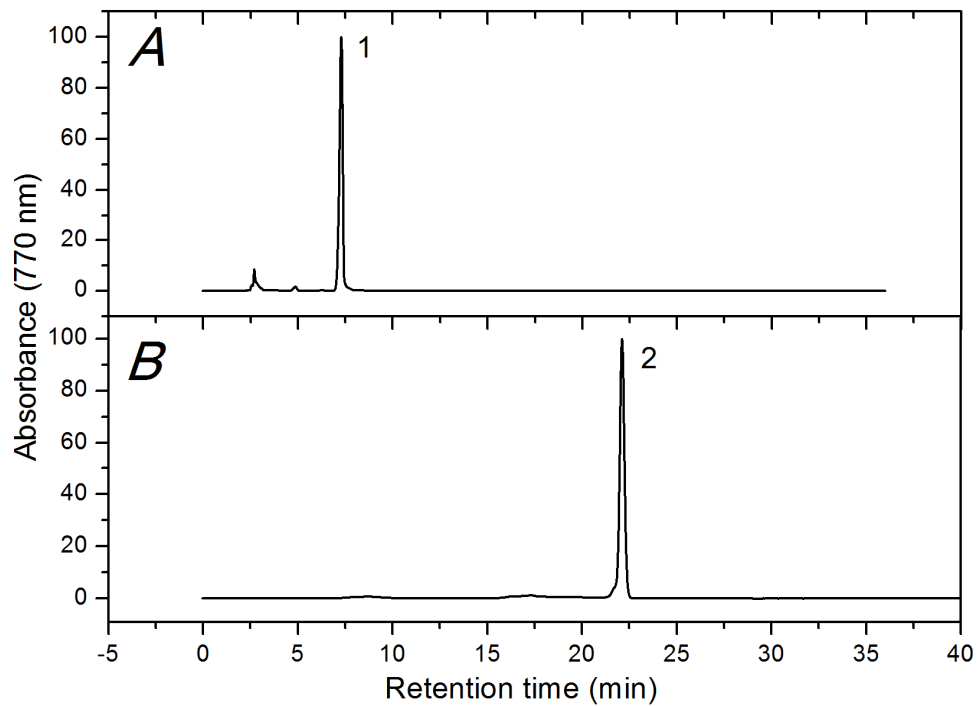


Fig. 7 Pigment analysis by HPLC. (A) Extract from the *bchG* mutant of *Rhodobacter capsulatus*. (B) Chromatogram of pigments from FMO protein. Peak 1 is BChlide *a* and peak 2 is BChl *a*.

suggests the 8th pigment is probably a BChlide *a*. However, detailed HPLC analysis of the FMO protein indicates that there is no BChlide *a* in the protein, as shown in Fig. 7. The extract of the *bchG* mutant of *Rhodobacter capsulatus*, in which only BChlide *a* is accumulated, shows an elution peak at ~7 min, while the chromatogram of the FMO shows a single peak eluted at 22 min. Although the traces shown in Fig. 7 are at 770 nm, the whole UV/Vis was monitored and no additional peaks were observed. Different columns and different solvents were used to analyze the FMO protein but no indication of BChlide *a* or similar pigments exist.

A possible explanation of the controversy of the native spray data (BChlide *a* as the 8th pigment) and the HPLC data (no BChlide *a* in FMO) is that the tail of the 8th pigment was cleaved off during the mass analysis under the native spray condition. To achieve a better desolvation of the native protein complexes, the in-source collision induced dissociation (ISCID) was turned on and sometimes a collision energy up to 180 eV was used to keep the complex intact and to achieve better resolutions. In addition, the collision energy in the collision cells was increased to 20 eV instead of the common 10 eV used in normal electrospray process. To check whether the harsh desolvation condition in the native spray caused the fragmentation of the BChl *a*, the FMO protein denatured by 50% methanol was analyzed by mass spectrometry using similar parameters of the native spray. As shown in Fig. 8, besides the BChl *a* ion peak ($m/z = 911.5$), a strong BChlide *a* ion ($m/z = 633.2$) peak shows up, which is not normally seen under normal spray condition. The $m/z = 611.3$ and $m/z = 889.6$ ions are bacteriopheophytin *a* and pheophorbide *a*, respectively.

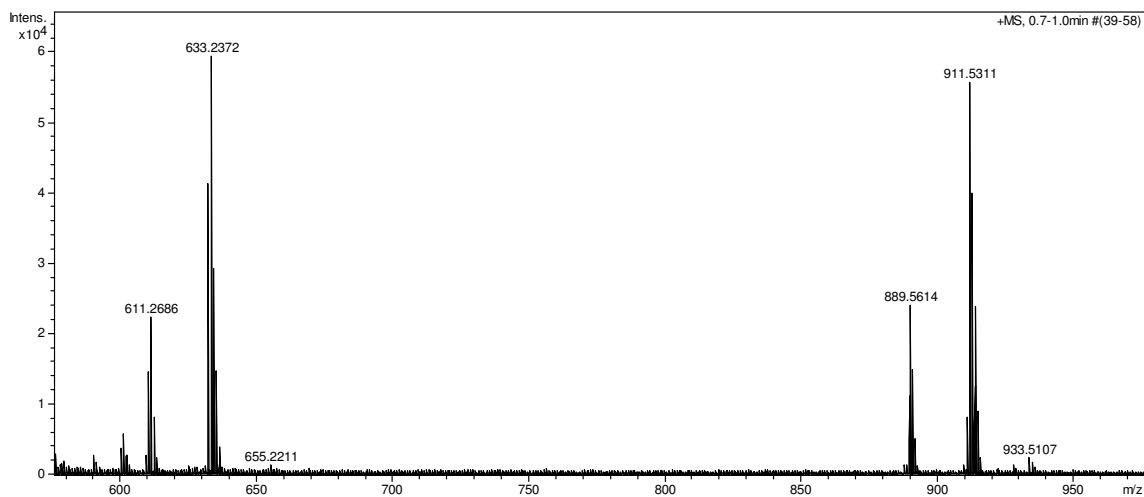


Fig. 8 The BChl *a* in the FMO protein has an average mass at 911.5 Da. Under MS measurement conditions, it also gave another mass at 889.6 Da, which is generated by replacing the central Mg with two hydrogens. The 633.2 Da ion is the fragment of the BChl *a* without the phytol tail (ie. BChlide *a*). The 611.3 Da ion is the BChlide *a* with its central Mg replaced by two hydrogens.

In conclusion, the results discussed above and the observations from the structures (17) suggest the 8th pigment in the FMO is a BChl *a* and the dominant fraction of trimers in the preparation have the 8th BChl *a* not fully occupied. The 8th BChl *a* is located in a cleft at the surface of the complex (Fig. 3C, 3D), while the others are completely protected from solvent. Our results clearly show that a fraction of the BChl *a* binding at the 8th site is lost during purification. The FMO extraction by Na₂CO₃ is more gentle compared to the detergent extraction, since the occupancy of the 8th BChl *a* is higher in the Na₂CO₃ extracted FMO.

Possible Function of the 8th pigment

This pigment is separated from the other seven core BChl *a* and is located in a cleft in the protein surface (Fig. 3C). Linear dichroism studies (28) and chemical labeling and mass spectrometry data (29, and also chapter 4) have established the orientation of the FMO protein on the membrane. The side of the protein containing BChl *a* #3 is near the cytoplasmic membrane and the side containing BChl *a* #1 is toward the chlorosome. The newly discovered eighth pigment is in the region of the protein that is toward the chlorosome and its orientation may facilitate energy transfer from the chlorosome baseplate to the reaction center. The location of this pigment bridges the distance between the baseplate pigments and the core BChl *a* in the FMO, and will thus increase the energy-transfer efficiency. In addition, the orientation of this pigment serves to increase the efficiency of energy transfer between the donor baseplate BChl *a* and this new pigment. This is because the Q_y transition dipole moment of the eighth pigment is

oriented in a similar way as the BChl *a* in the baseplate, as reported on the basis of fluorescence anisotropy of single chlorosomes (30).

Structural mass spectrometry by native spray

Recent developments in mass spectrometry (MS) makes it possible to analyze intact protein complexes, allowing the molecular weight of the complex to be recorded, thus unambiguously defining the stoichiometry of the interacting components (31-34).

The FMO antenna protein, a water-soluble protein found in the photosynthetic green sulfur bacteria, is an ideal model system to understand protein interactions with non-covalently bound cofactors and protein-protein interactions to form larger complexes. Here we used the FMO protein as a model system and successfully measured the mass of the whole complex, which directly tells us that it is a trimer. The stoichiometry and nature of the 8th pigment were also indicated, although some uncertainties remain.

In general, to assign functions to protein complexes, a critical step before an atomic-resolution structure is available is to determine the overall oligomeric state of these complexes, the number of copies of each type of subunits, the architecture, and topology of the complexes (35, 36). The current methods utilized (i.e. Blue-native PAGE (BN PAGE), gel filtration, analytical ultracentrifugation or dynamic light scattering (DLS)) are often not accurate enough to give conclusive results in terms of large multi-subunit complexes with a large number of distinct types of subunits. Mass measurement of intact protein complexes by native electrospray may allow us to determine unambiguously the stoichiometry of protein complexes. By coupling stripping off the peripheral protein

subunits by collision- or chemically-induced dissociations, the topology of the protein complexes could be built.

Materials and Methods

FMO protein purification

Cells of the green sulfur bacterium *P. aestuarii* 2K and *P. phaeum* were grown anaerobically at room temperature with a light intensity of 150 μ E for 2 days in two 15 L carboys. The *C. tepidum* culture was grown at 40 °C. The cells were harvested by centrifugation at 7,500 rpm for 15 min. After the cells were resuspended and washed with 20 mM Tris/HCl (pH = 8.0) buffer, they were run through the centrifuge again. This pellet was resuspended and then broken by sonication. A 4.0 M Na₂CO₃ solution was slowly added until a 0.2 M final concentration was reached, and the solution was stirred gently for 20 h in the dark at 4 °C. Cell debris and unbroken cells were then removed by centrifuging at 10,000 \times g for 15 min. More Na₂CO₃ solution was added until a final concentration of 0.4 M was reached. The solution was gently stirred in the dark for 20 h. The solution was ultracentrifuged for 2 hr. The supernatant containing the FMO protein was carefully decanted and dialyzed against 20 mM Tris/HCl (pH = 8.0) for a day. The solution was then loaded on a SuperQ-650S ion-exchange column and washed with NaCl step gradients. The FMO protein was eluted with around 80–100 mM NaCl elution solution. Further protein purification was achieved by loading the protein on an S-300 gel filtration column and the fractions with $OD_{267nm}/OD_{371nm} < 0.6$ were selected and pooled. The final product was concentrated using the Amicon YM30 and stored for crystallizations and mass spectrometry analysis.

The FMO protein was also prepared by membrane extraction using zwitterionic detergent SB-12 (Anatrace, USA). The cytoplasmic membrane was incubated with 50 mM SB-12 for 1 hr. The extracted protein complexes were collected as supernatant after ultracentrifugation at 225,000 xg for 2 hr. The solution was loaded onto a linear sucrose gradient with densities from 10% (g/v) to 45% (g/v). The FMO band shows light blue color and was collected, concentrated and loaded onto Superdex200 (GE Healthcare, USA) gel filtration column. After this step, the detergent was removed and the FMO protein was enriched. Another round of ion exchange chromatograph is required to get the protein pure by using QSHP media (GE Healthcare, USA).

Absorbance spectroscopy

Each FMO protein was dissolved in 20 mM Tris/HCl buffer (pH = 8.0), diluted into 80% glycerol and was slowly cooled to 77 K in a temperature-controlled cryostat (OptistatDN, Oxford Instruments, UK). The spectra were taken by Lamda 950UV/Vis spectrophotometer (Perkin Elmer, USA).

MS measurement

Mass measurement of the denatured and native FMO protein was carried out on a maxis micrOTOF instrument equipped with a nanoelectrospray source (Bruker Daltonics, Bremen, Germany) coupled either to a PHD ULTRA™ syringe pump (Harvard Apparatus, MA, USA), or to an nanoACQUITY UltraPerformance LC (Waters Corp., MA, USA). To measure the mass of the denatured FMO polypeptide and the bacteriochlorophyll *a*, the FMO protein was diluted into acetonitrile or methanol with

0.1% formic acid. For the native spray, the FMO complex was buffer exchanged to 0.75 M ammonium acetate (pH = 7.5) and concentrated to ~ 15 μ M. The solutions were loaded to the mass spectrometer by infusion. The nanoelectrospray was generated from a home-pulled silica capillary needle at a voltage of 850 – 1500 V. The needle was pulled by the P-200 Laser Puller (Sutter Instrument CO., Novato, CA) using the fused silica capillary tubing (Polymicro Technologies LLC, Phoenix, AZ). The capillary tubing with ID 150 μ m (OD: 356.8 μ m) works better under most conditions. The flow rate for all the measurements was between 20 nL/min to 0.1 μ L/min.

The ion transfer parameters were optimized by direct infusion of an ESI tuning mix (Bruker, part # 18220) before measuring the samples. For the denatured samples, the following spray conditions were normally used under positive ion mode: capillary voltage, 1500 V; dry gas, 5 L/min; dry gas temperature, 100 – 150 °C. In order to achieve better native spray signal, the capillary voltage was lowered to 850 – 1200 V once the spray was initiated by 1500 V and kept stable. The collision energy in the collision cell normally needs to be increased to 20 – 40 eV to observe good native spray signals. In certain instances, the in-source collision induced dissociation was turned on and energy up to 25 eV was used, which seemed to help solvent desorption.

The Bruker Data analysis Software (Bruker, Germany) was used to analyze the data. The charge deconvolution for the native spray was manually calculated.

Pigment analysis by HPLC

The purified FMO protein (10 uL, OD₈₀₈ ~ 10 cm⁻¹) was directly loaded onto to an XDB C18 reversed-phase column (4.6 by 250 mm; pore size: 100 Å; Agilent Technologies) by an Agilent series 1100C high-performance liquid chromatography (HPLC) system. Pigments were eluted by a methanol/water gradient that started with 60% methanol and increased to 100% methanol in 10 min and kept constant for another 20 min. The flow rate was 1 mL/min. The photodiode-array detector was set to detect 770, 670, 500 and 280 nm. Pigments eluted by HPLC were collected for further mass analysis.

Bacteriochlorophyllide *a* was used as a standard, extracted from the BChG mutant of *Rhodobacter capsulatus* (37), in which bacteriochlorophyllide *a* was accumulated.

References

1. Blankenship, R. E., Olson, J. M. & Miller, M. (1995). Antenna complexes from green photosynthetic bacteria. In *Anoxygenic Photosynthetic Bacteria* (Blankenship, R. E., Madigan, M. T. & Bauer, C. E., eds), pp. 399-435, Kluwer Acad. Pub., Dordrecht.
2. Olson J, Romano C (1962) A new chlorophyll from green bacteria. *Biochim Biophys Acta* 59:726–728
3. Fenna, R. E. & Matthews, B. W. (1975). Chlorophyll arrangement in a bacteriochlorophyll protein from *Chlorobium limicola*. *Nature*, 258, 573-577.
4. Tronrud, D. E., Schmid, M. F. & Matthews, B. W. (1986). Structure and X-ray amino acid sequence of a bacteriochlorophyll *a* protein from *Prosthecochloris aestuarii* refined at 1.9Å resolution. *J. Mol. Biol.* 188, 443-454.
5. Li Y, Zhou W, Blankenship R, Allen J (1997) Crystal structure of the bacteriochlorophyll *a* protein from *Chlorobium tepidum*. *J Mol Biol* 271:456–471
6. Milder MT, Brüggemann B, van Grondelle R, Herek JL. (2010) Revisiting the optical properties of the FMO protein. *Photosynth Res*. DOI 10.1007/s11120-010-9540-1

7. Olson JM, Ke B, Thompson KH (1974) Exciton interaction among chlorophyll molecules in bacteriochlorophyll *a* protein and bacteriochlorophyll *a* reaction center complexes from green bacteria. *Biochim Biophys Acta* 430:524–537 Errata (1976). 440, 763
8. Pearlstein RM (1992) Theory of the optical spectra of the bacteriochlorophyll *a* antenna protein trimer from *Prosthecochloris aestuarii*. *Photosynth Res* 31:213–226.
9. Louwe RJW, Vrieze J, Hoff AJ, Aartsma TJ (1997b) Toward an integral interpretation of the optical steady-state spectra of the FMO-complex of *Prosthecochloris aestuarii*. 2. Exciton simulations. *J Phys Chem B* 101(51):11280–11287.
10. Savikhin S, Buck DR, Struve WS (1997) Pump-probe anisotropies of Fenna–Matthews–Olson protein trimers from *Chlorobium tepidum*: a diagnostic for exciton localization? *Biophys J* 73:2090–2096.
11. Vulto SIE, de Baat MA, Louwe RJW, Permentier HP, Neef T, Miller M, van Amerongen H, Aartsma TJ (1998) Exciton simulations of optical spectra of the FMO complex from the green sulphur bacterium *Chlorobium tepidum* at 6 K. *J Phys Chem B* 102(47):9577–9582.
12. Müh F, Madjet ME-A, Adolphs J, Abdurahman A, Rabenstein B, Ishikita H, Knapp E-W, Renger T (2007) α -Helices direct excitation energy flow in the Fenna–Matthews–Olson protein. *Proc Natl Acad Sci USA* 140:16862–16867.
13. Brixner T, Stenger J, Vaswani HM, Cho M, Blankenship RE, Fleming GR (2005) Two-dimensional spectroscopy of electronic couplings in photosynthesis. *Nature* 434:625–628.
14. Engel GS, Calhoun TR, Read EL, Ahn TK, Mančal T, Cheng YC, Blankenship RE, Fleming GR (2007) Evidence for wavelike energy transfer through quantum coherence in photosynthetic systems. *Nature* 446:782–786.
15. Zhou W, LoBrutto R, Lin S, Blankenship RE (1994) Redox effects on the bacteriochlorophyll *a*-containing Fenna-Matthews-Olson protein from *Chlorobium Cepidum*. *Photosyn Res* 41:89–96
16. Ben-Shem A, Frolow F, Nelson N (2004) Evolution of photosystem I - from symmetry through pseudo-symmetry to asymmetry. *FEBS Lett* 564:274–280.

17. Tronrud DE, Wen J, Gay L, Blankenship RE (2009) The structural basis for the difference in absorbance spectra for the FMO antenna protein from various green sulfur bacteria. *Photosynth Res* 100:79-87.
18. Frolov D, Marsh M, Crouch LI, Fyfe PK, Robert B, van Grondelle R, Hadfield A, Jones MR. (2010) Structural and spectroscopic consequences of hexacoordination of a bacteriochlorophyll cofactor in the *Rhodobacter sphaeroides* reaction center. *Biochemistry* 49:1882-1892.
19. Lu B, Xu T, Park SK, Yates JR 3rd. (2009) Shotgun protein identification and quantification by mass spectrometry. *Methods Mol Biol.* 564:261-88.
20. Yates JR, Ruse CI, Nakorchevsky A. (2009) Proteomics by mass spectrometry: approaches, advances, and applications. *Annu Rev Biomed Eng.* 11:49-79.
21. Liu T, Belov ME, Jaitly N, Qian WJ, Smith RD. (2007) Accurate mass measurements in proteomics. *Chem Rev.* 107:3621-53.
22. Loo JA (2000) Electrospray ionization mass spectrometry: a technology for studying noncovalent macromolecular complexes. *Int. J. Mass Spectrom.* 200:175-186
23. Sobott F, Robinson CV (2002) Protein complexes gain momentum. *Curr Opin in Struct Biol* 12:729-734
24. Benesch JLP, Robinson CV (2006) Mass spectrometry of macromolecular assemblies: preservation and dissociation. *Curr Opin in Struct Biol* 16:245-251
25. Hernández H, Robinson CV (2007) Determining the stoichiometry and interactions of macromolecular assemblies from mass spectrometry. *Nature Protocols* 2:715-726
26. Ruotolo BT, Benesch JLP, Sandercock AM, Hyung SJ, Robinson CV (2008) Ion mobility-mass spectrometry analysis of large protein complexes. *Nature Protocols* 3:1139-1152
27. Kanu AB, Dwivedi P, Tam M, Matz L, Hill HH Jr. (2008) Ion mobility-mass spectrometry. *J. Mass Spectrom* 43:1-22
28. Melkozernov AN, Olson JM, Li YF, Allen JP, Blankenship RE (1998) Orientation and excitonic interactions of the Fenna-Matthews-Olson Protein in membranes of the green sulfur bacterium *Chlorobium tepidum*. *Photosynth Res* 56:315–328.
29. Wen J, Zhang H, Gross ML, Blankenship RE (2009) Membrane orientation of the FMO antenna protein from *Chlorobaculum tepidum* as determined by mass

- spectrometry-based footprinting. *Proc Natl Acad Sci USA* 106:6134–6139
30. Shibata Y, Saga Y, Tamiaki H, Itoh S (2007) Polarized fluorescence of aggregated bacteriochlorophyll *c* and baseplate bacteriochlorophyll *a* in single chlorosomes isolated from *Chloroflexus aurantiacus*. *Biochemistry* 46:7062–7068.
 31. Zhou M, Sandercock AM, Fraser CS, Ridlova G, Stephens E, Schenauer MR, Yokoi-Fong T, Barsky D, Leary JA, Hershey JW, Doudna JA, Robinson CV (2008) Mass spectrometry reveals modularity and a complete subunit interaction map of the eukaryotic translation factor eIF3. *Proc Natl Acad Sci USA*. 105:18139-18144
 32. Barrera NP, Bartolo ND, Booth PJ, Robinson CV (2008) Micelles protect membrane complexes from solution to vacuum. *Science* 321:243-246
 33. Ruotolo BT, Giles K, Campuzano I, Sandercock AM, Bateman RH, Robinson CV (2005) Evidence for Macromolecular Protein Rings in the Absence of Bulk Water. *Science* 310:1658-61
 34. van Duijn E, Barendregt A, Synowsky S, Versluis C, Heck AJR (2009) Chaperonin complexes monitored by Ion Mobility Mass Spectrometry. *J. Am. Chem. Soc.*, 131: 1452–1459
 35. Kirchhoff H (2008) Significance of protein crowding, order and mobility for photosynthetic membrane functions. *Biochem. Soc. Trans.* 36: 967 - 970
 36. Robinson CV, Sali A, Baumeister W. (2007) The molecular sociology of the cell. *Nature* 450: 973-82.
 37. Bollivar DW, Wang S, Allen JP, Bauer CE. (1994) Molecular genetic analysis of terminal steps in bacteriochlorophyll *a* biosynthesis: characterization of a *Rhodobacter capsulatus* strain that synthesizes geranylgeraniol-esterified bacteriochlorophyll *a*. *Biochemistry* 33:12763-12768.

Chapter 3.
**Pigment mutants of the FMO antenna protein from green
photosynthetic bacteria***

** This chapter is based on the published work: Biochemistry, 2010, 49 (26), pp 5455–5463*

Abstract

The Fenna-Matthews-Olson (FMO) light harvesting antenna protein has been a model system to understand pigment/protein interactions in the energy transfer process in photosynthesis. All previous studies utilized wild type FMOs from several species. Here we report the purification and characterization of the first FMO mutant generated by replacing the phytyl group at the C-17 propionate residue of bacteriochlorophyll *a* (BChl *a*) to geranylgeranyl, which possesses three more double bonds. The FMO protein still assembles with the modified pigment, but both the whole cell absorption and the biochemical purification indicate that the mutant cells contain much less mature FMO protein. The gene expression was checked using quantitative real time PCR, and all the genes coded for BChl *a* binding proteins are not strongly regulated. The smaller amount of the FMO protein in the mutant cell is probably due to the degradation of the apo-FMO protein at different stages after it cannot bind the normal pigment. The absorption, fluorescence and CD spectra of the purified FMO mutant protein are similar to the wild type FMO protein except the conformations of most pigments are more heterogeneous, which broadens the spectral bands. Interestingly, the lowest energy pigment binding site seems to be unchanged and is the only peak that can be well resolved in 77 K absorption. The excited state lifetime of the mutant FMO protein is unchanged from wild type and shows a similar temperature dependent modulation as does the wild type. The mutant FMO protein is less thermally stable than the wild type. The assembly of the FMO protein and also the implications of the decreased FMO/chlorosome stoichiometry are discussed in terms of the topology of these two antennas on the cytoplasmic membrane.

Introduction

In the photosynthetic green sulfur bacteria, light absorbed by the large peripheral antenna complex called the chlorosome (1-4) is transferred through the baseplate protein (5-7) and the Fenna-Matthews-Olson (FMO) protein (8) to the reaction center (RC) where charge separation occurs (9). The FMO protein forms a bridge to connect the chlorosome to the cytoplasmic membrane structurally and functionally to direct the excitation energy collected from the chlorosome to the RC (10, 11). Ever since the FMO protein was first discovered in the early 1960s (12) and its atomic resolution structure was solved in the 1970s (13), the analysis of this protein has been a major source of our understanding of how pigments bind to photosynthetic proteins and the nature of pigment-pigment interactions.

The FMO protein is a water-soluble protein that is remarkably stable. This makes it a very attractive system for structural and functional studies. The X-ray structures of the FMO protein were determined from two species of green sulfur bacteria *Prosthecochloris aestuarii* (*P. aestuarii*) and *Chlorobaculum tepidum* (*C. tepidum*) (14-18), and a third structure of FMO from *Pelodictyon phaeum* in which bacteriochlorophyll *e* is the dominant chlorosomal pigment has recently been completed in collaboration with Allen and co-workers (unpublished data). The FMO protein forms a compact trimer with three-fold symmetry (Fig. 1A). A large portion of the protein scaffold is beta sheet secondary structure, which forms a “taco shell” to create a highly hydrophobic cavity to hold seven bacteriochlorophyll *a* (BChl *a*) molecules in each monomer. Three monomers join together by both electrostatic and hydrophobic interactions to form a stable structure (16).

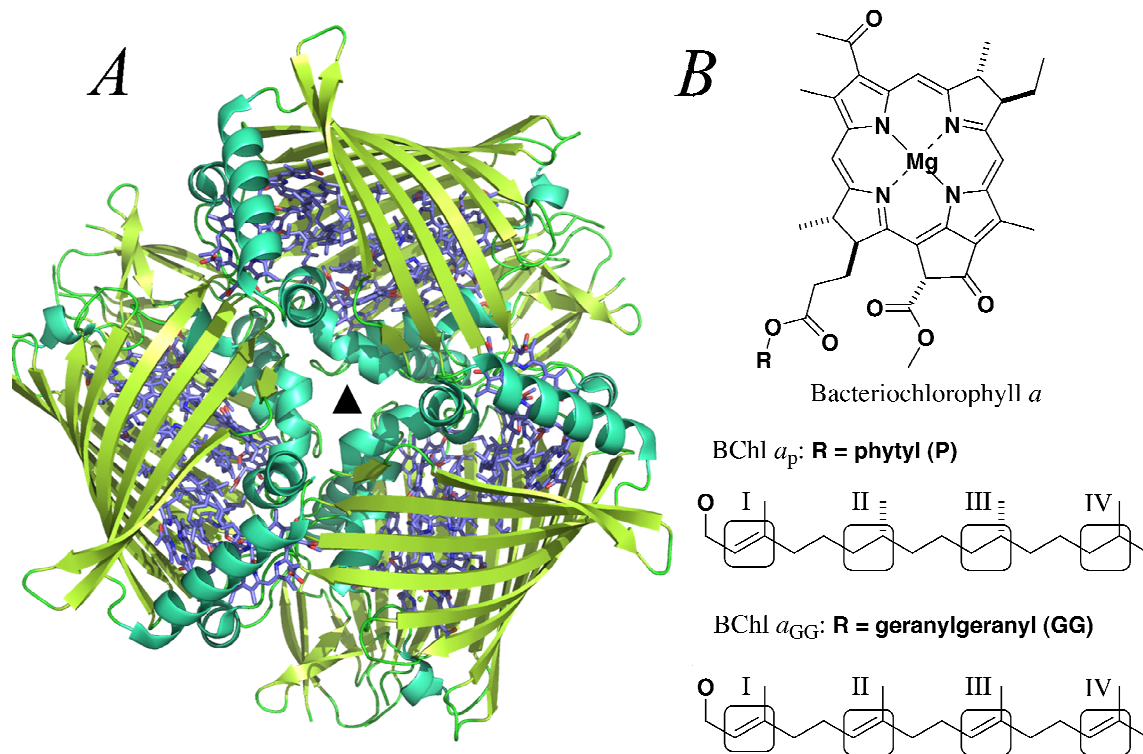


Fig. 1 (A) Structure of FMO protein from *C. tepidum* (PDB code: 3ENI). (B) Bacteriochlorophyll *a* (BChl *a*) with phytyl (P) and geranylgeranyl (GG) tails.

The seven BChl *a* molecules hold very specific conformations inside the protein with their bacteriochlorin rings forming hydrogen bonds and axial ligation with the surrounding protein and water. The tails of the BChl *a* also have unique orientations and may play important structural roles, which have not been elucidated. Recently, the structure of FMO from *P. aestuarii* was solved at 1.3 Å resolution, under which almost every individual non-hydrogen atom could be resolved (15). Surprisingly, an 8th BChl *a* was discovered in the monomer connection region, although it had long been known to crystallographers who determined the structures that there was unresolved electron density between the subunits (14). A preliminary report from Nelson and co-workers suggested that another pigment was in this position (17). A comparison of the binding region in the refined FMO structures from *C. tepidum* and *P. aestuarii* allowed Tronrud *et al.* (15) to recognize a specific binding motif and possible structural change for binding the 8th pigment in the two species. Site-directed mutations of the FMO protein will help to understand these issues, although such mutants have not yet been produced.

The FMO protein is quite highly conserved, with amino acid sequence identities among the various green sulfur bacteria typically on the order of 80%. It has been used as a marker gene to classify green sulfur bacteria (19, 20). The known structures are also very similar, but the optical properties, such as 77 K absorption, linear and circular dichroism, show some differences, the reasons for which are not well understood.

Recently, a sixth phylum of phototrophic bacteria has been discovered in hot springs in Yellowstone National Park (21). Remarkably, this organism, *Candidatus*

Chloracidobacterium thermophilum, which is a member of the acidobacteria, also contains a clear homolog of the FMO protein. However, this FMO protein is significantly diverged from the ones found in the green sulfur bacteria, and has only about 50% identity with the green sulfur FMOs (22). This FMO variant also has somewhat different spectral features (22), which provide an attractive system for comparative studies.

Due to the relatively small number of pigments coupled in the protein and especially the ability to resolve partially the exciton peaks at low temperature, the FMO protein has been an interesting system for both theoretical and spectroscopic studies to understand the dynamics of the energy transfer process (23-26). The prediction of the site energies of individual pigments has been developed from the initial simple fitting of the experimental spectra (27, 28) to direct quantum calculations based on the detailed structures (11, 29). General optical features, such as steady-state spectra and dynamic energy transfer, have been explained and functions of specific amino acids have been predicted (29), although these have not been experimentally verified. All these achievements have on one hand deepened our understanding of light harvesting process, while, on the other hand, raised interesting questions and provided targets for mutagenesis studies.

Recently, the FMO protein was used as a model system in the development of the two dimensional electronic spectroscopy pioneered in the Fleming group (30-32). The pathway of energy flow within the molecule was determined by observing off-diagonal peaks in the 2D spectrum, which directly reveals the strength of the excitonic coupling of the pigments (30). Later, a long-lived quantum coherence in the FMO protein was

observed (33-35) and also in another light harvesting antenna called PC645 (36). These findings have generated intense interest in many areas of science including discussions of possible relevance to quantum computing (37-40). An interesting question is how nature manipulates the specific pigment-protein architecture to preserve such long-lived coherence and how we might be able to control it. The ability to produce specific FMO mutants will shine light on these issues.

The genome of *C. tepidum* was sequenced (41) and analyzed in detail (42). The genetic system in *C. tepidum* first developed by Wahland and Madigan (43) was developed significantly by Bryant and co-workers (2, 42, 44). However, the desirable FMO mutants have never been generated, probably because *fmo* is an essential gene for photosynthesis and the green sulfur bacteria are obligate photoautotrophs. Here we report the first FMO mutant, which was generated by replacing the phytyl at the C-17 propionate residue of the BChl *a* (BChl *a_P*) by geranylgeranyl (BChl *a_{GG}*) (Fig. 1B) by deleting the geranylgeranyl reductase (*bchP*) gene (45, 46). Properties of this mutant FMO are the subject of this chapter.

Results

1. Cell absorption and biochemical purification indicate less FMO protein is present in the mutant cells.

Conversion of the phytyl tail of the BChl *a* (also the primary electron acceptor chlorophyll *a* in the RC) to geranylgeraniol did not induce a lethal defect in the cell growth. The mutant cells grew well and could reach a similar cell density as the wild type

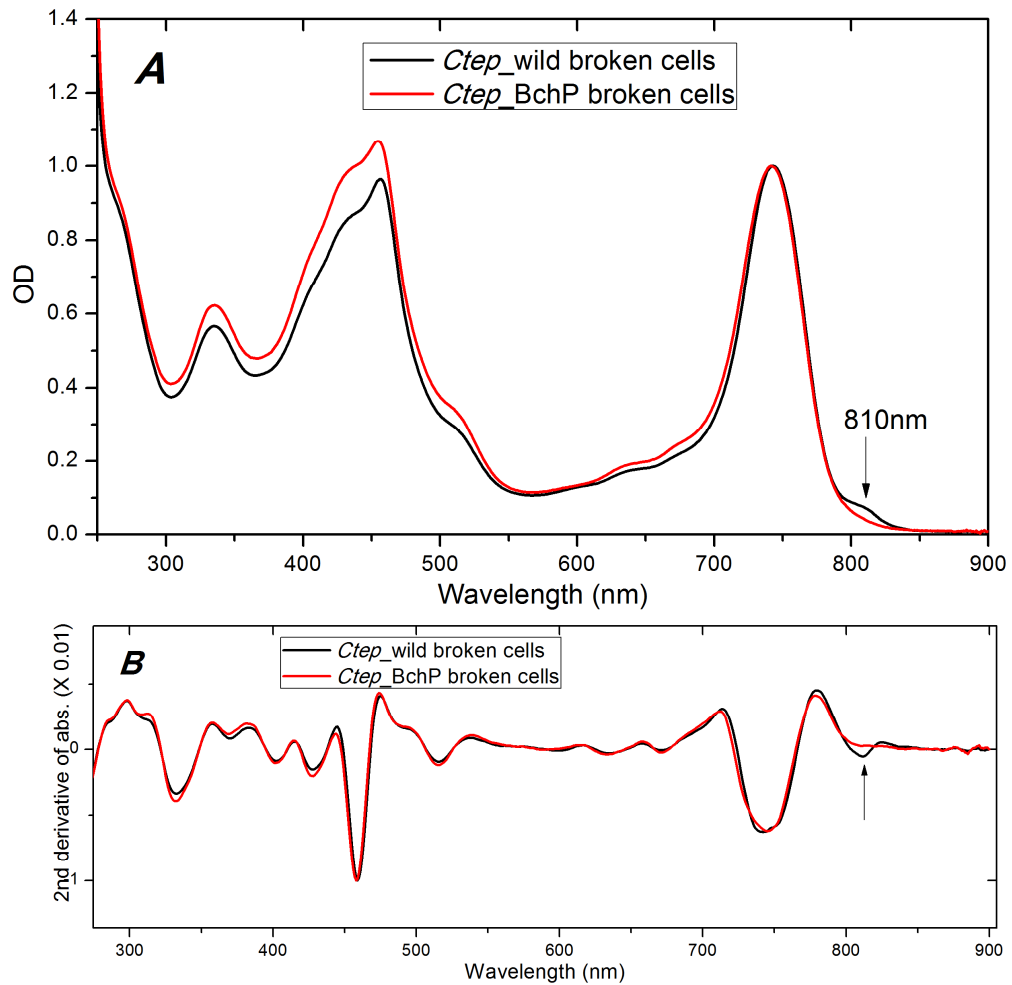


Fig. 2 (A) Absorption of broken whole cells. Wild type cells show a shoulder at the 810 nm region which is the Qy peak of the FMO protein. There is almost no shoulder in the BchP cells. (B) Second derivative of the broken whole cell absorption shows the absence of the 810 nm shoulder in the BchP cells.

as reported by Harada *et al* (45). Fig 2A shows the absorption of the broken whole cells of wild type and BchP mutant after normalization at the chlorosome Qy peak at 743 nm. Compared to the wild type cells, the BchP cells have a higher carotenoid peak in the 400-500 nm region which overlaps with the Soret band of chlorosomes. The FMO shoulder at approximately 810 nm is almost invisible in the mutant cells. The difference is also clearly shown in the corresponding 2nd derivative of the absorption of the broken whole cells. It is clear that if there is any intact FMO in the BchP cells, the amount is small compared to the wild type, although there is another possibility that the FMO in the BchP mutant cells has a very different Qy absorbance spectrum from the wild type; that is, it may be blue shifted and hidden by the dominant chlorosome peak, which is shown below not to be the case.

Na₂CO₃ treatment of the BchP mutant membrane following the same procedure as purifying the wild type FMO indicates there are FMO in the BchP cells (as characterized below). The same amounts of *C. tep* wild and mutant membranes (normalized on the chlorosome peaks) were treated with Na₂CO₃. The supernatants collected after ultracentrifugation from the mutant membrane solution showed FMO-like absorption at 806 nm with an OD = 0.3, while the supernatant of the wild type cells has an OD = 1.6. Only around 1/5 of the FMO protein could be extracted from the BchP mutant membranes compared to the wild type membranes. The FMO protein (FMO_BchP) in the supernatant from the mutant membrane solution was purified until it shows one band on the SDS-PAGE and was characterized as shown below.

2. Pigment analysis of the FMO_BchP

We first checked whether the FMO_BchP incorporated BChl a_{GG} or BChl a_P as the binding pigments. The HPLC analysis of pigments from the purified FMO_BchP protein and also the wild type FMO protein is shown in Fig. 3. Under the elution conditions described in the Methods section, the pigment from the wild type FMO (BChl a_P) elutes at 11 min while that from the BchP mutant elutes at 7 min, showing the same absorption as BChl a_P (Inset of Fig. 3A). Although other detection wavelengths were also monitored, no other elution peaks were observed. Earlier HPLC studies (45, 48, 49) indicated that BChl a_{GG} is less hydrophobic than BChl a_P owing to more double bonds in the tail. Clearly the FMO_BchP contains a type of BChl a different from BChl a_P , and it is anticipated that the component that elutes at 7 min is BChl a_{GG} . Further identification of the pigment was achieved by mass spectrometry using MALDI-TOF.

The BChl a_P collected from the wild type FMO protein shows four main peaks in the MALDI-TOF mass spectrum: MW 910.8, 888.9, 632.4 and 610.5 (Fig. 3B). The m/z 910.8 ion is the monoisotopic peak of BChl a_P ($[C_{55}H_{74}MgN_4O_6]^+$), while the m/z 888.9 ion is the BChl a_P with its central Mg replaced by two hydrogen atoms (bacteriopheophytin a , BPhe a_P , $[C_{55}H_{76}N_4O_6]^+$). After they lost the phytyl tails, BChl a_P and BPhe a_P ions gave the m/z 632.4 (bacteriochlorophyllide a , $[C_{35}H_{36}MgN_4O_6]^+$) and 610.5 (bacteriopheophorbide a , $[C_{35}H_{38}N_4O_6]^+$) ions, respectively. This fragmentation was proved, as also shown in Fig. 4, by MS/MS analysis of the m/z 911.8 and 888.9 precursor ions. The pigment collected from the FMO_BchP shows a similar mass pattern with four main peaks at MW 904.8, 882.8, 632.4 and 610.4 (Fig. 3C). The 904.8 and

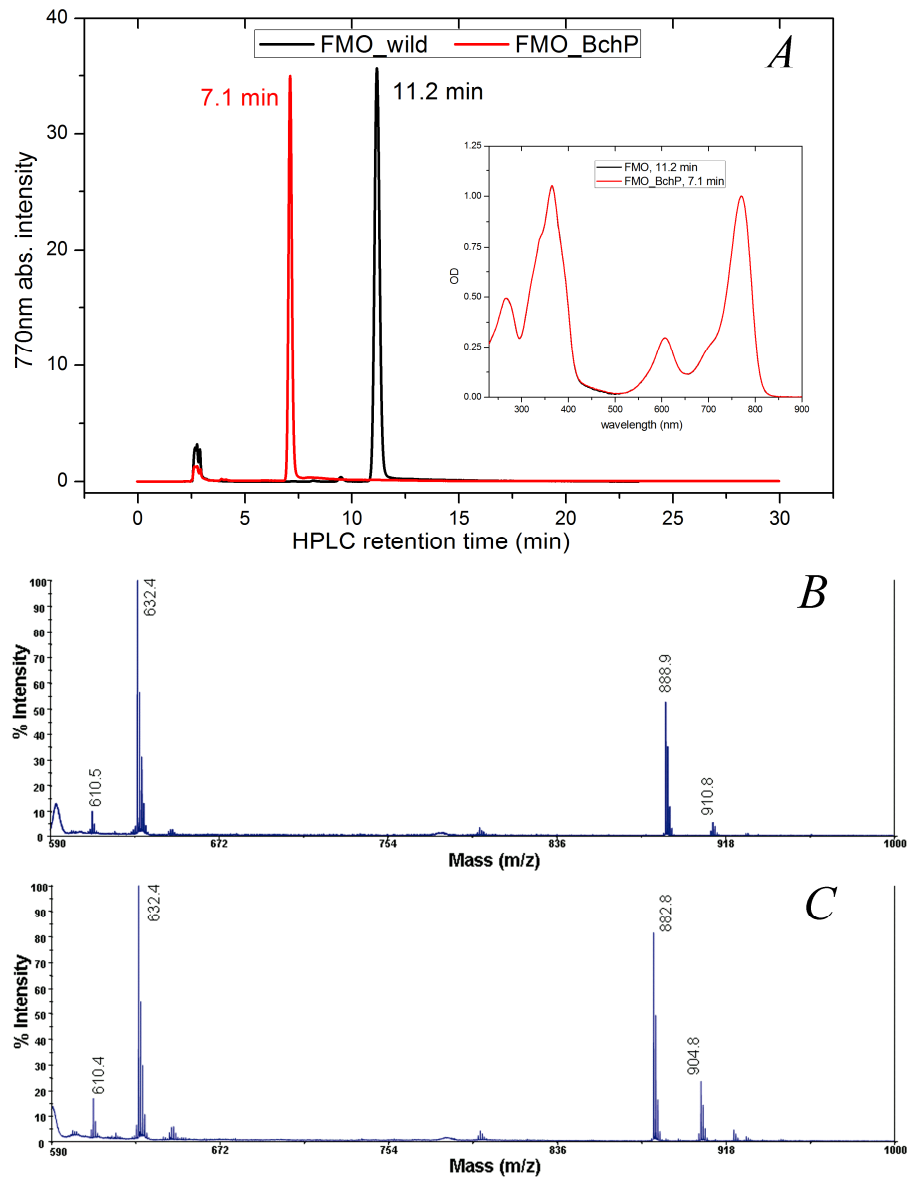


Fig. 3 (A) HPLC analysis shows the different elution times of pigments in the wild and BchP FMO. Both pigments have a typical BChl *a* absorption as shown in the inset. MALDI-TOF mass spectral analysis of the pigments from FMO_wild and FMO_BchP are shown in (B) and (C), respectively.

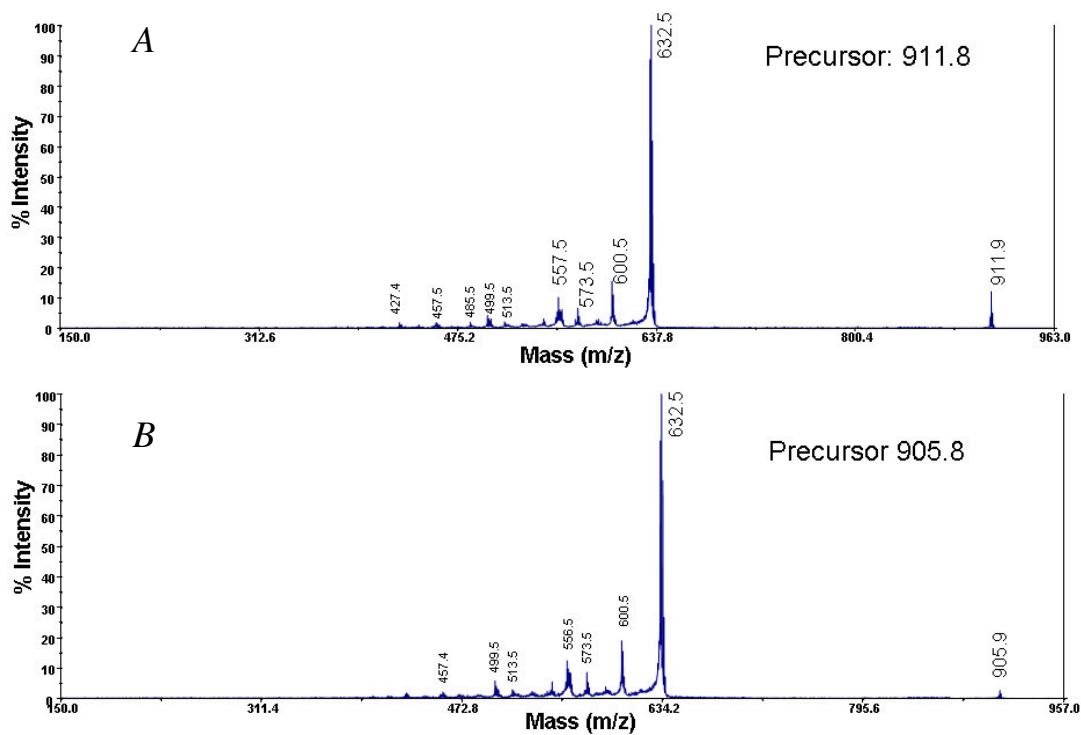


Fig. 4 Product-ion spectra of precursor ions m/z 911.9 from the wild type FMO (A) and m/z 905.9 from the FMO mutant (B). This confirms that the 6 Da mass shift in the pigment from FMO mutant is coming from the tail, because the macrocycle of the bacteriochlorophyll ring (632.5 Da) is the same as that from the BChl a_P in the wild type FMO (A).

882.8 peaks are 6 Da less than the mass of BChl a_P and BPhe a_P , respectively, and they match the predicted mass of the BChl a_{GG} and BPhe a_{GG} very well (49). The 6 Da mass shift arises from the change of the tail since the 632.4 and 610.4 peaks of the macrocycle were also found in BChl a_P (Figs. 3B, 3C and Fig. 4). The results show that three more double bonds are in the tail of the pigment from FMO_BchP. Thus, we concluded that the FMO purified from the BchP cells assembled with BChl a_{GG} .

3. Steady-state optical spectra of FMO_BchP

Room temperature UV/Vis absorption spectra of the FMO_BchP were measured and compared with the wild type as shown in Fig. 4. After the FMO_wild and FMO_BchP absorption spectra were normalized at the Soret band, we found that the intensities of the Q_x and Q_y peaks of the FMO_BchP are weaker than those of the wild type (Fig. 5A). In addition, the wild type FMO shows more structure in the Q_y region as indicated by the 2nd derivative of the absorption spectra (Fig. 5B). Three peaks were resolved at 825.7, 813.5 and 805 nm. FMO_BchP clearly resolve the lowest energy peak at 825.7 nm and a peak at 810 nm with a shoulder on the high energy side. Interestingly, the Q_x peak of the FMO_BchP shows more spectral features than that of the wild type, and two clear peaks at 594 and 608 nm were resolved. The wild type FMO only shows a single peak at 603 nm.

If the absorption spectra are normalized at the Q_y peak (Fig. 5C), it is clear that the full width at half maxima (FWHM) of both Q_y and Q_x of the FMO_BchP are larger than those of the FMO_wild. The FWHM of Q_y and Q_x of the wild type FMO are 28.3 and

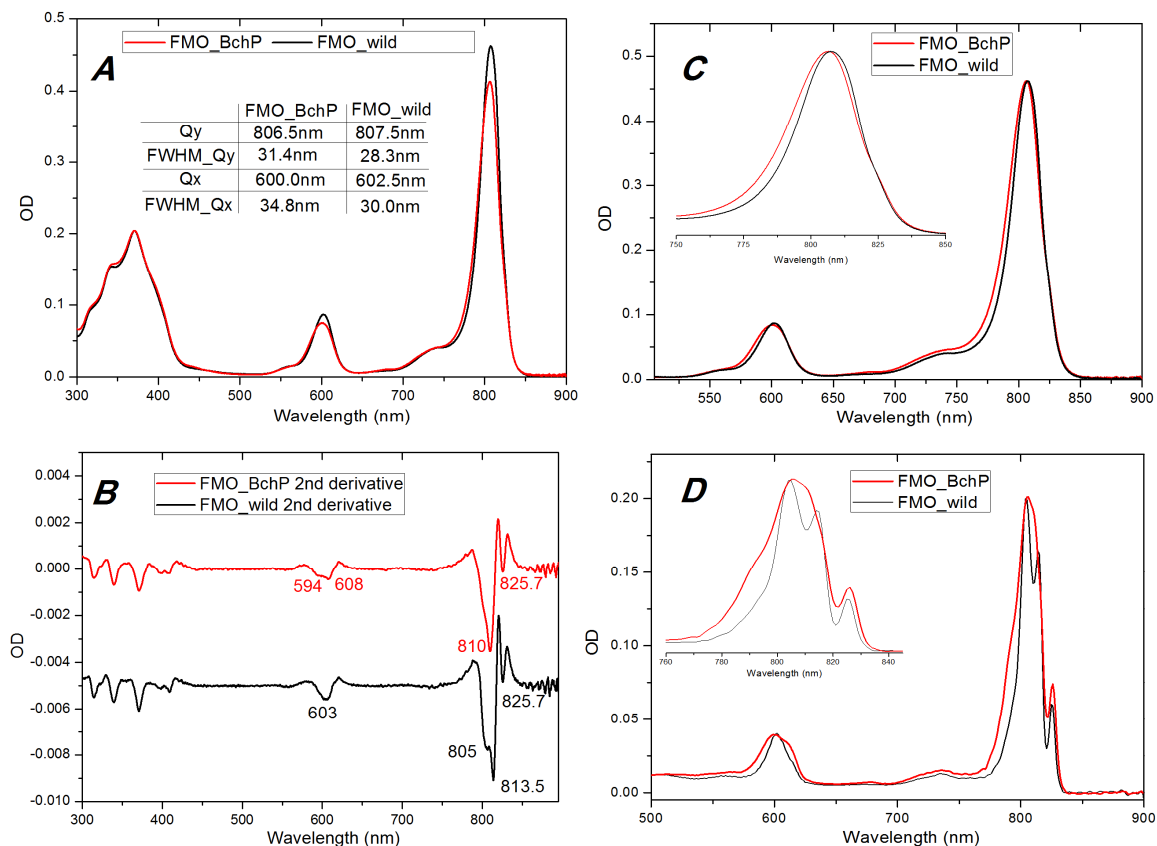


Fig. 5 (A) RT absorption of FMO_BchP and FMO_wild type normalized at the Soret bands. Peak positions and bandwidths are shown in the inset. (B) Second derivative of the absorption spectra of FMO_BchP and FMO_wild. (C) Qy and Qx regions of the absorptions of FMO_BchP and FMO_wild normalized at the Qy peak (inset). FMO_BchP has blue shifted and also broadened Qy and Qx peaks. (D) 77 K absorption of FMO_BchP and FMO_wild. The Qy region is zoomed in and shown in the inset.

30.0 nm, respectively, whereas they are 31.4 and 34.8 nm for the FMO_BchP, respectively. The broader spectrum of FMO_BchP may indicate more heterogeneous pigment conformations in the FMO_BchP, which broadens the peaks inhomogeneously. Moreover, the Q_y and Q_x peaks of the FMO_BchP are also blue shifted around 1-2 nm compared to the wild FMO. A similar spectral shift effect was also reported in the BchP mutant of RC (50), LH1 (48) and LH2 (51) complexes in purple bacteria.

At 77 K (Fig. 5D), the wild FMO protein showed three distinct peaks at 825, 814 and 804 nm. In contrast, the FMO_BchP showed a broad peak at 806 nm with shoulders on both the high and low energy sides. Only the lowest energy peak at 826 nm could be well resolved, which suggests that the conformation of the corresponding pigment(s) is/are not affected much by changing the tail. However, the peak of the lowest energy band of FMO_BchP is shifted 1 nm to the red (Fig. 5D inset), indicating a slightly lower energy level compared to the wild type FMO. It is also noted that the Q_x peak of FMO_BchP is also much broader than that of the wild type. The 77 K absorption spectrum further confirms a more heterogeneous conformational distribution of all the other pigments, which gave inhomogeneous peak broadening and, thus, could not be resolved at 77 K.

At room temperature, the FMO_BchP shows a broader fluorescence peak centered at 822 nm with FWHM of 34.0 nm, whereas the wild type FMO shows an emission peak at 825 nm with FWHM of 31.9 nm (Fig. 6A). The broader emission peak from FMO_BchP further implicates the more heterogeneous pigment conformations in the mutant.

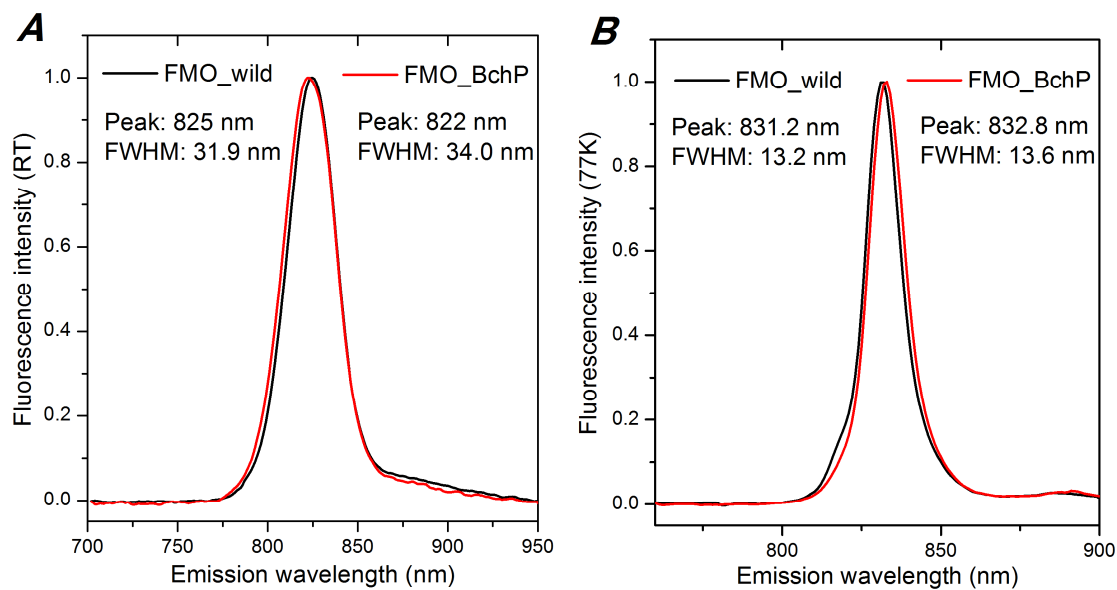


Fig. 6 RT (A) and 77 K (B) fluorescence spectra of FMO_BchP and FMO_wild (excitation at 370 nm).

In contrast, the emission peak widths of FMO_BchP and FMO_wild at 77 K are quite similar with FWHMs of 13.6 nm and 13.2 nm, respectively (Fig. 6B), which is consistent with the conclusion from 77 K absorption that the conformation of the lowest energy pigment(s) is/are more similar. However, the emission peak of the FMO_BchP is slightly red-shifted (1.6 nm) compared to the wild type which indicates a slightly lower energy level of FMO_BchP that was previously suggested in the 77 K absorption. Comparing the 10.2 nm fluorescence peak shift of FMO_BchP from RT to 77 K (822 nm → 832.8 nm) with the 6.2 nm peak shift of FMO_wild (825 nm → 831.2 nm), we suggest there is probably a stronger thermal equilibrium between the exciton states of different pigments in the mutant at room temperature. This thermal equilibrium causes the blue-shifted emission peak of FMO_BchP at RT due to backward energy transfer, but the equilibrium was interrupted at 77 K and all the high energy excitonic states transfer energy to the lowest excitonic state and this process was irreversible at 77 K causing the emission only from the lowest excitonic state.

FMO_BchP shows a similar CD spectrum as the wild type except a slightly weaker CD signal in the Q_y region (Fig. 7), suggesting a weaker excitonic coupling strength compared with the wild type.

Overall, the FMO_BchP has quite similar steady-state optical properties as the wild type FMO except more heterogeneous pigment conformations, which may affect the energy transfer as suggested from the RT and 77 K fluorescence. Interestingly, the lowest excitonic state seems not to be changed significantly. The absence of the 810 nm

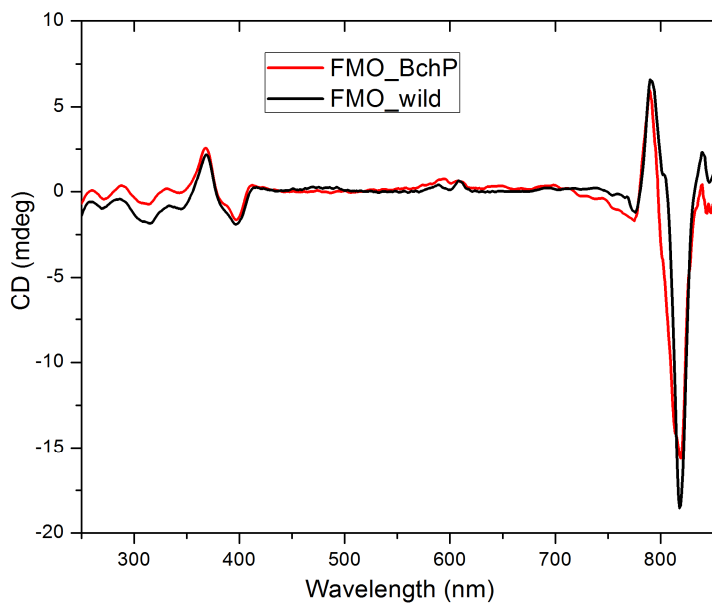


Fig. 7 CD spectral comparison, normalized at the Soret band absorption.

shoulder in the whole cell absorption clearly indicates that there is a smaller number of FMO complexes in the mutant, which is consistent with the biochemical purification that BchP cells have much less FMO that can be extracted.

4. Fluorescence dynamics

The fluorescence decay kinetics of the FMO_BchP was probed by excitation in the Soret band using time-correlated single photon counting. In Fig. 8, the measured fluorescence decay curves at RT and 77 K and the fitted decay curves, together with the corresponding instrument response function (IRF) are shown. It is clear that the fluorescence decay of FMO_BchP at RT (824 nm) is significantly faster than the decay at 77 K. The former can be fitted very well with three exponentials having lifetimes of 2.3 ns (40%), 0.75 ns (17%) and 0.094 ns (43%). The 77 K fluorescence decay (832 nm) can be best described by a biexponential decay with time constants of 2.5 ns (45%) and 0.78 ns (55%). The lifetime of wild type FMO was measured under the same condition and gave virtually the same results (Fig. 9) in agreement with previous reports (52). It has long been known that the lifetime of FMO depends on the redox condition of the solution (53) and also the temperature (54); however, the molecular mechanism of this excited state modulation is still unclear. Here a similar temperature-regulated fluorescence lifetime in the FMO_BchP was shown. The fast decay component 0.094 ns of FMO_BchP at RT was not observed at 77 K, and the relative contribution of the slow components increased.

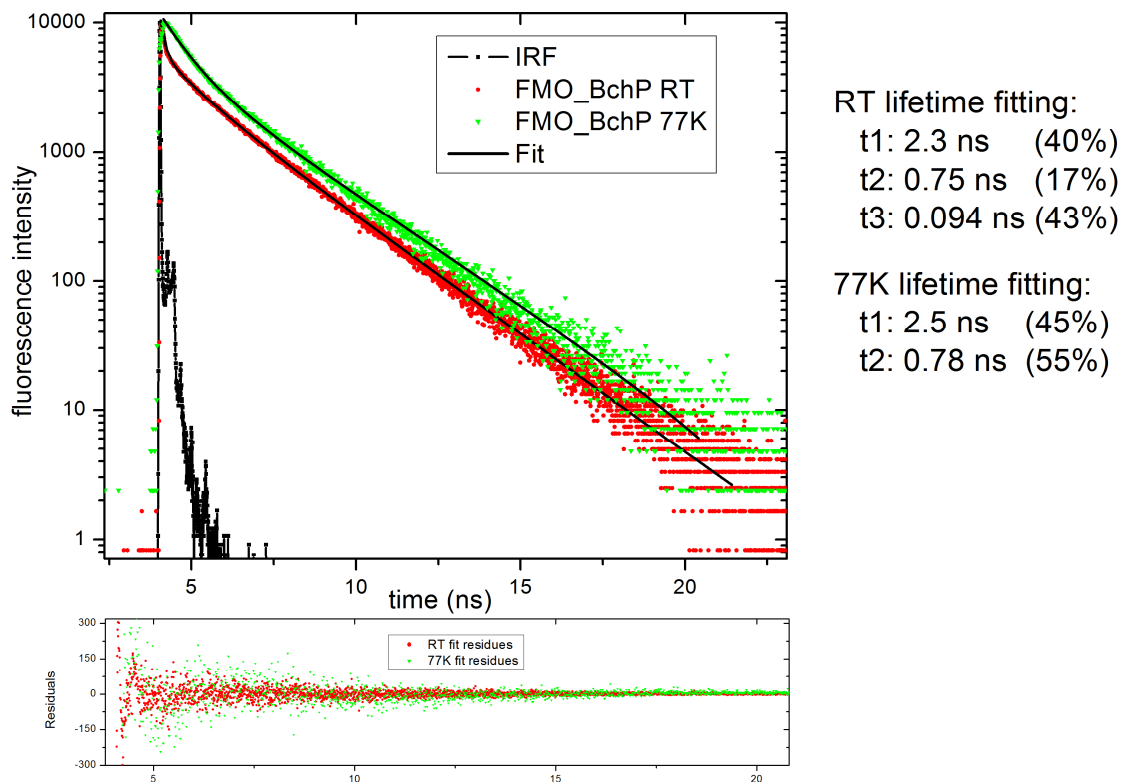


Fig. 8 RT and 77 K lifetime of FMO_BchP. Three exponential decays can fit the RT fluorescence kinetics very well. The dominant lifetime components are 94 ps and 2.3 ns, which account for 43% and 40% of the amplitude, respectively. Two exponential decays can give a reasonable fit of the 77 K fluorescence decay. The lifetime increases to 2.5 ns and 0.78 ns, which account for 45% and 55% of the amplitude. The lower panel shows the residues between the fitting and the experimental data.

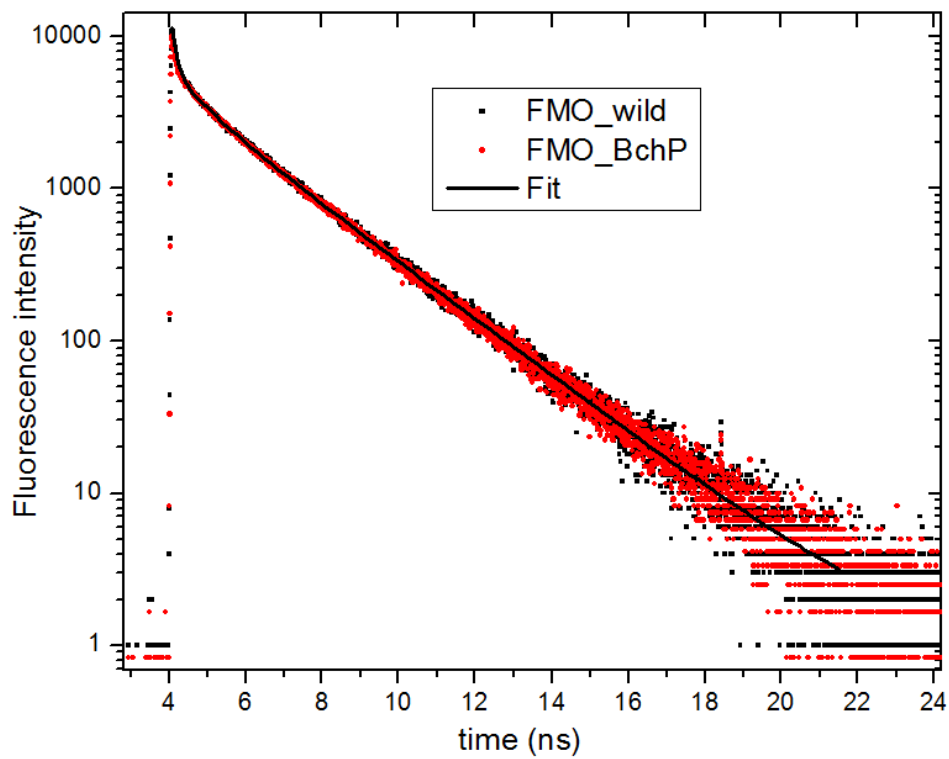


Fig. 9 FMO_BchP and FMO_wild have the same decay kinetics.

5. Thermal stability of FMO_BchP

The *C. tepidum* BchP mutant can still grow photosynthetically, although the growth rate decreased at a higher temperature (45). It is possible that the geranylgeranyl tail caused the BChl *a* binding proteins to be unstable under high temperatures. Therefore, the thermal stability of the FMO_BchP was studied in comparison with the wild type FMO protein by monitoring the amplitude of the Qy peak. The thermally-induced FMO unfolding process was irreversible, so the change of free energy could not be quantified. However, it is still clear that the FMO_BchP is less thermally stable and has a sharp downturn at 67 °C (Fig. 10). The wild type FMO, instead, has a downturn point at around 73 °C (Fig. 10). Below 60 °C, the Qy band of wild type FMO is more sensitive to temperature as it has a larger slope compared to the FMO_BchP. The pigments start to degrade, and the protein forms aggregates above 80 °C, causing the continuous decrease of the absorption in the Qy region.

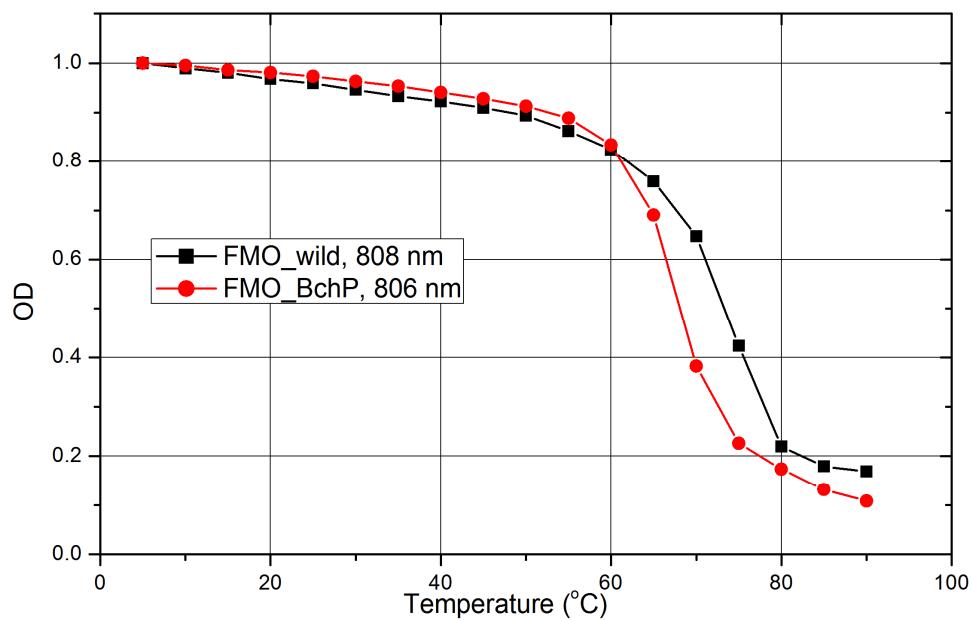


Fig. 10 Thermal stability of FMO_BchP and FMO_wild monitored at the Qy absorption peaks from 5 °C to 90 °C with a temperature step size of 5 °C. The solution was equilibrated for 5 min at each temperature point.

6. Gene expression profiles

To elucidate further the amount of FMO in the BchP mutant cells and understand its regulation, upstream genes were followed on FMO and all the other BChl *a* binding or related proteins (CsmA, CsmD, PscA) by qRT-PCR analysis of the mRNA level. Normalized ΔC_T data using 16S rRNA as the house-keeping gene from *C. tep* wild cells were compared to data from *C. tep* BchP cells, in which $\Delta\Delta C_T = \Delta C_T^{\text{Ctep_BchP}} - \Delta C_T^{\text{Ctep_wild}}$. If a certain gene is down-regulated in the mutant cells, the mRNA level of this gene will be low. In the qRT-PCR, it will need more amplification cycles for this gene to reach the threshold, thus giving a bigger ΔC_T and a positive $\Delta\Delta C_T$ when compared with those of the wild type. As shown in Table 1, the $\Delta\Delta C_T$ of all the genes are approximately zero except the *pscA* gene which shows a slightly negative value. It seems the mRNA levels of all the proteins were not significantly changed except for a small up-regulation of the *pscA* gene in the BchP mutant. The smaller amount of FMO holo-protein in the BchP mutant might be a result of less efficient assembly with the wrong pigment so that the translated FMO apo-protein is degraded quickly by the cell. Actually, the ratio of FMO apo-protein in the wild type and BchP mutant cells depending on the cell growth phase and the duration of protein processing could range from ~ 2 to ~ 6 as seen by the western blot using anti-FMO antibody.

Table 1. ΔCt and $\Delta\Delta\text{Ct}$ of selected genes in qRT-PCR

Gene	ΔCt (wild)	ΔCt (BchP)	$\Delta\Delta\text{Ct}$
<i>16S rRNA</i>	0	0	0
<i>csmA</i>	6.4 ± 0.3	6.4 ± 0.3	0 ± 0.3
<i>csmD</i>	8.0 ± 0.2	7.9 ± 0.4	-0.1 ± 0.4
<i>pscA</i>	8.6 ± 0.5	7.3 ± 0.3	-1.3 ± 0.5
<i>fmo</i>	7.2 ± 0.2	6.3 ± 0.3	-0.9 ± 0.3

Discussion

1. FMO assembly

The replacement of phytyl tail in the BChl *a* by geranylgeranyl (Fig. 1B) should add more rigidity owing to the torsional restrictions from the double bonds. However, the change from phytyl to geranylgeranyl does not introduce a lethal defect on the cell growth. In *C. tep*, BChl *a* is distributed in the CsmA protein, FMO protein and the RC. In the crystal structure of the FMO protein (PDB codes: 1M50, 3ENI), the tails of BChl *a* are tightly packed and have well-defined conformations (Figs. 1A and 11). The torsion angles at one double and three single bond positions in the BChl *a_P* were measured and are listed in Table 2. Although there are some variations in the conformation of tails in the two structures of the same FMO protein (PDB codes: 1M50, 3ENI), the tail of BChl *a_P* #4 seems to be less affected by changing from phytyl to geranylgeranyl in both structures. All the other BChls *a_P* seem to have to adopt new conformations to release the torsion restriction. In any case, only torsion angles at regions II and III of certain BChl *a_P* will be affected more in the BchP mutant since region IV is at the end of the tail which should have more flexibility to adopt the double bond.

Both the whole cell absorption spectra and the biochemical extraction of the FMO protein all indicated fewer FMO protein complexes in the BchP mutant. The upstream *fmo* gene expression level seems to be not changed, as checked by qRT-PCR. Thus, the smaller amount of native FMO in the mutant probably results from the failure of assembling native FMO complexes owing to the mismatched pigment composition. The lack of atomic resolution structures for the CsmA and RC makes it difficult to evaluate the BChl

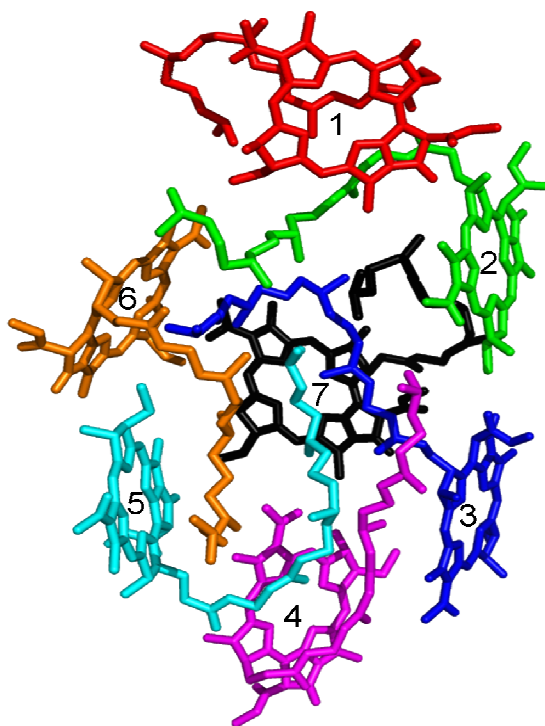


Fig. 11 Conformation of the BChl a_p in an FMO monomer with each pigment highlighted in different colors and numbered, the 8th pigment was omitted since the tail is invisible in the structure.

Table 2. Torsion angles of the tails in the FMO structures from *C. tepidum* (PDB code: 1M50 and 3ENI)* and *P. aestuarii* (PDB code: 3EOJ)

2-1) FMO from *C. tepidum* (PDB code: 1M50)

Pigments	Torsion angles			
	I	II	III	IV
BChl a_P 1	179.7	177.3	132.8	179.3
BChl a_P 2	179.8	179.8	153.7	178.4
BChl a_P 3	177.8	178.1	136.6	179.5
BChl a_P 4	178.7	178.3	169.1	178.6
BChl a_P 5	179.0	177.4	163.1	179.5
BChl a_P 6	178.9	178.6	146.7	178.9
BChl a_P 7	177.0	177.5	163.9	178.5

In FMO structure 1M50, the torsion angles of BChl a_P at regions I, II and IV (refer to text Fig. 1B) are very close to 180°, thus BChl a_P to BChl a_{GG} will probably not have effects at these regions. The mutation of the tail from phytyl to geranylgeranyl will affect region III of pigments # 1, 2, 3 and 6 more than others.

2-2) FMO from *C. tepidum* (PDB code: 3ENI)

Pigments	Torsion angles			
	I	II	III	IV
BChl a_P 1	179.6	176.9	114.2	156.8
BChl a_P 2	178.5	136.8	108.9	156.3
BChl a_P 3	178.1	122.9/98.2	178.3/101.4	168.5
BChl a_P 4	178.6	165.1	179.2	166.8
BChl a_P 5	177.8	126.8	177.9	170.8
BChl a_P 6	178.7	106.6	170.1	172.5
BChl a_P 7	179.1	99.4	132.9/129.7	164.4

In FMO structure 3ENI, the torsion angles of BChl a_P at regions I and IV are very close to 180° of which region I is originally a double bond. The change of BChl a_P to BChl a_{GG} will mainly have effects at regions II and III. BChl a_P 4 seems to be less affected at these regions compared to others. The tails of certain pigment show two conformations in this refined structure. The torsion angles in both conformations are listed.

* note: There are some variations in the conformation of tails in the two structures of the same FMO protein, which is probably coming from different structure refinement methods the authors adopted.

2-3) FMO from *P. aestuarii* (PDB code: 3EOJ)

Pigments	Torsion angles			
	I	II	III	IV
BChl a_p 1	179.6	174.5	112.7	153/154
BChl a_p 2	173.2	175.9	176	177.3
BChl a_p 3	176	140/114.9	109.3/168.1	172.3/160.3
BChl a_p 4	179.3	159	176.2	175.3
BChl a_p 5	179.2	120.4	159.2	173.6
BChl a_p 6	179	107	171.7	144.1
BChl a_p 7	179	168	109.6/108	164.7/161.5

The torsion angles of BChl a_p at regions I to IV in the FMO structure (PDB code: 3EOJ) from *P. aestuarii* were also listed as a comparison.

a binding sites and the assembly of these two proteins. Although at the gene expression level, it seems the *csmA* gene is not regulated and the *pscA* gene is slightly up-regulated in the mutant, it would be important in the future to see whether there is any regulation at the active protein complex level as is the case for the FMO protein.

There have been several studies that also indicate that the type of esterifying alcohol is an important component for the synthesis of a fully functional photosystem (48, 50, 51, 55). For example, it was observed that the amount of mature LH2, LH1 and RC complexes in both *Rhodobacter sphaeroides* (48) and *Rhodobacter capsulatus* (50) were severely reduced after replacing the tail of BChl *a* from phytol to geranylgeranyl. In an extreme situation, if the tail esterifying step was blocked, no such complexes were assembled and the cells lost the ability to do photosynthesis (50). The biological significance of the ester groups of the 17-propionate substituent was recently reviewed by Tamiaki *et al* (55).

2. Optical properties and thermal stability

When the favorable BChl *a_P* is not available, the FMO protein will incorporate the more rigid BChl *a_{GG}*, albeit less efficiently. First, this directly results in a partial failure of the protein assembly as discussed above. Second, the conformation of the BChl *a_{GG}* in the assembled FMO mutant is more heterogeneously distributed, which broadens the spectral peak inhomogeneously. This was demonstrated by both the absorption and fluorescence spectra at RT and 77 K (Figs. 5 and 6). Interestingly, the only excitonic state that can be resolved at 77 K is that represented by the 826 nm peak, which is the excitation trap. As discussed above, the conformation of BChl *a* #4, which partially contributed to the lowest

excitonic state (26, 27) seems to be unchanged. Third, although there are some FMO proteins successfully assembled, they are less thermally stable than the wild type (Fig. 10).

Because the tail is not part of the conjugated electron system of the tetrapyrrole, it is commonly accepted to be neutral and optical silent (55, 56). The difference of the spectra of the wild type and mutant FMOs is probably due to an altered packing of the BChl to release the torsion restriction, resulting in changes in the interactions between BChl and other components of the FMO protein.

3. Membrane topology

The smaller number of mature FMO complexes in the BchP mutant cells results in a significant change in the stoichiometry of chlorosome to FMO, which might give some indication of the topology of chlorosome and FMO on the membrane. The purified chlorosomes from both the wild type and mutant cells show a similar size as checked by sucrose density gradients. If all the FMO proteins are covered by the chlorosomes in vivo, the density of FMO on the cytoplasmic membrane in the BchP cells should be smaller than that of the wild type. It will be interesting to compare the binding affinity of the chlorosome to the cytoplasmic membrane and the stoichiometry of CsmA to FMO in the *C. tepidum* wild and BchP mutant cells. However, if the density of FMO under the chlorosome is the same, the smaller amount of FMO protein in the mutant cells must mean that there are FMO proteins that are not covered by the chlorosome, at least in the wild type cells. It has been widely discussed in the past in terms of how many FMO per

RC are present in the wild type RC (57, 58), with the numbers ranging from 5-6 to only one FMO tightly bound to the RC. The BchP mutant may be a good comparison system to re-investigate this question in the future.

In conclusion, the success to generate the first FMO mutant by replacing the phytol tail of BChl *a* to geranylgeranyl allows us to examine the assembly of the FMO protein. Although the FMO protein could still be assembled, the amount is much less in the mutant cells, which raises interesting questions of the topology of FMO on the cell membrane. The assembled FMO mutant shows generally similar optical properties as the wild type, but the conformations of the pigments are more heterogeneously distributed due to the rigidity of more double bonds, as seen in the spectral broadening. An atomic resolution structure of the FMO_BchP will be extremely helpful to understand the structural and functional differences from that of the wild type FMO.

Experimental procedures

***C. tepidum* mutagenesis, culture conditions and FMO purification**

The *C. tepidum* *bchP* deletion mutant conferring resistance to gentamycin was generated according to Harada *et al* (45). Both the wild type and mutant cells were grown in sealed carboys under $150 \mu\text{E m}^{-2}\text{s}^{-1}$ light intensity at 35 °C for two days. For the BchP mutant, 5 μM of gentamycin was added to the growth media. Thirty grams of wet cells of *C. tepidum* wild type and BchP mutant respectively, were used for the FMO purification following the method described by Wen *et al* (10). The cells were broken by ultrasonication and the cytoplasmic membranes were enriched by ultracentrifugation. Both

membranes were suspended into 150 ml of 20 mM Tris/HCl buffer (pH = 8.0), which gave $OD_{745\text{nm}} \sim 150 \text{ cm}^{-1}$. The FMO protein was released from the re-suspended membrane by incubation with 0.2 M Na_2CO_3 for 24 hr and 0.4 M Na_2CO_3 for another 24 hr. The released FMO protein was collected in the supernatant after ultracentrifugation. The optical density (OD) at 808 nm of the supernatant from the wild type and mutant cells were 1.6 and 0.3, respectively. The protein was further purified by a combination of ion exchange and gel filtration columns until $OD_{267\text{nm}}/OD_{371\text{nm}} < 0.6$.

Pigment analysis by HPLC

The pigment from purified FMO protein was extracted by methanol and applied to an Agilent series 1100C high-performance liquid chromatography (HPLC) system with an XDB C18 reversed-phase column (4.6 by 250 mm; pore size: 100 Å; Agilent Technologies). Pigments were eluted by 100% methanol with a flow rate of 1 ml/min for 25 min. The photodiode-array detector was set to detect 770 nm, 670 nm, 490 nm and 280 nm. Pigments eluted by HPLC were collected for further mass analysis.

Pigment analysis by MALDI-TOF

The pigment fractions collected after HPLC were dried by speed vac (Millipore, USA) and re-suspended into methanol to OD at 777 nm = 5. 1 μL of pigment solution was mixed with 1 μL of matrix (10 mg/ml 2',4',6'-trihydroxyacetophenone monohydrate in 50% $\text{CH}_3\text{CN}/\text{H}_2\text{O}$, 0.1% trifluoroacetic acid) by vortexing and 0.3 μL was spotted on an ABI-192-AB stainless steel plate. The samples were analyzed using MALDI-TOF (Applied Biosystems 4700 proteomics analyzer) instrument under reflection positive

acquisition and processing modes. Each spectrum was averaged by summing 40 sub-spectra with 50 laser shots/sub-spectrum. The laser intensity was 3800 arbitrary units (AU). For the MS/MS experiment, a precursor ion was selected with a molecular weight (MW) ± 2 window, and reflection positive MS/MS acquisition and processing modes were used. The laser intensity was increased to 6700 AU. Collision induced dissociation was used to fragment the precursor ions. The expansion chamber pressure was maintained at 570 Torr during the MS/MS analysis.

Steady-state optical spectra

Absorption spectra were recorded with a Lambda 950 UV/VIS spectrophotometer (Perkin Elmer, USA). Fluorescence emission spectra were taken using a Photon Technology International fluorometer at 4 nm spectral bandwidth with an avalanche photodiode detector (Model 27, Advanced Photonics Inc., USA). The excitation wavelength was 370 nm with a 350–540 nm pass-through filter. A 1 cm path-length cuvette was used, and the absorption of the samples at 807 nm was OD = 0.1. CD spectra were recorded on a Jasco J-815 CD spectrometer using a 0.1 cm path-length quartz cell and averaged over eight scans for each sample with a scan speed of 50 nm/min and bandwidth of 1 nm. The protein solution was diluted into 70% glycerol and cooled to 77 K using a temperature-controlled cryostat (OptistatDN, Oxford Instruments, UK) for low temperature measurements.

Fluorescence lifetimes

The excited state lifetime of the FMO protein was measured by time-correlated single

photon counting. A mode-locked Ti:sapphire laser (Tsunami, Spectra-Physics) pumped by a frequency-doubled Nd:YVO₄ laser (Millenia Xs, Spectra Physics) was used to generate 740 nm light pulses. The Ti:sapphire laser was operated at a repetition rate of 81 MHz with a pulse width of <120 fs (full width at half maximum, FWHM). The repetition rate was controlled using a pulse picker (3980, Spectra Physics). A frequency doubler was used to generate the excitation light pulses at 370 nm. The applied excitation power at 800 KHz for all the measurements was 2.2 μ W corresponding to excitation densities of 1×10^8 - 1×10^9 photons/(pulse \cdot cm²) which was chosen after testing a range of intensities to make certain no excitation annihilation effects were present. The fluorescence signal was collected in a 90°-geometry after passing through a monochromator, and arrival times were stored in 4096 channels of a multichannel photomultiplier analyzer. The excitation light had a bandwidth of 12 nm and the emission bandwidth was 6 nm. The instrument response function (IRF, 35 ps FWHM) for the entire TCSPC setup was recorded by measuring the scattered light from a piece of metal placed in the sample chamber. Fluorescence decay curves were fitted to a sum of exponentials, convoluted with the instrument response function using Origin or Asufit. The quality of a fit was judged from the χ^2 -value and by visual inspection of the residuals. The number of exponentials was considered sufficient if the addition of one extra decay component did not significantly improve the fit.

Thermal stability

The thermal stability of the FMO protein and the mutant was investigated by monitoring the decrease of the Q_y peak after increasing the temperature. Temperature was controlled

using the Peltier 1+1 temperature controlling accessory (PerkinElmer, USA), which controls and monitors two electronically thermostatted cells placed in the sample compartment of the spectrophotometer. The temperature was raised from 5 °C to 90 °C in increments of 5 °C. The sample was equilibrated at the desired temperature for 5 min before measurement. The temperature stability was ± 0.2 °C. The protein was dissolved in 20 mM Tris buffer with 0.1 M NaCl and was gently stirred.

RNA purification and quantitative real-time PCR (qRT-PCR).

C. tepidum wild and mutant cells were harvested after 2 days growth under the same conditions. The RNA purification and qRT-PCR were done following Tang *et al* (47). In brief, RNA was isolated from the cell pellets using TRIzol reagent (Invitrogen) and possible DNA contamination was further removed by DNase treatment. Three independent RNA samples were prepared with A_{260}/A_{280} ratio > 2 . cDNA was synthesized from 1 μ g RNA and 100 μ M random 9-mer DNA using Superscript III reverse transcriptase (Invitrogen). The qRT-PCRs were performed via the ABI 7500 real-time PCR system. The primers for qRT-PCRs (shown in Table 3) were designed using the Primer Express 2.0 software program (Applied Biosystems) and analyzed by the OligoAnalyzer 3.0 program (Integrated DNA Technologies). An initial denaturation step (15 min at 95 °C), followed by 40 amplification cycles (15 s at 95 °C, 30 s at 60 °C, and 45 s at 72 °C) and then 1 dissociation cycle (15 s at 95 °C, 1 min at 60 °C, and then 15 s at 95 °C) were applied for the PCR using Power SYBR green master mix (Applied Biosystems). In the data analysis, the threshold cycle (C_T) was calculated as the cycle number at which ΔRn (the magnitude of the fluorescence intensity generated by the given

set of PCRs) crossed the baseline. Data were normalized by calculating $\Delta C_T = C_T$ of the target gene – C_T of the housekeeping gene (16S rRNA). Each experiment was repeated three times for validation, and the mean value was reported (Table 1).

Table 3. Primers used for the qRT-PCR studies

Gene	Forward primers (5' – 3')	Reverse primers (5' – 3')
<i>16S rRNA</i>	GGGTGAGTAAGGCATAGGTAATCTG	CGCTGCATCATCTGGTATTGTC
<i>csmA</i>	CCAGTGACCTTCGACCATAACC	GAGGCGTCTTTACCGACATTTT
<i>csmD</i>	TGACAAATTCAGCCGTTTCG	CGATCCGATAGCGTTTGTGA
<i>pscA</i>	TCCGTTTCGCTGAAACAGAAA	CGGAGCATCGGTCATTAAAGA
<i>Fmo</i>	CGTGCCCAACCCGATCTAC	GCGGAACTTTCATGAGGATGTC

References

1. Ganapathy S, Oostergetel GT, Wawrzyniak PK, Reus M, Gomez Maqueo Chew A, Buda F, Boekema EJ, Bryant DA, Holzwarth AR, de Groot HJ (2009) Alternating syn-anti bacteriochlorophylls form concentric helical nanotubes in chlorosomes. *Proc Natl Acad Sci USA* 106, 8525-8530.
2. Frigaard NU, Li H, Milks KJ, Bryant DA (2002) Nine mutants of *Chlorobium tepidum* each unable to synthesize a different chlorosome protein still assemble functional chlorosomes. *J Bacteriol* 186, 646-653.
3. Oostergetel GT, van Amerongen H, Boekema EJ. (2010) The chlorosome: a prototype for efficient light harvesting in photosynthesis. *Photosynth Res*. DOI 10.1007/s11120-010-9533-0
4. Saga Y, Shibata Y, Tamiaki H (2010) Spectral properties of single light-harvesting complexes in bacterial photosynthesis. *J. Photochem. Photobiol., C* 11, 15-24
5. Pedersen MO, Linnanto J, Frigaard NU, Nielsen NC, Miller M. (2010) A model of the protein-pigment baseplate complex in chlorosomes of photosynthetic green bacteria. *Photosynth Res* DOI 10.1007/s11120-009-9519-y
6. Pedersen MØ, Underhaug J, Dittmer J, Miller M, Nielsen NC (2008) The three-dimensional structure of CsmA: a small antenna protein from the green sulfur bacterium *Chlorobium tepidum*. *FEBS Lett* 582, 2869-2874.
7. Montañó GA, Wu HM, Lin S, Brune DC, Blankenship RE (2003) Isolation and characterization of the B798 light-harvesting baseplate from the chlorosomes of *Chloroflexus aurantiacus*. *Biochemistry* 42, 10246-51.
8. Olson JM (2004) The FMO protein. *Photosynth Res* 80, 181-187.
9. Hauska G, Schoedl T, Remigy H, Tsiotis G (2001) The reaction center of green sulfur bacteria. *Biochim Biophys Acta* 1507, 260-277
10. Wen J, Zhang H, Gross ML, Blankenship RE (2009) Membrane orientation of the FMO antenna protein from *Chlorobaculum tepidum* as determined by mass spectrometry-based footprinting. *Proc Natl Acad Sci USA* 106, 6134–6139
11. Adolphs J, Renger T (2006) How proteins trigger excitation energy transfer in the FMO Complex of Green Sulfur Bacteria. *Biophys J* 91, 2778-2797

12. Olson J, Romano C (1962) A new chlorophyll from green bacteria. *Biochim Biophys Acta* 59, 726–728
13. Fenna RE, Matthews BW (1975) Chlorophyll arrangement in a bacteriochlorophyll protein from *Chlorobium limicola*. *Nature* 258, 573-577.
14. Tronrud DE, Schmid MF, Matthews BW (1986) Structure and x-ray amino acid sequence of a bacteriochlorophyll *a* protein from *Prosthecochloris aestuarii* refined at 1.9 Å resolution. *J Mol Biol* 188, 443-454.
15. Tronrud DE, Wen J, Gay L, Blankenship RE (2009) The structural basis for the difference in absorbance spectra for the FMO antenna protein from various green sulfur bacteria. *Photosynth Res* 100, 79-87.
16. Li YF, Zhou W, Blankenship RE, Allen JP (1997) Crystal structure of the bacteriochlorophyll *a* protein from *Chlorobium tepidum*. *J Mol Biol* 271, 456-471.
17. Ben-Shem A, Frolow F, Nelson N (2004) Evolution of photosystem I - from symmetry through pseudo-symmetry to asymmetry. *FEBS Lett* 564, 274-280.
18. Camara-Artigas A, Blankenship RE, Allen JP (2003) The structure of the FMO protein from *Chlorobium tepidum* at 2.2Å resolution. *Photosynth Res* 75, 49-55
19. Alexander B, Andersen JH, Cox RP, Imhoff JF (2002) Phylogeny of green sulfur bacteria on the basis of gene sequences of 16S rRNA and of the Fenna-Matthews-Olson protein. *Arch.Microbiol.* 178, 131-140.
20. Imhoff JF (2003) Phylogenetic taxonomy of the family Chlorobiaceae on the basis of 16S rRNA and *fmo* (Fenna-Matthews-Olson protein) gene sequences. *Int. J. Syst. Evol. Micro.* 53, 941- 951.
21. Bryant DA, Costas AM, Maresca JA, Chew AG, Klatt CG, Bateson MM, Tallon LJ, Hostetler J, Nelson WC, Heidelberg JF, Ward DM (2007) *Candidatus Chloracidobacterium thermophilum*: an aerobic phototrophic Acidobacterium. *Science* 317, 523-526.
22. Tsukatani Y, Wen J, Blankenship RE, and Bryant DA (2010) Characterization of the FMO protein from the aerobic chlorophototroph, *Candidatus Chloracidobacterium thermophilum*. *Photosyn Res* DOI 10.1007/s11120-009-9517-0
23. Cheng YC, Fleming GR (2009) Dynamics of Light Harvesting in Photosynthesis. *Ann. Rev. Phys.Chem.* 60, 241-262.

24. Milder MTW, Brüggemann B, van Grondelle R, Herek JL (2010) Revisiting the optical properties of the FMO protein. *Photosyn Res* DOI 0.1007/s11120-010-9540-1
25. Renger T (2009) Theory of excitation energy transfer: from structure to function. *Photosynth Res* 102, 471–485
26. Blankenship RE, Matsuura K (2003) Antenna complexes from green photosynthetic bacteria. In: *Light-Harvesting Antenna in photosynthesis* (Green BR, Parson WW eds). pp 195-217, Kluwer Academic Publishers, Dordrecht, The Netherlands,.
27. Johnson S, Small G (1991) Excited-state structure and energy-transfer dynamics of the bacteriochlorophyll *a* antenna complex from *Prosthecochloris aestuarii*. *J Phys Chem* 95, 471–479
28. Pearlstein R (1992) Theory of the optical spectra of the bacteriochlorophyll *a* antenna protein trimer from *Prosthecochloris aestuarii*. *Photosynth Res* 31, 213–226
29. Müh F, Madjet Mel-A, Adolphs J, Abdurahman A, Rabenstein B, Ishikita H, Knapp EW, Renger T. (2007) α -Helices direct excitation energy flow in the Fenna-Matthews-Olson protein. *Proc Natl Acad Sci USA* 104, 16862-16867
30. Brixner T, Stenger J, Vaswani HM, Cho M, Blankenship RE, Fleming GR (2005) Two-dimensional spectroscopy of electronic couplings in photosynthesis. *Nature* 434, 625-628.
31. Read EL, Schlau-Cohen GS, Engel GS, Wen J, Blankenship RE, Fleming GR (2008) Visualization of Excitonic Structure in the Fenna-Matthews-Olson Photosynthetic Complex by Polarization-Dependent Two-Dimensional Electronic Spectroscopy. *Biophys J*. 95, 847-856.
32. Cho M, Brixner T, Stiopkin I, Vaswani H, Fleming GR (2006) Two Dimensional Electronic Spectroscopy of Molecular Complexes. *J. Chin Chem Soc* 53, 15-24.
33. Engel GS, Calhoun TR, Read EL, Ahn TK, Mančal T, Cheng YC, Blankenship RE, Fleming GR (2007) Evidence for wavelike energy transfer through quantum coherence in photosynthetic systems. *Nature* 446, 782–786.
34. Ishizaki A, Fleming GR (2009) Theoretical examination of quantum coherence in a photosynthetic system at physiological temperature. *Proc. Natl. Acad. Sci. USA* 106, 17255-17260.

35. Panitchayangkoon G, Hayes G, Fransted KA, Caram JR, Harel E, Wen J, Blankenship RE, Engel GS (2010) Long-lived quantum coherence in photosynthetic complexes at physiological temperature. arXiv:1001.5108v1
36. Collini E, Wong CY, Wilk KE, Curmi PMG, Brumer P, Scholes GD (2010) Coherently wired light-harvesting in photosynthetic marine algae at ambient temperature. *Nature* 463, 644-648
37. Mohseni M, Rebentrost P, Lloyd S, Aspuru-Guzik A (2008) Environment-assisted quantum walks in energy transfer of photosynthetic complexes. *J Chem Phys* 129, 174106.
38. Beljonne D, Curutchet C, Scholes GD, Silbey RJ (2009) Beyond Forster Resonance Energy Transfer in Biological and Nanoscale Systems. *J. Phys. Chem. B* 113, 6583-6599.
39. Palmieri B, Abramavicius D, Mukamel S (2010) Interplay of slow bath fluctuations and energy transfer in 2D spectroscopy of the FMO light-harvesting complex: benchmarking of simulation protocols. *Phys. Chem. Chem. Phys.* 12, 108-114.
40. Rebentrost P, Mohseni M, Aspuru-Guzik A (2009) Role of Quantum Coherence and Environmental Fluctuations in Chromophoric Energy Transport. *J. Phys. Chem. B* 113, 9942–9947
41. Eisen JA, Nelson KE, Paulsen IT, Heidelberg JF, Wu M, Dodson RJ, Deboy R, Gwinn ML, Nelson WC, Haft DH, Hickey EK, Peterson JD, Durkin AS, Kolonay JL, Yang F, Holt I, Umayam LA, Mason T, Brenner M, Shea TP, Parksey D, Nierman WC, Feldblyum TV, Hansen CL, Craven MB, Radune D, Vamathevan J, Khouri H, White O, Gruber TM, Ketchum KA, Venter JC, Tettelin H, Bryant DA, Fraser CM (2002) The complete genome sequence of *Chlorobium tepidum* TLS, a photosynthetic, anaerobic, green-sulfur bacterium. *Proc Natl Acad Sci USA* 99, 9509-9514.
42. Frigaard NU, Chew AGM, Li H, Maresca JA, Bryant DA (2003) *Chlorobium tepidum*: insights into the structure, physiology and metabolism of a green sulfur bacterium derived from the complete genome sequence. *Photosynth Res* 78, 93-117.
43. Wahlund TM, Madigan MT (1995) Genetic transfer by conjugation in the thermophilic green sulfur bacterium *Chlorobium tepidum*. *J Bacteriol* 177, 2583-2588.

44. Frigaard NU, Bryant D (2004) Seeing green bacteria in a new light: genomics-enabled studies of the photosynthetic apparatus in green sulfur bacteria and filamentous anoxygenic phototrophic bacteria. *Arch Microbiol* 182, 265-276.
45. Harada J, Miyago S, Mizoguchi T, Azai C, Inoue K, Tamiaki H (2008) Accumulation of chlorophyllous pigments esterified with the geranylgeranyl group and photosynthetic competence in the CT2256-deleted mutant of the green sulfur bacterium *Chlorobium tepidum*. *Photochem. Photobiol. Sci.* 7, 1179-1187.
46. Chew AGM, Frigaard NU, Bryant DA (2008) Identification of the *bchP* gene, encoding geranylgeranyl reductase in *Chlorobaculum tepidum*. *J. Bacteriol.* 190, 747-749.
47. Tang K-H, Wen J, Li X and Blankenship RE (2009) The role of the AcsF protein in *Chloroflexus aurantiacus*. *J. Bacteriol.* 191, 3580-3587.
48. Addlesee HA, Hunter CN (1999) Physical mapping and functional assignment of the geranylgeranyl-bacteriochlorophyll reductase gene, *bchP*, of *Rhodobacter sphaeroides*. *J. Bacteriol.* 181, 7248-7255
49. Mizoguchi T, Harada J, Tamiaki H. (2006) Structural determination of dihydro- and tetrahydrogeranylgeranyl groups at the 17-propionate of bacteriochlorophylls-a. *FEBS Lett.* 580, 6644-6648.
50. Bollivar DW, Wang S, Allen JP, Bauer CE. (1994) Molecular genetic analysis of terminal steps in bacteriochlorophyll *a* biosynthesis: characterization of a *Rhodobacter capsulatus* strain that synthesizes geranylgeraniol-esterified bacteriochlorophyll *a*. *Biochemistry* 33, 12763-12768.
51. Addlesee HA, Hunter CN. (2002) *Rhodospirillum rubrum* possesses a variant of the *bchP* gene, encoding geranylgeranyl-bacteriopheophytin reductase. *J Bacteriol.* 184, 1578-86.
52. Freiberg A, Lin S, Timpmann K, Blankenship RE (1997) Exciton dynamics in FMO bacteriochlorophyll protein at low temperatures. *J. Phys. Chem. B* 101, 7211-7220
53. Zhou W, LoBrutto R, Lin S, Blankenship RE (1994) Redox effects on the bacteriochlorophyll *a*-containing Fenna-Matthews-Olson protein from *Chlorobium Cepadum*. *Photosyn Res* 41, 89-96

54. Rätsep M, Freiberg A (2007) Unusual temperature quenching of bacteriochlorophyll a fluorescence in FMO antenna protein trimers. *Chemical Physics Letters* 434, 306 – 311
55. Tamiaki H, Shibata R, Mizoguchi T. (2007) The 17-propionate function of (bacterio)chlorophylls: biological implication of their long esterifying chains in photosynthetic systems. *Photochem Photobiol.* 83, 152-162.
56. Fiedor L, Kania A, Myśliwa-Kurdziel B, Orzeł Ł, Stochel G. (2008) Understanding chlorophylls: central magnesium ion and phytyl as structural determinants. *Biochim Biophys Acta.* 1777, 1491-1500.
57. Francke C, Permentier HP, Franken EM, Neerken S, Amesz J (1997) Isolation and properties of photochemically active reaction center complexes from the green sulfur bacterium *Prosthecochloris aestuarii*. *Biochemistry* 36, 14167-14172.
58. Rémy HW, Stahlberg H, Fotiadis D, Müller SA, Wolpensinger B, Engel A, Hauska G, Tsiotis G (1999) The reaction center complex from the green sulfur bacterium *Chlorobium tepidum*: a structural analysis by scanning transmission electron microscopy. *J Mol Biol* 290, 851–858.

Chapter 4.

Membrane Orientation of the FMO Antenna Protein from
***Chlorobaculum tepidum* as Determined by Mass Spectrometry-Based**
Footprinting*

* *This chapter is based on the published work: Proc Natl Acad Sci U S A. 2009 106(15): 6134–6139.*

Abstract

The high excitation energy-transfer efficiency observed in photosynthetic organisms relies on the optimal pigment-protein binding geometry in the individual protein complexes and also on the overall architecture of photosystems. In green sulfur bacteria, the membrane-attached Fenna-Matthews-Olson (FMO) antenna protein functions as a “wire” to connect the large peripheral chlorosome antenna complex with the reaction center (RC), which is embedded in the cytoplasmic membrane (CM). Energy collected by the chlorosome is funneled through the FMO to the RC. Although there has been considerable effort to understand the relationships between structure and function of the individual isolated complexes, the specific architecture for in-vivo interactions of the FMO protein, the CM, and the chlorosome, ensuring highly efficient energy transfer, is still not established experimentally. Here we describe a novel mass spectrometry- based method that probes solvent-exposed surfaces of the FMO by labeling solvent-exposed aspartic and glutamic acid residues. The locations and extents of labeling of FMO on the native membrane in comparison with it alone and on a chlorosome-depleted membrane afford an answer. The large differences in the modification of certain peptides show that the Bchl *a* #3 side of the FMO trimer interacts with the CM, which is consistent with recent theoretical predictions. Moreover, the results also provide direct experimental evidence to confirm the overall architecture of the photosystem from *Chlorobaculum tepidum* (*C. tepidum*) and give information on the packing of the FMO protein in its native environment.

Introduction

Photosynthesis is a fundamental biological process that harvests solar energy to power the life cycle on earth (1). A diverse family of pigment-protein complexes and elegant architectures accomplish the necessary light-harvesting and energy-storage processes (2-5). In photosynthetic green sulfur bacteria, light absorbed by a large antenna complex known as a chlorosome (6-8) is transferred through a protein named the Fenna-Matthews-Olson or FMO protein (9) to the reaction centers, which are embedded in the CM. Together, they form a funnel-like architecture to facilitate energy transfer. The specific orientation of the critical linker, the FMO protein, however is unknown (Fig. 1A).

The structure of the FMO protein was the first (bacterio)chlorophyll binding protein to be determined by X-ray crystallography. Structures of this protein from two species, *Prosthecochloris aestuarii* 2K (10, 11) and *C. tepidum* (12) are now available, and they show strong structural and spectral similarities. The FMO protein consists of three identical subunits of mass ~40 kDa related by a 3-fold axis of symmetry. The three monomers form a disc with a C₃ symmetry axis perpendicular to the disc plane (Fig. 1B). There are seven BChl *a* molecules in each monomer, although an eighth pigment has been resolved in newly solved structures (13, 14). Each pigment experiences a different local environment (Fig. 1C), and their site energies are fine-tuned by specific interactions with the protein. Bchl *a* #3 and Bchl *a* #1, for example, are on the opposite sides of the FMO protein from the side view of the FMO trimer (Fig. 1C).

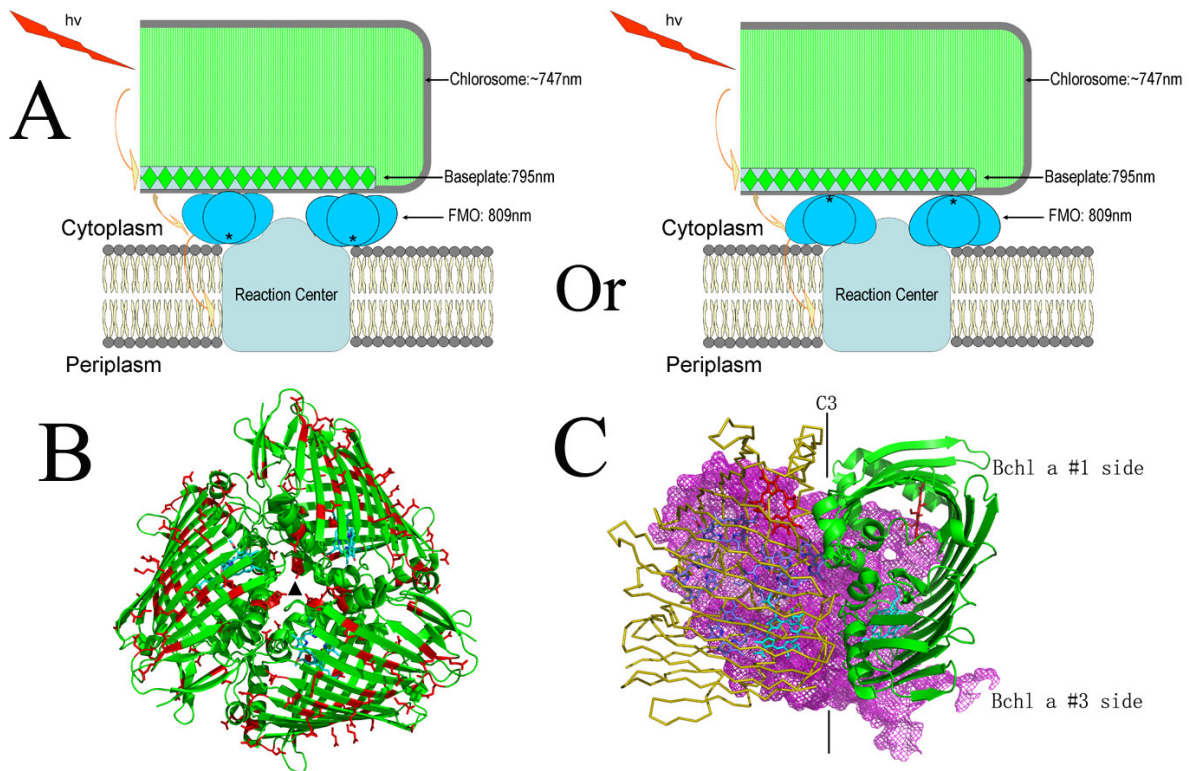


Fig. 1 Photosystem from *C. tepidum* and structure of FMO. A. Model architecture of photosystem from *C. tepidum*. The two possible orientations of FMO on the CM are presented. Bchl *a* #3 is shown as a star. B. Top view of the FMO trimer with the Bchl *a* #3 side shown. All the pigments are omitted except Bchl *a* #3 which is colored cyan. The side chains of all the D/E residues are highlighted as red sticks. In each FMO monomer, there are 21 D and 20 E residues plus a C-terminal carboxyl group. C. Side view of the FMO trimer shown as cartoon, ribbon and mesh for clarity. Positions of Bchl *a* #3 (cyan) and Bchl *a* #1 (red) are labeled in the monomer shown by cartoon. All the phytol tails of pigments are omitted for clarity.

Given that the FMO protein plays a critical role in the energy transfer pathway, significant effort has been made to understand its electronic structure. Quantum effects (15-20), which were recently clarified in this complex, may function to improve the energy-transfer efficiency. A defined energy-transfer pathway was also elucidated by both 2D electronic spectroscopy (21) and novel theoretical calculations (20). The pigment with the lowest site energy, the assignment of which was historically controversial (22-24), is predicted to be Bchl *a* #3 on the basis of coupling with the dipole of adjacent alpha helices (19). This energy-sink pigment is expected to be close to the CM to ensure efficient energy transfer from the FMO protein to the RC (20). Thus, this side of the FMO trimer (Bchl *a* #3 side) should be in close contact with the RC in the CM.

The opposite orientation, however, was predicted from the structure of the isolated protein. Hydrophobicity analysis of the FMO protein favors an interaction of the Bchl *a* #1 side of the protein with the CM (12), in accord with another suggestion based on the existence of an extra pigment (13). In this latter model, the resolved extra pigment forms an energy transfer bridge between the FMO and the RC.

The experimental evidence related to the orientation of the FMO comes from linear dichroism (25) and 3D reconstitution data based on STEM images (26). Both suggest that the FMO disc sits flat on the CM with its C3 symmetry axis perpendicular to the plane of the membrane. However, the specific orientation of the disc (i.e., which side interacts with the CM), which must have high impact on the efficiency of energy transfer, cannot be determined using these methods.

Moreover, the overall architecture, including the relative orientation and the extent of the interaction between the individual antenna complexes, to insure efficient energy transfer is also poorly understood. The interaction between the flat surface of the FMO trimer and the RC, shown by the STEM image (26), is not as strong as proposed on the basis of protein hydrophobicity, which suggests the FMO is probably partially buried in the CM (12). On the chlorosome side, the detailed interaction between the FMO and the CsmA protein is not clear, although surface plasmon resonance (27) and cross-linking data (28) suggest that FMO protein directly interacts with the CsmA protein and is probably partially buried in the CsmA layer (28). In short, a comprehensive interaction map at the molecular level of the various components, chlorosome, FMO and RC, is still needed.

We report here a method that combines carboxyl group modification with mass spectrometry to afford surface mapping or footprinting (29, 30) of the protein, revealing the interaction of proteins associated with membranes. We chose for mapping the reagent, glycine ethyl ester (GEE), which is used to label any solvent accessible carboxyl groups from glutamic acid (E), aspartic acid (D), or the C-terminus by zero-length crosslinking (28, 31-33). Although the use of labeling reagents for mapping and crosslinking are not new and liquid chromatography/tandem mass spectrometry (LC/MS/MS) is commonly used in complex proteomics, their combination, made highly specific with highly accurate mass measurements, is a new approach.

Three states of the protein were investigated for comparison: the isolated FMO protein, the protein attached to the CM but with chlorosomes removed, and the protein in the

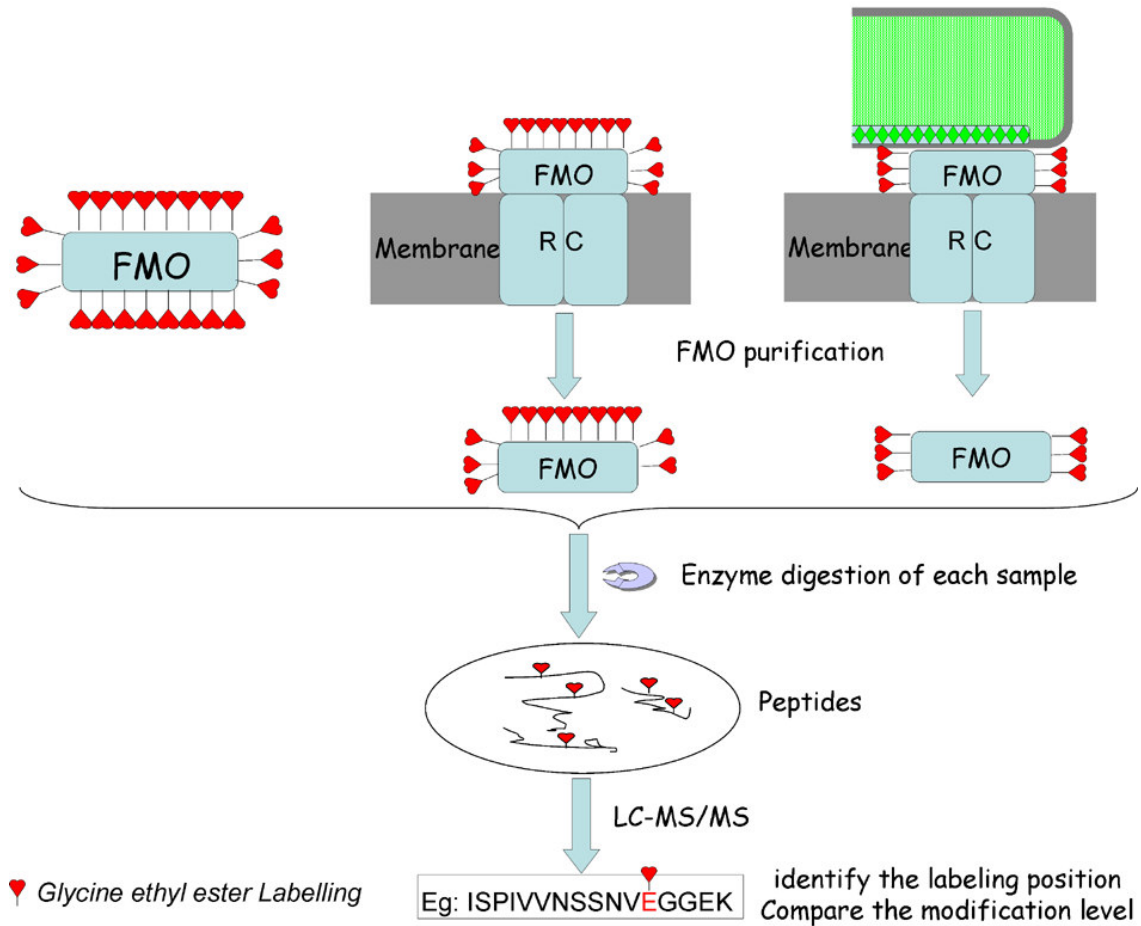


Fig. 2 Schematic experimental design and procedure. The solvent-exposed surface of isolated FMO protein, FMO from chlorosome-depleted membrane and FMO from native membrane was probed by a small molecule, which can be covalently attached to certain residues. The labeling sites were determined by MS after protein purification and enzyme digestion. The modification level of different peptides was compared to determine the interaction interface.

native membrane (i.e., with chlorosomes attached). The labeled sites on the FMO protein from these three samples were located by LC-MS/MS analysis of peptides produced by in-gel trypsin digestion of the protein following its isolation (Fig. 2). The modification levels of various peptides from the three samples, upon quantitative analysis on the basis of selected ion chromatograms (SIC) (34), show that the Bchl *a* #1 side of the FMO protein in the native membrane was modified to a lesser extent compared to that after the chlorosome was removed. When the FMO protein is attached to the CM, with or without chlorosomes, the modification levels of the Bchl *a* #3 side of the FMO protein were never as high as those for the free protein. Thus, it is the Bchl *a* #3 side of the protein that is in contact with the CM.

Results

Three samples were prepared and subjected to chemical modification: the isolated FMO protein as a control (Fig. 3A), the chlorosome-depleted membrane (Fig. 3B), and the native membrane (Fig. 3C). In the native membrane, the strong chlorosome absorption at 746 nm, 457 nm and 336 nm obscures the spectral features of the other components (Fig. 3C), and the Q_y absorption band of the FMO is just a shoulder. After chlorosome depletion by the chaotropic reagent NaI, the FMO protein is still attached to the CM and shows the characteristic absorption. Peaks from the RC (671 nm) and from carotenoids in the 400-500 nm region are recognizable in the absorption of chlorosome-depleted membranes (Fig. 3B). The isolated FMO protein showed identical absorption spectra before and after GEE modification (Fig. 3A), which indicated no significant conformational change after protein modification.

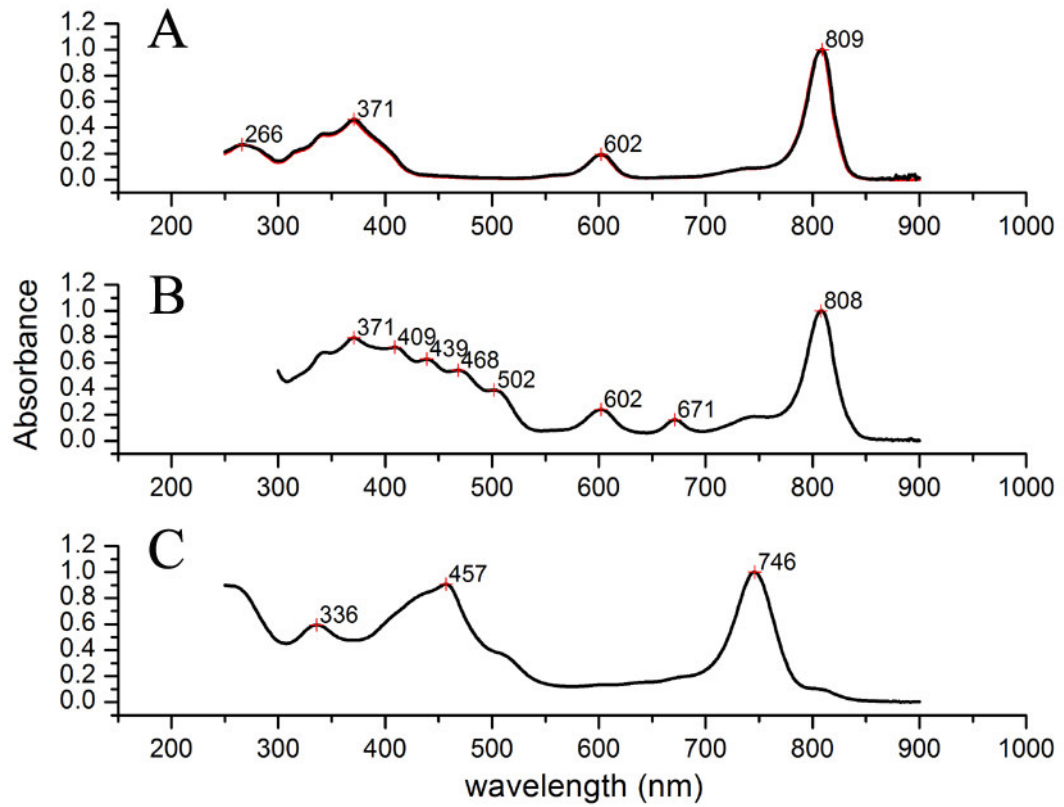


Fig. 3 Characteristic absorption spectra. A. Absorption spectra of purified FMO protein (red) and FMO protein after GEE modification (black). B. Chlorosome-depleted membrane. C. Native membrane from *C. tepidum*.

The modification of the D/E residues on the FMO protein by GEE was done under physiological conditions by using the zero-length crosslinker, 1-ethyl-3-(3-dimethylaminopropyl)carbodiimide hydrochloride (EDC). The mechanism of the modification is shown in Fig. 4. Once the three samples were modified, they were submitted to SDS-PAGE. Separate samples of the FMO protein, visualized in appropriate gel bands were in-gel digested, and the peptides were loaded to LC to identify and quantify the modification sites by MS/MS.

In the LC-MS analysis (an example is shown in Fig. 5), peptides and their modifications were identified by both accurate mass measurement (accuracy < 10 ppm) and tandem mass spectrometry (MS/MS, Fig. 6). The accurate mass is needed to add specificity for analysis of the complex mixtures that arise by protein digestion. The modification of one D/E site by GEE shifts the peptide mass +85.0528 Da (C_4H_7NO) (Fig. 5D). The added ester group also undergoes hydrolysis under either the basic conditions during protein purification or under the acidic conditions used for LC/MS, or both. After hydrolysis, the mass shift for a given one-site modified peptide changes to +57.0215Da (C_2H_3NO) (Fig. 5C). The hydrolysis conserves a carboxyl group, producing little conformational stress and maintaining the stabilization of the protein. The +57.0215 Da peptide generally eluted at approximately the same time as or a little earlier than the unmodified peptide, whereas the +85.0528 Da peptide always eluted approximately 1-3 min later than the unmodified peptide, consistent with its increased hydrophobicity. This unique pattern helps in the identification of the modified peptides (Fig. 11).

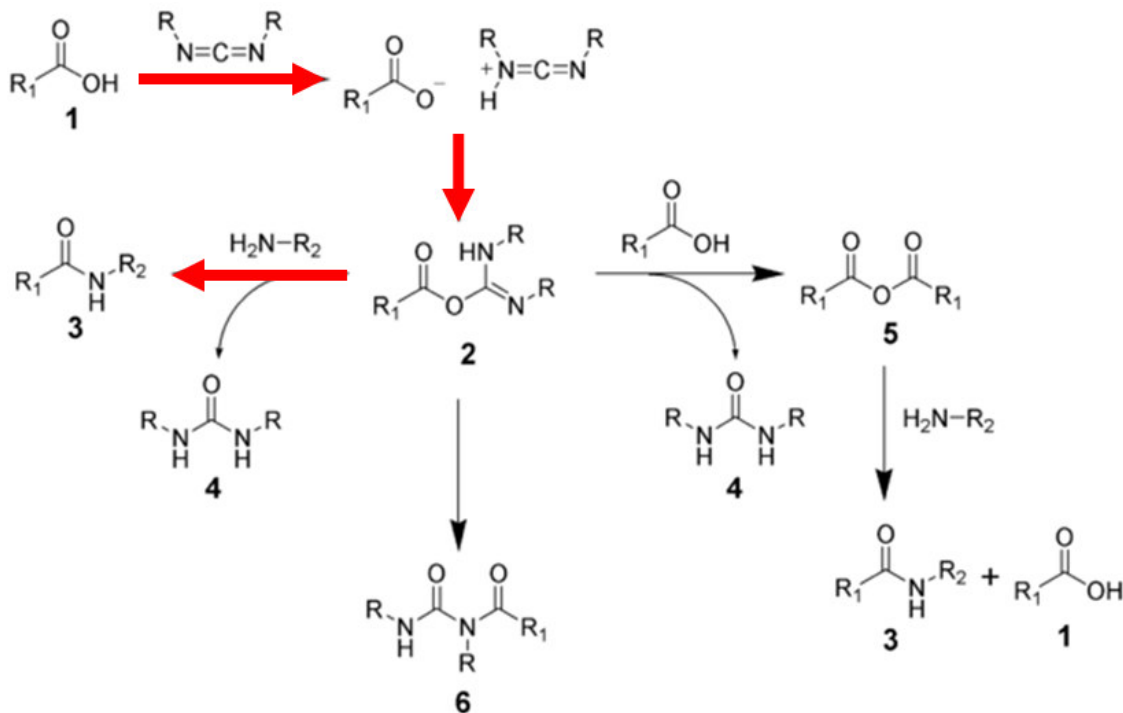


Fig. 4 Mechanism of protein carboxyl group modification by amine with the zero-length crosslinker EDC. A slightly acidic condition will protonate the nitrogen on the carbodiimide, which will activate the carbon to be stronger electrophile. The deprotonated carboxyl group attacks the activated carbon to form a new bond (compound 2), and the attached carbodiimide is a good leaving group. With free amine groups around (H₂N-R₂), a substitution reaction will happen and a stronger amide bond will form (compound 3). Side reactions might happen from compound 2. However, the main reaction will follow the red arrow in reality, since a large amount of free amine (glycine ethyl ester) was added to the solution. (Figure adapted from <http://en.wikipedia.org/wiki/Carbodiimide>)

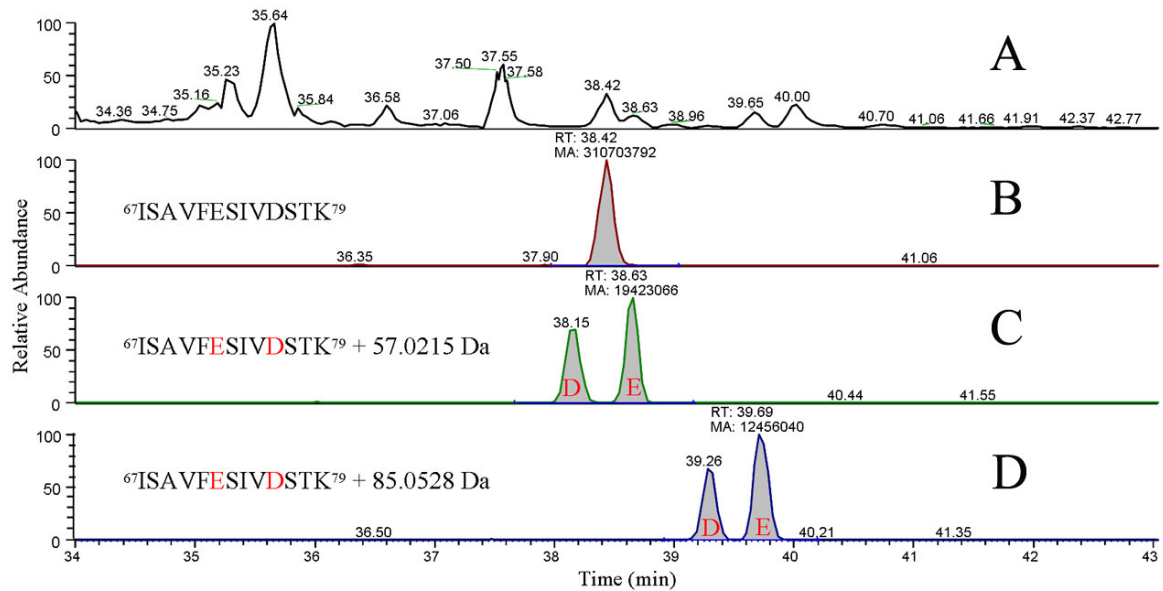


Fig. 5 Typical chromatograms from LC/MS showing a peptide and the peptide with D/E modifications. A. LC chromatogram of the trypsin-digested FMO protein. B. Selected ion chromatogram (SIC) of the unmodified peptide ($m/z = 698.3719$ Da). C. SIC of the peptide with D/E modification (+ 57.0215 Da). D. SIC of the peptide with D/E modification (+ 85.0528 Da). The D/E modification sites were determined by the product ions (Fig. 5). The retention times of the peptides and the areas of SIC were labeled, and the mass accuracy was better than 10 ppm.

Chapter 4

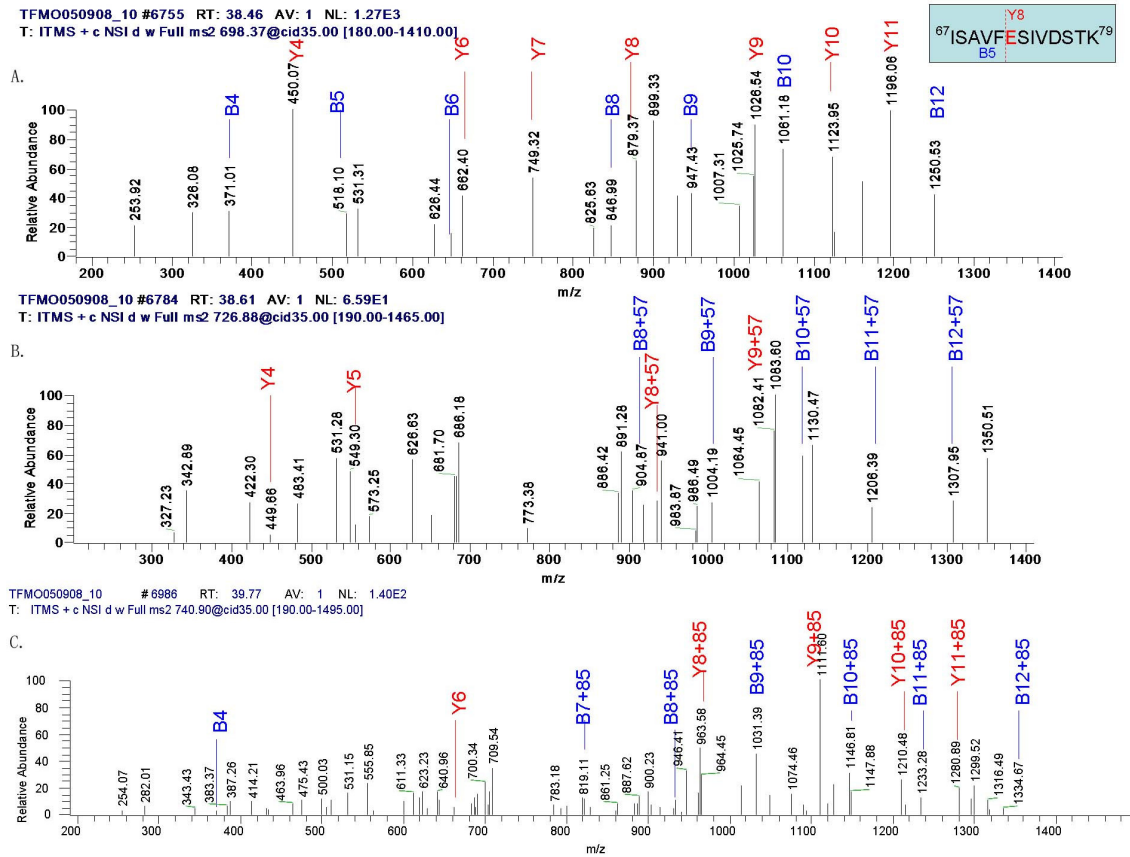


Fig. 6. Identification of the D/E modification sites by tandem mass (take peptide 67-79 as an example). A. Product ions of the unmodified peptide. B. Product ions of the peptide with E6 being modified (+ 57 Da). C. Product ions of the peptide with E6 being modified (+ 85 Da). B and Y ions are labeled.

Quantitative MS analysis was accomplished by obtaining selected ion chromatogram (SIC) of the trypsin-digested peptides. The modification level of a given peptide was

computed to be the ratio of the SIC of D/E modified peptides by the total ion chromatogram signals, which is the sum of ion currents of both modified and unmodified peptides. For example, the modification level of peptide 67-79 from the modified free protein, shown in Fig. 5, is equal to $(1.94 \times 10^7 + 1.24 \times 10^7) / (1.94 \times 10^7 + 1.24 \times 10^7 + 3.11 \times 10^8) \times 100\% = 9\% \pm 2\%$. The same peptides from the treated FMO protein in chlorosome-depleted membranes and in native membranes were analyzed separately. This peptide has two possible modification sites. Remarkably, the modification of either site was identified and they were well separated by the HPLC method we adopted. An SIC signal for the modification of both sites of the same peptide (mass increments of +114.0430 Da, +170.1056 Da or +142.0743 Da) could not be detected at a signal-to-noise ratio of 2:1. In general, the SIC signal corresponding to multiple modifications of any peptide containing two or more carboxyl side chains was at or below the noise level, and they were not considered further in the analysis (Fig. 7).

If there are no sites missed in the trypsin digestion, the FMO protein will be digested into 25 peptides that contain at least six amino acids. Five peptides (132-143, 216-222, 287-303, 325-331, and 340-347) do not have D/E residues, and they all were observed. Of the remaining twenty peptides, five peptides (169-181, 182-199, 225-238, 348-354 and 355-366) have D/E residues, but the D/E residues are located in the connection region utilized to form a trimer, and they are buried under the trimer surface. The signals from these unmodified peptides were identified, but no modifications could be observed. When the

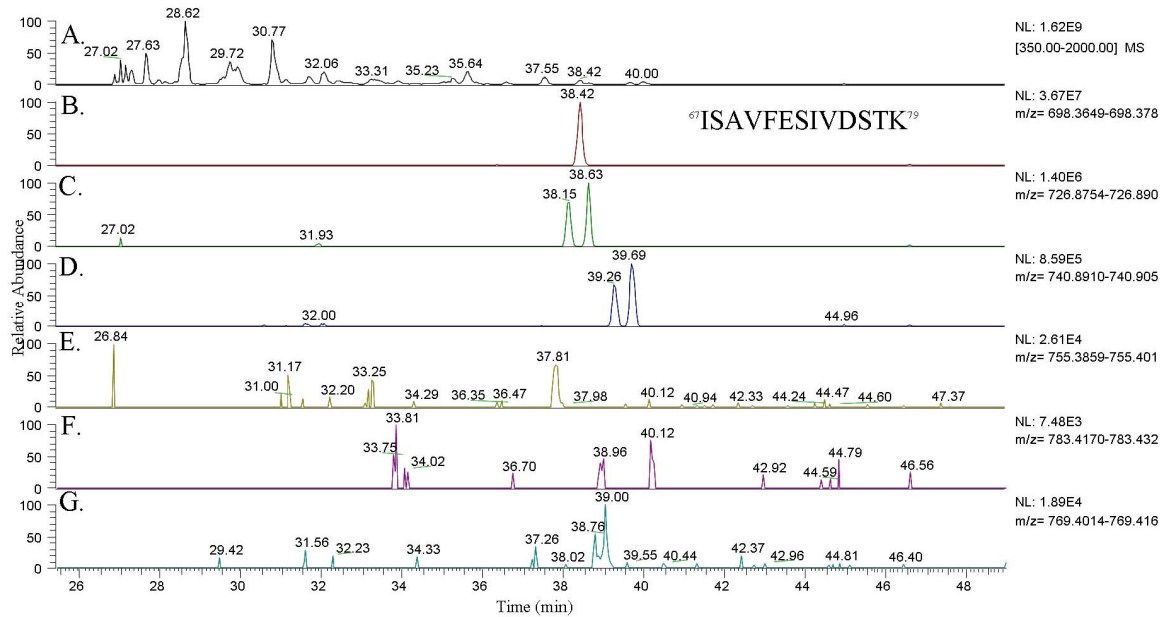


Fig. 7. Mass spectrometric analysis showing selected ion chromatograms for the unmodified peptide, the +57.0215 Da peptide, and the +85.0528 Da peptide. Signals from multiple modifications of certain peptides with more than one D/E modification site were generally noisy (e.g., peptide 67-79). A. LC chromatogram of the trypsin-digested FMO protein. B. Selected ion monitoring (SIM) of the unmodified peptide ($m/z = 698.3719$). C. SIM of the peptide with D/E modification (+ 57.0215 Da). D. SIM of the peptide with D/E modification (+ 85.0528 Da). E. SIM of the peptide with both D and E residues modified (+ 57.0215 x 2 Da). F. SIM of the peptide with both D and E residues modified (+ 85.0528 x 2 Da). G. SIM of the peptide with both D and E residues modified (+ 85.0528 + 57.0215 Da). The retention times of the peptides and the areas of SIC were labeled, and the mass accuracy was 10 ppm or better. Peptides with either D or E residues modified (panels C and D) show strong signals whereas the signals for peptides containing modifications of both D and E residues are in the noise level (panels E, F and G).

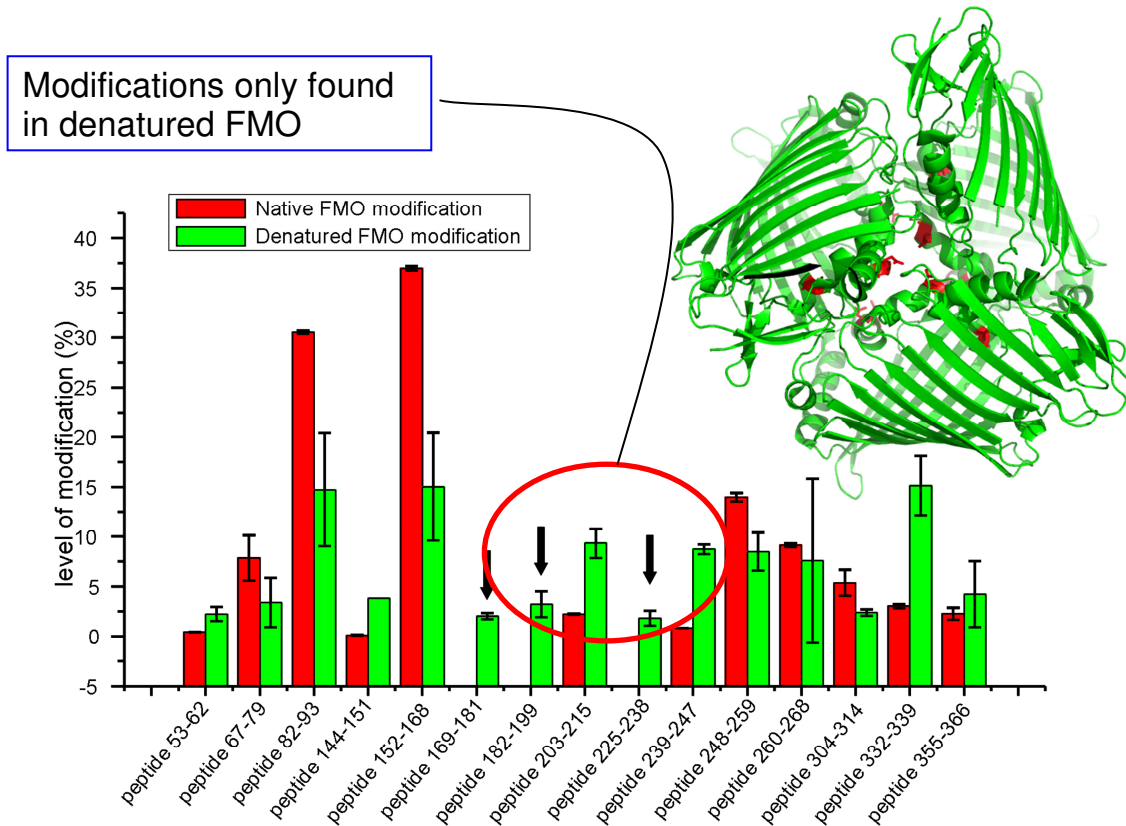


Fig. 8 Certain D/E residues can only be modified after the protein is denatured. Red bars: the identified D/E modified peptides of the native protein. Green bars: the identified D/E modified peptides of the denatured protein. Modification of the D/E residues on peptides 169-181, 182-199 and 225-238 are possible only when the FMO trimer is denatured. These D/E residues are located on the monomer connection region of the trimer, which are labeled in red in the inset protein structure. When the FMO protein is denatured, the modification level of each peptide is more or less similar, losing the signature of that of the native protein (for example, peptides 82-93 and 152-168 could be modified to much higher level in the native protein.)

FMO trimers were denatured, however, these sites could be easily modified (Fig. 8), indicating stable binding of the three monomers to form the trimer. Two long tryptic peptides (1-29 and 97-126) were not detected in the LC/MS experiment. The loss of large peptides is a common problem in in-gel trypsin digestion. Signals for peptides 82-93, 152-168 and 269-285 were barely above the noise level and only occasionally could be found; they also are not considered further.

All other tryptic peptides were detected in the three samples; they are classified and listed in three groups in Fig. 9. Peptides 36-52, 67-79 and 304-314 (group A) of the modified FMO protein purified from chlorosome-depleted membranes and from the native membranes were not modified as extensively as those from the GEE-modified free FMO protein (compare the red bar with the green and blue bars in Fig. 9A), indicating that the corresponding regions of the protein are clearly protected. The modification levels of these peptides, from FMO either in the chlorosome-depleted membrane or in the native membrane, are approximately identical whether or not the chlorosome is removed from the membrane. This indicates that protection comes from the membrane and not from the chlorosomes.

In contrast, several peptides, 53-62, 144-151, 203-215, 239-247 (group B), showed a statistically significant increase in modification after the chlorosome was removed from the CM (compare the green bars with the blue bars in Fig. 9C). In the native environment, the protein regions corresponding to these peptides are likely to be covered by the bulky chlorosomes, but they become available for labeling when the chlorosomes are not

present, regardless of the presence or absence of the membrane.

Higher modification levels of peptides (green bars in Fig. 9C) are seen when the chlorosome was removed and the membrane remains than when the protein is free (red bars in Fig. 9C). This is likely due to the dimerization of the free FMO protein under low ionic strength. Such dimers have been shown by Blue-native PAGE and analytical ultracentrifugation analysis of the FMO protein. Recently, H/D exchange of the FMO protein under different concentrations clearly shows that these peptides are self-protected in the high protein concentration condition. Thus, protection of peptides in group A by the membrane is apparent from the results.

There are also several peptides (Fig. 9E) that show no apparent trend as those seen for peptides in groups A and B. The modification levels of peptides 248-259 and 260-268 in the isolated FMO protein, for example, are the same as or slightly higher than those from FMO associated with the chlorosome-depleted membrane and with the native membrane. Both peptides are located in the middle and on the side of the FMO protein (highlighted in orange in Fig. 9F). They show slight protection when the membrane is present. Peptide 332-339 is modified to a somewhat higher level in FMO taken from the chlorosome-depleted membrane and from the native membrane than from the free protein. The D/E residues in this peptide are located in a flexible loop at the bottom region of the FMO disc and stick out of the protein body (blue colored in Fig. 9F). The local environment of these residues in the three different samples is expected to be similar; thus, this peptide may be an indicator of the amount of labeling reagents that can approach the FMO

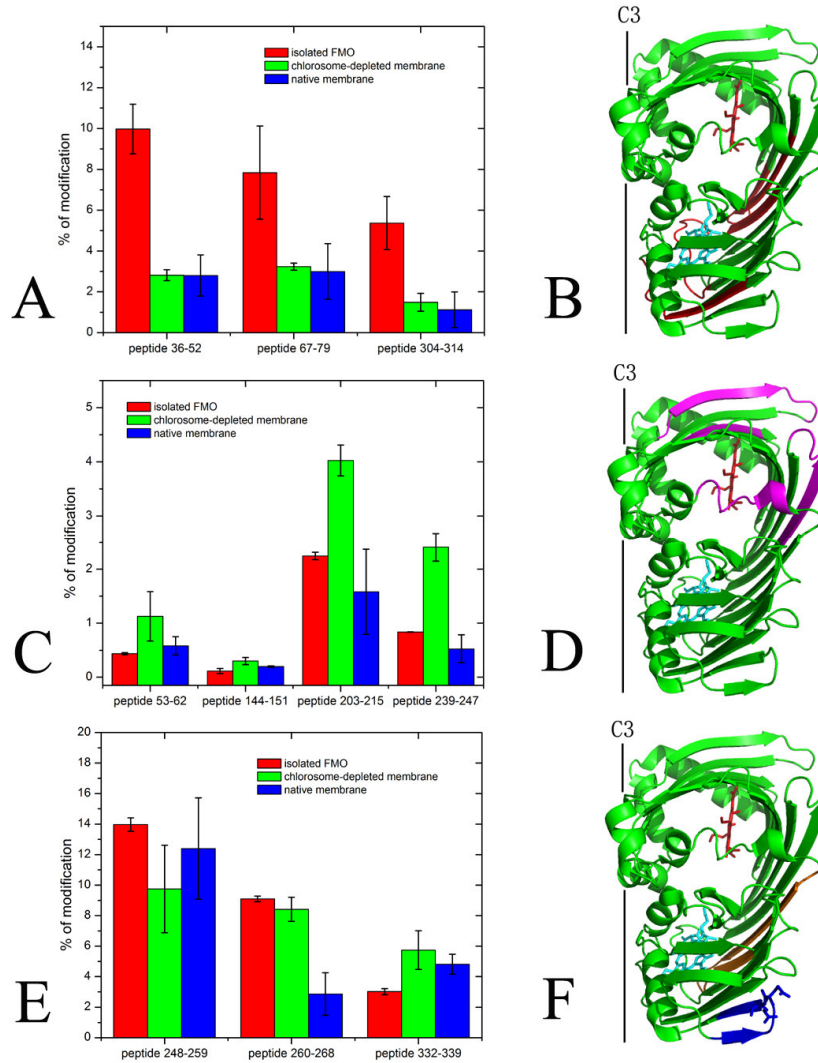


Fig. 9 Modification level of certain peptides and their location in the protein 3D structure. A. Identified cytoplasmic membrane-protected peptides of FMO (group A); B. Location of peptides in group A (highlighted in red); C. Identified chlorosome-protected peptides of FMO (group B); D. Location of peptides in group B (highlighted with purple); E. Peptides that are identified and showed an approximately similar modification level; F. Location of peptides 248-259 and 260-268 (highlighted in orange) and location of peptide 332-339 (highlighted in blue). In panels B, D and F, the side view of the FMO monomer is presented for clarity. Only Bchl *a* #3 (cyan) and Bchl *a* #1 (red) are labeled to show the orientation.

protein held in the chlorosome-depleted membrane and in the native membrane.

In the ESI MS analysis, some peptides show different charge-state distributions; furthermore, a small fraction of certain peptides undergo other modifications (e.g., methionine oxidation and N/Q deamidation). Larger peptides from a few missed cleavages can also be found. These complications can affect in a small way the calculation of modification levels, but they do not change the trends (Fig. 10, 11). In the analysis, we always chose the dominant fractions, considered only the unmodified peptide, the +57.0215 peptide, and the +85.0528 peptide, except for peptide 36-52 and peptide 144-151. For peptide 36-52, the dominant material is a C propionamide (+ C_3H_7NO) formed by reaction with free acrylamide during SDS-PAGE, whereas that for peptide 144-151 is an M-oxidized species (Fig. 12).

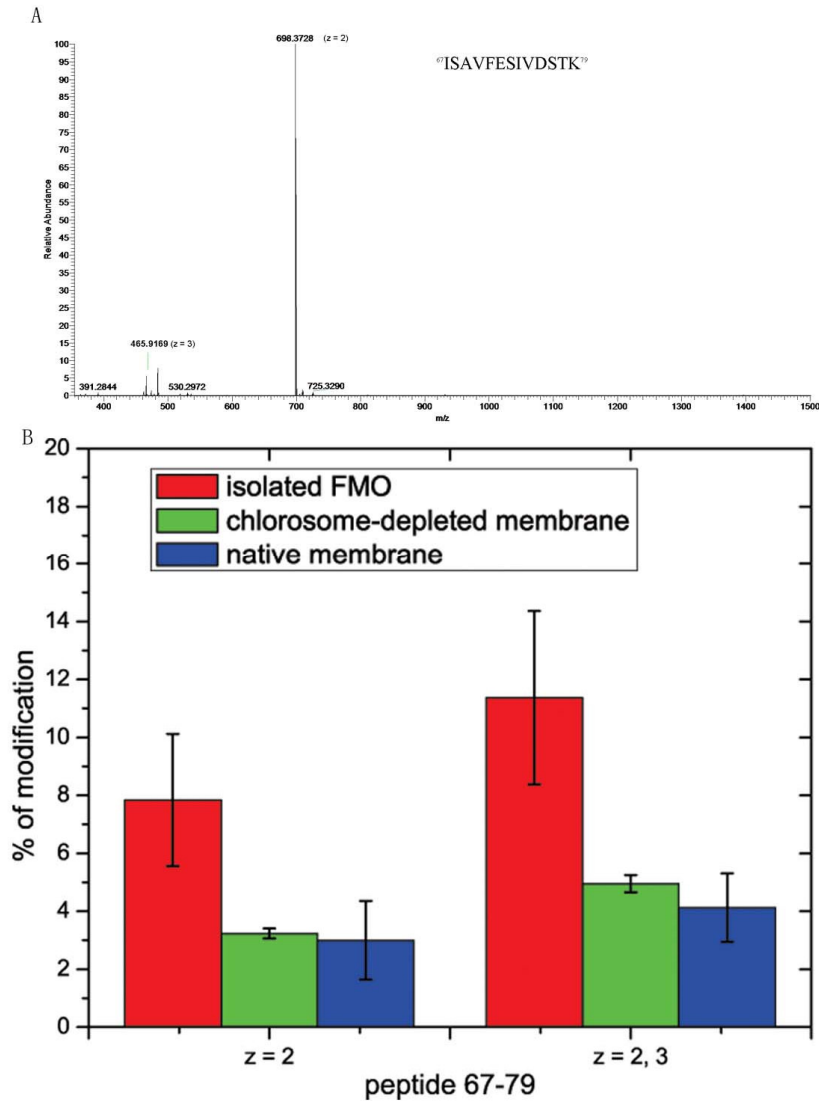


Fig. 10. Results showing that charge distributions do not affect the calculation of the peptide modification levels (consider peptide 67-79 as an example). A. Peptide 67-79 showed two charge distributions $z = 2$ and $z = 3$. The dominant fraction is the signal from $m/z = 698.3728$ ($z = 2$). The $m/z = 465.9169$ ($z = 3$) fraction accounts for less than 6% of the total protein. B. After taking both the $z = 2$ and $z = 3$ fractions into account (bars on the right), the calculated modification levels of this peptide from three samples slightly increased, but the overall trend was retained.

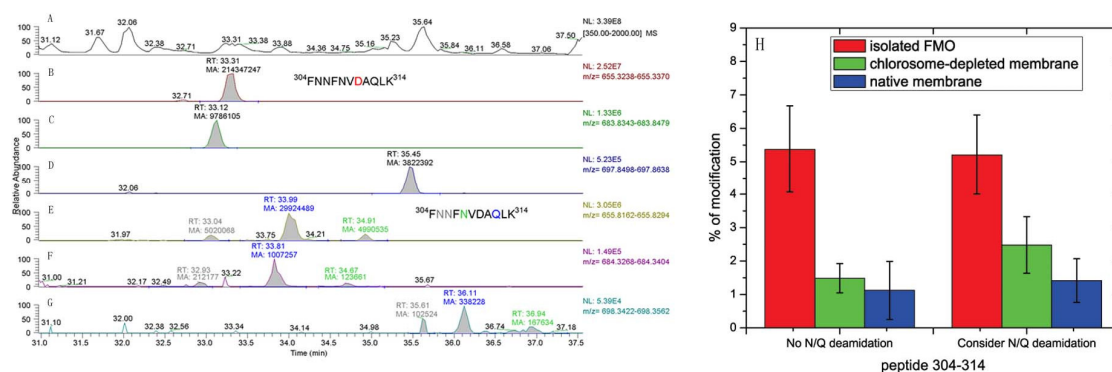


Fig. 11. Other modifications have little effect on the calculation of the peptide modification levels (consider N/Q deamidation on peptide 304-314 as an example). A. LC chromatogram of the trypsin-digested FMO protein. B. SIM of the unmodified peptide ($m/z = 655.3304$ Da). C. SIM of the peptide with D/E modification (+ 57.0215 Da). D. SIM of the peptide with D/E modification (+ 85.0528 Da). E. SIM of the peptide with N/Q deamidation (+ 0.9848 Da). F. SIM of the peptide with N/Q deamidation and D/E modification (+ 57.0215 + 0.9848 Da). G. SIM of the peptide with N/Q deamidation and D/E modification (+ 85.0528 + 0.9848 Da). In panels B, C and D, the elutions of the unmodified peptide and the D/E modified peptide followed the trends discussed in the text. The +57.0215 peptide eluted slightly earlier than the unmodified peptide, and the +85.0528 Da peptide eluted approximately 2 min after the unmodified peptide. There are three groups of N/Q in this peptide (colored gray, green and blue in panel E). Deamidation was found in all these three groups, the isomeric peptides were well separated, and they were colored according to the deamidation site. The D/E modified deamidated peptides also separated into three groups (panels F and G) and showed the elution pattern described above. H. After taking N/Q deamidation into account, the modification levels of this peptide from the three samples (bars on the right) are approximately the same as those without considering the N/Q deamidation (bars on the left).

Chapter 4

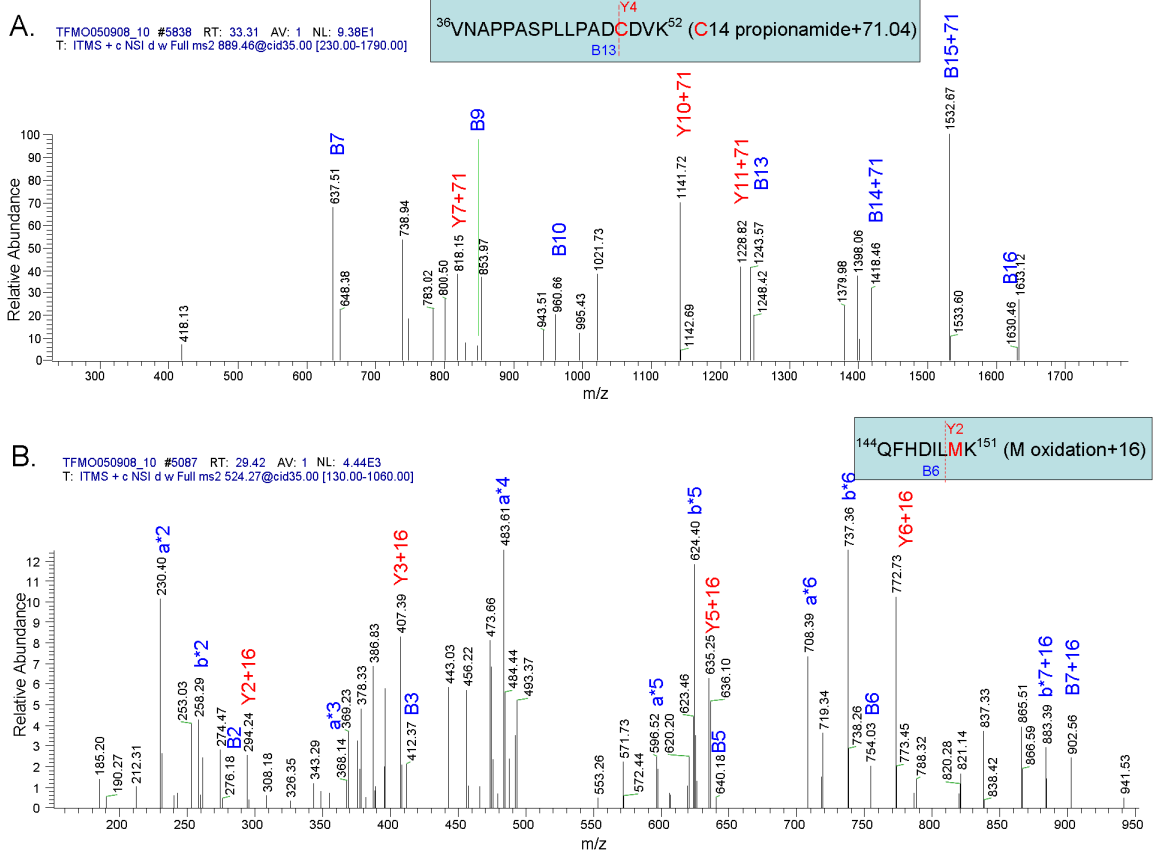


Fig. 12. Identification of cysteine propionamide in peptide 36-52 and methionine oxidation in peptide 144-151. A. Product ions of peptide 36-52 with Cys propionamide. The b and y ions are labeled. B. Product ions of peptide 144-151 with M oxidation. The abundant b, y, b* and a* ions are labeled.

Discussion:**Membrane Orientation of FMO.**

When peptides in group A are mapped onto the known FMO 3D structure (PDB code: 1M5B), we see that all are located on the Bchl *a* #3 side of the protein (Fig. 9B). In contrast, peptides in group B are all located on the Bchl *a* #1 side of the protein (Fig. 9D). Considering both peptide sets, we are able to pinpoint the interactions between both the FMO protein and the chlorosome and the FMO and the CM. That is, the Bchl *a* #3 side of the protein interacts with the CM whereas the Bchl *a* #1 side interacts with the chlorosome. This orientation of the FMO trimers on the CM indicates that the newly resolved eighth Bchl *a* in the FMO protein (*13,14*) is located close to the chlorosome baseplate, suggesting that this new pigment functions as a linker to facilitate the energy transfer from the baseplate protein to the core pigments of the FMO protein.

This orientation, the first to be determined experimentally, does confirm recent theoretical predictions that Bchl *a* #3 functions as a trap and transfers excitation to the RC (*15, 19-21*). Nevertheless, the question of how this pigment connects to the energy-acceptor pigment in the RC is still unanswered. A detailed analysis of the docking of FMO and RC and the energy transfer process from the FMO to the RC requires an atomic-resolution structure of the whole complex.

Packing of the chlorosome, FMO and CM layers.

Having answered the principal question, what is the orientation of the FMO protein in the CM, we turn to some additional questions about the architecture of the system. One

question concerns the packing between the chlorosome, FMO, and the CM layers because the packing must affect the energy transfer efficiency and other cellular processes. The labeling results, obtained using small probes to map solvent-exposed surfaces, also allows some tentative conclusions to be made about the packing of the three layers.

First, for peptides in group A, the presence of the CM doesn't preclude modification (green and blue bars in Fig. 9A); rather the extent of modification is decreased to 30-40% compared to the free FMO protein. This outcome indicates that the interaction between the FMO protein and the CM is not sufficiently strong to lock the protein in the CM, a conclusion that is consistent with the STEM results (26). Further, peptide 332-339 (Fig. 9E) of FMO in both the chlorosome-depleted membrane and the native membrane was modified to a similar extent as that from the free protein. If the Bchl *a* #3 side of the FMO was tightly locked with or significantly immersed in the CM, such a high level modification of this peptide on the CM would not be expected.

Second, the comparable extents of some peptide modification from the chlorosome-protected FMO and the free FMO (compare blue and red bars in Fig. 9C) indicate that the packing between the FMO and chlorosome layers has permeability to solvent water carrying the mapping reagent. It is likely that the FMO protein is available for labeling because it is not buried in the CsmA layer; indeed, 15-20 amino acids from the C-terminus of CsmA stick out of the chlorosome envelope (35). In addition, the newly resolved eighth Bchl *a* and the possible linker function, as described above, may diminish the packing of the two layers.

All previously reported models (2, 36-37) of this membrane system hold that the FMO proteins are located beneath the chlorosomes and function mainly to transfer excitation energy from the chlorosomes to the RCs. Nevertheless, some FMO proteins may be present that are not covered by the chlorosomes. If so, moderate modification of chlorosome-protected peptides from FMO in the native membrane would be expected and is observed. Those uncovered proteins that increase the extent of modification are unlikely to be unbound because we did pellet both the purified chlorosome-depleted membrane and native membrane and took measures to remove any unbound FMO proteins.

When the FMO protein was oriented through gel squeezing, linear dichroism experiments found that the C3 symmetry axis of a fraction of FMO trimers was not perfectly perpendicular to the membrane surface (25). In fact, such a tilt might explain why there is still low-level modification of peptides when FMO is interacting with the chlorosome (blue bars in Fig. 9C). The fraction of FMO proteins deviating from 90° is expected to be small and does not affect our overall conclusion on the orientation of the FMO proteins in the membrane.

The probe molecule (GEE) used here, due to its small and compact size with its active group on the end (diameter: ~ 2.5 Å; length: ~ 7 Å), may not be sufficiently sensitive to the distances between the interacting bodies except when the binding is tight and strong. A new series of probes with different sizes and shapes are now being sought to probe the packing between the three layers in a way that is more sensitive to distance.

Packing of FMO on the CM.

Bryant and coworkers (36-37) estimate that approximately 150-200 FMO trimers and 25-40 RCs are present per chlorosome on the basis of pigment extraction. A range of 4-8 FMO trimers are associated with each RC. Although the stoichiometry of the purified FMO-RC complex is still uncertain, it appears that each RC only has one or two FMO binding sites according to the STEM images (26). Therefore, there may be lateral energy transfer from FMO to FMO on the native CM, and this would require tight packing of the FMO proteins to increase the energy-transfer efficiency.

The STEM images of the FMO-RC complex (26), however, indicate that the two possible FMO binding sites are not closely associated with each other. Biophysical studies of the purified FMO protein also are in accord with the proposal that there is little energy coupling between the three monomers of a FMO trimer even though they are tightly packed (23-24). Another concern is that ferredoxin should be able to move freely to accept the electron delivered from the RC. There should be enough space or channels between the chlorosomes and CM to permit its diffusion, although in a proposed model in which all the RCs are on the edge of the chlorosome (36), such channels are not required. Considering all these concerns, efficient lateral energy transfer does not appear to be possible.

Due to the complexity of the system, it is difficult to predict the labeling pattern of the side of the FMO protein on the CM. Nevertheless, it is interesting to note that peptides 248-259 and 260-268 were modified to a similar extent when the FMO protein is on the

CM compared to when it is free, which might indicate that there is no tight binding between them. A higher resolution experimental approach (possibly AFM) is required to determine the distribution of FMO on the CM.

To conclude, the green sulfur photosynthetic bacteria contain a remarkably efficient and complex architecture to harvest sunlight and transfer the energy, step by step, to the RC, where electron transfer quenches the excitation. Specific protein-membrane and protein-protein interactions play a crucial role in accomplishing the high efficiency transfer. We were able to establish for the first time the orientation of the FMO protein in its native setting. Furthermore, from a semi quantitative consideration of the labeling results, we were able to conclude the packing of the FMO layer is permeable to solvent water carrying the mapping reagent. These conclusions arise from results taken by a novel and efficient protein footprinting method. Indeed, the reagent used in this research works remarkably well under physiological conditions. Given that D/E residues are common in most soluble proteins, we believe this method can be extended to study a wide variety of protein-protein, protein-membrane, and protein-ligand interactions.

Materials and Methods

Cells of the thermophilic green sulfur bacterium *Chlorobium tepidum* strain TLS were grown anaerobically at 45 °C, 150 uE light intensity for 2 days. The cells were harvested by centrifugation at 10,000xg for 15 min.

Native Membrane Preparation.

After the harvested cells were washed with 50 mM phosphate buffer (pH = 7.6), they were broken by sonication; the cell debris was pelleted by low-speed centrifugation, and the supernatant liquid was ultracentrifuged at 150,000xg for 2 hr. The pellet, containing the native membrane, was collected for later analysis.

FMO Protein Purification.

The FMO protein from *C. tepidum* was isolated according to a modification of the method described by Li *et al* (12). The main difference is that the starting material was the native membrane instead of the broken cells. After Na₂CO₃ incubation and ultracentrifugation, the supernatant containing the FMO protein was dialyzed against 100 times volume of 20 mM Tris-HCl buffer (pH = 8.0) to remove residual CO₃²⁻. The solution was then purified by using ion exchange and gel filtration chromatography until OD₂₆₇/OD₃₇₁ < 0.6. The FMO protein was concentrated by Centricon 100MWCO and stored for further use.

Chlorosome-Depleted Membrane Preparation.

A method modified from Feick *et al* (38) was used to purify the chlorosome-depleted membrane from *C. tepidum*. 10% sucrose and 2 M NaI (Mallinckrodt Inc. Paris, KY) were added to the membrane suspension. The mixture was sonicated for 10 min in a water-bath sonicator. 0.05% of Deriphath 160c detergent (Henkel Corp. Ambler, PA) was added to prevent the membrane aggregation. A subsequent centrifugation at 80,000 xg for 60 min resulted in a floating pellet, which is mainly chlorosome, and a supernatant. The supernatant was ultracentrifuged at 180,000 xg for 150 min and the supernatant was

harvested as the chlorosome-depleted membrane. Another round of centrifugation and ultracentrifugation yielded clean chlorosome-depleted membranes.

Carboxyl Group Modification.

The modification reaction was carried out for 2 hr at 4 °C, dark, phosphate buffer at pH = 7.6, with 0.3 M glycine ethyl ester (GEE) (Sigma, St. Louis, MO) and 50 mM 1-ethyl-3-(3-dimethylaminopropyl) carbodiimide hydrochloride (EDC) (Pierce, Rockford, IL). The reaction was quenched by adding the same volume of 1 M sodium acetate, and the samples were immediately loaded onto SDS-PAGE gel to isolate the FMO protein. Before the modification reaction, both the native membrane and the chlorosome-depleted membrane were ultracentrifuged again to pellet the membranes and to ensure that there was no free FMO protein in the sample. The pellets were resuspended in 50 mM phosphate buffer (pH = 7.6), and the modification reaction carried out. The OD₈₀₉ of the chlorosome-depleted membrane was approximately 0.8. The OD₇₄₇ of the chlorosome peak in the native membrane was approximately 70. The isolated FMO protein was originally in Tris buffer; buffer exchange was done by diluting the concentrated protein stock into phosphate buffer, then concentrated, and diluted again several times. The OD₈₀₉ of the FMO protein was approximately 4.

LC-MS/MS

The FMO band was cut from the SDS-PAGE gel, and the in-gel protein was trypsin digested following the manufacturer's instructions by using proteomic grade trypsin from Sigma. The LC-MS/MS running method was adapted from Sperry *et al* (39). The peptide

solution was loaded onto a reverse-phase C₁₈ column (0.075 mm × 150 mm) custom-packed with silica media (5 μm, 120 Å, Michrom Bioresources, Inc.) The peptides were separated over 70 min using an Eksigent NanoLC-1D (Livermore, CA) with the LC gradient from 2% to 60% acetonitrile with 0.1% formic acid for 60 min and then from 60% to 80% acetonitrile with 0.1% formic acid for 10 min at 260 nL/min followed by a 12 min re-equilibration step by de-ionized water with 0.1% formic acid. The solution was sprayed directly from the column into the LTQ-Orbitrap mass spectrometer (Thermo-Scientific, San Jose, CA) using a PicoView Nanospray Source (PV550, New Objective, Woburn, MA) with an spray voltage of 1.8 kV, no sheath gas and capillary voltage of 27 V. Mass spectra of the tryptic peptides (m/z range: 350-2000) were acquired at mass resolving power of 60,000 (at $m/z = 400$) with an Orbitrap mass spectrometer while product-ion scans (MS/MS) of the six most abundant ions were performed in the ion trap part of the LTQ instrument at 35% of the normalized collision energy. An isolation width of 2 Da and an activation time of 30 milliseconds were used.

Peptides and the D/E modifications were identified from the peptide accurate masses and product-ion sequencing by searching against the bacteria entries in the NCBI database using Mascot (Matrix Science, London, UK). The selected ion chromatograms were used to give quantitative information about chemical modification level on each peptide, as described in the Results section. Peak areas were obtained by integration of the various peaks by using Qual Browser (Xcalibur, Thermo-Scientific, San Jose, CA).

References

1. Blankenship RE (2002) *Molecular Mechanisms of Photosynthesis* (Blackwell Science, Malden, MA).
2. Blankenship RE, Olson JM, Miller M (1995) in *Anoxygenic Photosynthetic Bacteria*, eds Blankenship RE, Madigan MT, Bauer CE (Kluwer, Dordrecht, The Netherlands), pp 399–435.
3. Blankenship RE (1994) Protein structure, electron transfer and evolution of prokaryotic photosynthetic reaction centers. *Antonie van Leeuwenhoek* 65:311-329.
4. Bahatyrova S, *et al* (2004) The native architecture of a photosynthetic membrane. *Nature* 430:1058-1062
5. Şener MK, Olsen JD, Hunter CN, Schulten K (2007) Atomic-level structural and functional model of a bacterial photosynthetic membrane vesicle. *Proc Natl Acad Sci U S A*. 104:15723–15728
6. Staehelin LA, Golecki JR, Drews G (1980) Supermolecular organization of chlorosomes (chlorobium vesicles) and of their membrane attachment sites in *Chlorobium limicola* *Biochim. Biophys. Acta* 589:30-45
7. Oostergetela GT, *et al* (2007) Long-range organization of bacteriochlorophyll in chlorosomes of *Chlorobium tepidum* investigated by cryo-electron microscopy. *FEBS Letters* 581:5435–5439
8. Psencik J, *et al* (2004) Lamellar organization of pigments in chlorosomes, the light harvesting complexes of green photosynthetic bacteria. *Biophys J*. 87:1165–1172
9. Olson JM (2004) The FMO protein. *Photosynth Res* 80:181-187
10. Fenna RE, Matthews BW (1975) Chlorophyll arrangement in a bacteriochlorophyll protein from *Chlorobium-limicola*. *Nature* 258:573–577
11. Tronrud DE, Schmid MF, Matthews BW (1986) Structure and X-ray amino acid sequence of a bacteriochlorophyll *a* protein from *Prosthecochloris aestuarii* refined at 1.9 Å resolution. *J Mol Biol* 188:443–454.
12. Li YF, Zhou W, Blankenship RE, Allen JP (1997) Crystal structure of the bacteriochlorophyll *a* protein from *Chlorobium tepidum*. *J Mol Biol* 271:456–471.
13. Ben-Shem A, Frolow F, Nelson N (2004) Evolution of Photosystem 1 – from symmetry through pseudosymmetry to asymmetry. *FEBS Letters* 564:274-280

14. Tronrud DE, Wen J, Gay L, Blankenship RE (2009) The structural basis for the difference in absorbance spectra for the FMO antenna protein from various green sulfur bacteria. *Photosynth Res* 100: 79-87.
15. Engel GS, *et al* (2007) Evidence for wavelike energy transfer through quantum coherence in photosynthetic systems. *Nature* 446:782–786.
16. Read EL, *et al* (2007) Cross-peak-specific two-dimensional electronic spectroscopy. *Proc Natl Acad Sci USA* 104:14203–14208
17. Read EL, Schlau-Cohen GS, Engel GS, Wen JZ, Blankenship RE, Fleming GR (2008) Visualization of excitonic structure in the Fenna-Matthews-Olson photosynthetic complex by polarization-dependent two-dimensional electronic spectroscopy. *Biophys J* 95:847–856
18. Mohseni M, Rebentrost P, Lloyd S, Aspuru-Guzik A (2008) Environment-assisted quantum walks in energy transfer of photosynthetic complexes. *J Chem Phys.* 129:174106.
19. Müh F, *et al* (2007) α -Helices direct excitation energy flow in the Fenna-Matthews-Olson protein. *Proc Natl Acad Sci USA* 104:16862-16867
20. Adolphs J, Renger T (2006) How proteins trigger excitation energy transfer in the FMO Complex of Green Sulfur Bacteria. *Biophys J* 91:2778-2797
21. Brixner T, Stenger J, Vaswani HM, Cho M, Blankenship RE, Fleming GR (2005) Two-dimensional spectroscopy of electronic couplings in photosynthesis. *Nature* 434:625–628.
22. Pearlstein RM (1992) Theory of the optical spectra of the bacteriochlorophyll *a* antenna protein trimer from *Prosthecochloris aestuarii*. *Photosynth Res* 31:213–226
23. Gülen D (1996) Interpretation of the excited-state structure of the Fenna–Matthews–Olson pigment protein complex of *Prosthecochlori aestuarii* based on the simultaneous simulation of the 4K absorption, linear dichroism, and singlet-triplet absorption difference spectra: a possible excitonic explanations. *J Phys Chem* 100:17683–17689
24. Louwe RJW, Vrieze J, Hoff AJ, Aartsma TJ (1997) Toward the integral interpretation of the optical steady-state spectra of the FMO-complex of *Prosthecochloris aestuarii*. 2. Exciton simulations. *J Phys Chem* 101:11280–11287

25. Melkozernov AN, Olson JM, Li YF, Allen JP, Blankenship RE (1998) Orientation and excitonic interactions of the Fenna-Matthews-Olson Protein in membranes of the green sulfur bacterium *Chlorobium tepidum*. *Photosynth Res* 56:315–328.
26. Rémigy HW, *et al* (1999) The reaction center complex from the green sulfur bacterium *Chlorobium tepidum*: a structural analysis by scanning transmission electron microscopy. *J Mol Biol* 290:851–858.
27. Pedersen MØ, Borch J, Højrup P, Cox RP, Miller M (2006) The light-harvesting antenna of *Chlorobium tepidum*: Interactions between the FMO protein and the major chlorosome protein CsmA studied by surface plasmon resonance. *Photosynth Res* 89:63–69.
28. Li H, Frigaard NU, Bryant DA (2006) Molecular contacts for chlorosome envelope proteins revealed by cross-linking studies with chlorosomes from *Chlorobium tepidum*. *Biochemistry* 45:9095–9103.
29. Hambly DM, Gross ML (2007) Laser flash photochemical oxidation to locate heme binding and conformational changes in myoglobin. *Int. J. Mass Spectrom.* 259:124-129.
30. Zhu MM, Rempel DL, Du Z, Gross ML (2003) Quantification of protein-ligand interactions by mass spectrometry, titration, and H/D exchange: PLIMSTEX. *J Am Chem Soc* 125:5252-5253.
31. Swaisgood H, Nataka M (1973) Effect of Carboxyl Group Modification on Some of the Enzymatic Properties of L-Glutamate Dehydrogenase. *J. Biochem.* 74:77-86
32. Hoare DG, Koshland DE (1967) A method for the quantitative modification and estimation of carboxylic acid groups in proteins. *J. Biol. Chem.* 242:2447-2453
33. Burkey KO, Gross EL (1981) Effect of carboxyl group modification on redox properties and electron donation capability of spinach plastocyanin. *Biochemistry* 20:5495-5499
34. Ong SE, Mann M (2005) Quantitative mass spectrometry in proteomics: a critical review. *Nat. Chem. Biol.* 1: 252-262
35. Milks KJ, *et al* (2005) Chlorosome proteins studied by MALDI-TOF-MS: topology of CsmA in *Chlorobium tepidum*. *Photosynth Res* 86:113-121.

36. Frigaard NU, Chew AGM, Li H, Maresca JA, Bryant DA (2003) *Chlorobium tepidum*: insights into the structure, physiology, and metabolism of a green sulfur bacterium derived from the complete genome sequence. *Photosynth Res* 78:93-117.
37. Frigaard NU, *et al* (2005) Isolation and characterization of carotenosomes from a bacteriochlorophyll *c*-less mutant of *Chlorobium tepidum*. *Photosynth Res* 86:101-111.
38. Feick RG, Fitzpatrick M, Fuller RC (1982) Isolation and characterization of cytoplasmic membranes and chlorosomes from the green bacterium *Chloroflexus aurantiacus*. *J Bacteriol* 150:905-915
39. Sperry JB, Shi X, Rempel DL, Nishimura Y, Akashi S, Gross ML (2008) A mass spectrometric approach to the study of DNA-binding proteins: interaction of human TRF2 with telomeric DNA. *Biochemistry* 47:1797-1807

Chapter 5.

Conclusions and future directions

It is a great time to study photosynthesis. The current fossil fuel shortage and environmental problems have shifted public attention to promising alternative energy resources. Renewable bioenergy presents great potential to contribute to the global primary energy supply, although significant technical challenges exist to make it economically favorable (1). How we address the challenges and deliver a satisfactory solution will be the key to achieve a sustainable energy resource for the future.

The base of renewable bioenergy, no matter it is biomass, biodiesel, biohydrogen or artificial photosynthesis, is the fact that photosynthetic species, including plants, algae, and all kinds of photosynthetic bacteria, can directly utilize solar radiation as energy input, which is sustainable, to produce food and store the energy. As biochemists, one of our contributions to the area is to understand of the molecular architecture of the protein complexes involved in the photosynthetic energy storage process and their relevant functions.

There has been great advancement in understanding of the photosystem from green photosynthetic bacteria. The packing of the pigments BChl *c/d/e* inside the chlorosome has been intensively studied and a molecular model could be drawn (2, 3). We have started to know more about the baseplate protein (CsmA protein) (4-6). An 8th pigment was discovered in the FMO protein (7-9). Electronic quantum coherence was discovered in the FMO protein as the first report in any biological system (10-12). The understanding of the interaction between the FMO protein and the baseplate is improving (13-15). However, much more can be done.

The discovery of the 8th pigment in the FMO protein asks us to revisit its optical properties. In *P. aestuarii*, the 8th pigment has two axial ligands on the basis of the crystal structure, which is the first experimental report of this arrangement in a natural photosynthetic protein complex (7). The nature and function of this special ligation system should be understood. Careful resonance Raman spectral analysis might be used to study this bidentate ligation. In addition, theoretical calculations should play an important role in elucidating the functions of both the 8th pigment and the bidentate ligation. Moreover, it seems the 8th pigment is easy to be lost during the protein purification (7, 9). In the future, either an improved purification method that will prevent the lost of this pigment or an in vitro reconstitution method should be developed. Through such an in vitro method, the pigment can be put back to the protein. The key to such an assay is to develop a method to quickly check whether the 8th pigment is incorporated into the protein or not.

The study of the FMO_BchP mutant indicates more heterogeneous pigment conformations, but the lowest site energy was retained and can be clearly resolved at 77K as the wild type FMO (16). It is going to be interesting to see the structure of this mutant FMO, which will provide us some insights of the lowest energy pigment(s). The successful assembly of this mutant is good news for mutagenesis studies of the FMO protein. Site-directed FMO mutants, which are undergoing under the supervision of Dr. Connie Kang, will be extremely valuable samples for us to understand the pigment-pigment coupling and pigment-protein coupling in this protein. The nature of quantum coherence or the algorithm of energy transfer might be deciphered from these mutants.

The newly discovered *Candidatus Chloracidobacterium thermophilum* also contains FMO protein (FMO_Cab), although it only has a sequence similarity of ~ 50% to the FMOs from green sulfur bacteria (FMO_GSB) (17). The FMO_Cab has some different optical properties from the FMO_GSB. The protein has two emission peaks at room temperature but only one at 77 K. It seems there is a strong thermal equilibrium between the two populations at room temperature (18). A computer created FMO_Cab structure using homolog modeling indicates two major structural differences between the FMO_Cab and the FMO_GSB (Fig. 1). It turned out the unconserved region between residues 200-210 might be the CsmA binding region, since the same region on the FMO_GSB was predicted to be the CsmA binding region by H/D exchange (15), crystallization and molecular docking (unpublished data). It is quite possible that the 240-250 region, which is located on the side of trimer, is the RC binding region. This assignment agrees with the STEM image of the FMORC complex that the side of the FMO interacts with the RC (24). However, this needs to be tested by further experimental results. Overall, these two regions seem to not affect the protein's optical properties. The atomic resolution structure of the FMO_Cab is needed to understand the detailed binding sites of individual pigments and their site energy tuning by the environment.

The detailed interaction between the baseplate and FMO, including the binding sites, binding affinity and stoichiometry has been studied by H/D exchange using the C-terminal 20 amino acids of the CsmA as a ligand (15). The binding sites were also investigated in collaboration by crystallization using the same peptide and molecular docking and simulation. Similar approaches might be used to study the interaction

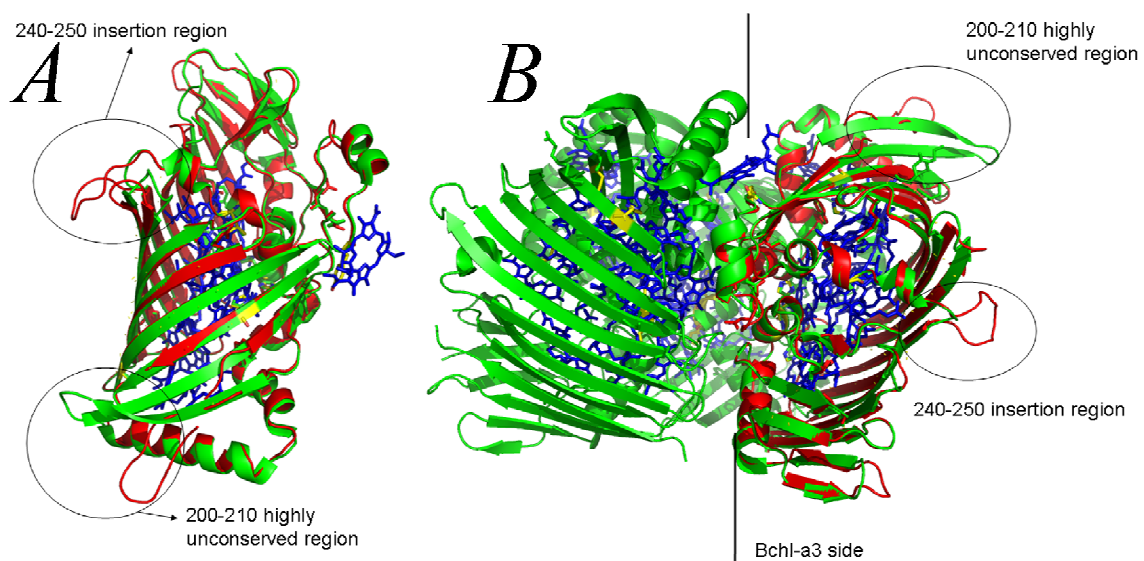


Fig 1. FMO_Cab structure predicted by homolog modeling using Swiss-Model. The predicted structure of FMO_Cab (red) was aligned with FMO structure from *C. tepidum* (green) (PDB code: 3ENI). Two regions show strong structural differences. The 200-210 region was predicted to be the CsmA binding region. The 240-250 region was proposed to be the RC binding region.

between the FMO and the RC. A tentative target as a ligand is the region predicted from the alignment of FMO_Cab and FMO_GSB as mentioned above. Another approach which might be more productive is to get the crystal structure of the FMORC complex.

The molecular mechanism of the redox regulation in the FMO protein has always been a mystery (19). Although intensive search of possible quencher(s) by both HPLC and MS analysis of possible post translational modifications is negative so far, there must be something sensitive to dithionite and to control the redox state of the protein. H/D exchange of the FMO protein and the FMO protein with dithionite indicates that dithionite will open the FMO trimer slightly by showing increased deuterium uptake at the center of the FMO trimer. However, the detailed molecular mechanism of the quenching is still missing. One possibility is that the fast decay component observed under normal or oxidizing conditions is due to the exciton delocalization among the three monomers in a trimer. Under reducing condition, such as when the protein is reduced by dithionite, the delocalization is blocked by opening the trimer. However, this analysis is contrary to the commonly accepted idea that the exciton delocalization among the monomers in a trimer is weak and can be ignored.

Beyond the FMO protein, the RC from green sulfur bacteria (and also heliobacteria) is a homodimer which is quite evolutionarily interesting, since the other RCs, like PSI, PSII and RC from purple bacteria, are heterodimers. Heliobacteria are extremely oxygen sensitive. At this point, the RC from GSB is a much more attractive system to study and there are some very interesting questions waiting to be answered (refer to a review 20).

The chlorosome from green photosynthetic bacteria is a kind of cellular organelle. The nature that BChl *c/d/e* self-assembled to form the chlorosome makes it a good candidate for developing bio-hybrid solar devices (21, 22). A very interesting fundamental question is the biogenesis of the chlorosome in the cell.

Green sulfur bacteria are photoautotrophs. They can grow on minimal media with the energy input from the sunlight and electron donor normally from sodium sulfide, and they fix carbon. The doubling time of *C. tepidum* is ~ 2 hr, close to yeast. A very attractive area is to genetically engineer species like *C. tepidum* to produce chemicals we need, like drugs. The nature of their food requirements will dramatically lower the cost.

Mass spectrometry is a very powerful technique. The method we developed using specific covalent labeling the surface exposed D/E residues on protein surfaces turned out to be very sensitive to the protein/protein and protein/ligand binding interface (13). This method might be applied to other systems in the photosynthetic research or other areas. Measuring protein complexes by mass spectrometry using native electrospray has demonstrated its power in determining the stoichiometry of a protein complex (9) and its topology (23). With a new 12 T FTICR machine equipped in the MS center at Washington University, the marriage between native spray and the ability to do top-down mass spectrometry by this new machine will open a new research area.

References

1. Rittmann BE, Krajmalnik-Brown R, Halden RU (2008) Pre-genomic, genomic and post-genomic study of microbial communities involved in bioenergy. *Nature Reviews Microbiology* 6:604-612
2. Ganapathy S, Oostergetel GT, Wawrzyniak PK, Reus M, Gomez Maqueo Chew A, Buda F, Boekema EJ, Bryant DA, Holzwarth AR, de Groot HJ (2009) Alternating syn-anti bacteriochlorophylls form concentric helical nanotubes in chlorosomes. *Proc Natl Acad Sci USA* 106, 8525-8530.
- 3 Oostergetel GT, Reus M, Gomez Maqueo Chew A, Bryant DA, Boekema EJ, Holzwarth AR. (2007) Long-range organization of bacteriochlorophyll in chlorosomes of *Chlorobium tepidum* investigated by cryo-electron microscopy. *FEBS Lett.* 581: 5435-5439.
4. Pedersen MO, Linnanto J, Frigaard NU, Nielsen NC, Miller M. (2010) A model of the protein-pigment baseplate complex in chlorosomes of photosynthetic green bacteria. *Photosynth Res* DOI 10.1007/s11120-009-9519-y
5. Pedersen MØ, Underhaug J, Dittmer J, Miller M, Nielsen NC (2008) The three-dimensional structure of CsmA: a small antenna protein from the green sulfur bacterium *Chlorobium tepidum*. *FEBS Lett* 582: 2869-2874.
6. Montaña GA, Wu HM, Lin S, Brune DC, Blankenship RE (2003) Isolation and characterization of the B798 light-harvesting baseplate from the chlorosomes of *Chloroflexus aurantiacus*. *Biochemistry* 42: 10246-51.
7. Tronrud DE, Wen J, Gay L, Blankenship RE (2009) The structural basis for the difference in absorbance spectra for the FMO antenna protein from various green sulfur bacteria. *Photosynth Res* 100: 79-87.
8. Ben-Shem A, Frolov F, Nelson N (2004) Evolution of photosystem I - from symmetry through pseudo-symmetry to asymmetry. *FEBS Lett* 564: 274-280.
9. Wen J, Zhang H, Gross ML, Blankenship RE (2010) Nature and stoichiometry of pigments in the FMO protein revealed by native spray mass spectrometry. (In preparation)

10. Engel GS, Calhoun TR, Read EL, Ahn TK, Mančal T, Cheng YC, Blankenship RE, Fleming GR (2007) Evidence for wavelike energy transfer through quantum coherence in photosynthetic systems. *Nature* 446: 782–786.
11. Ishizaki A, Fleming GR (2009) Theoretical examination of quantum coherence in a photosynthetic system at physiological temperature. *Proc. Natl. Acad. Sci. USA* 106: 17255-17260.
12. Panitchayangkoon G, Hayes G, Fransted KA, Caram JR, Harel E, Wen J, Blankenship RE, Engel GS (2010) Long-lived quantum coherence in photosynthetic complexes at physiological temperature. arXiv:1001.5108v1
13. Wen J, Zhang H, Gross ML, Blankenship RE (2009) Membrane orientation of the FMO antenna protein from *Chlorobaculum tepidum* as determined by mass spectrometry-based footprinting. *Proc Natl Acad Sci USA* 106: 6134–6139
14. Pedersen MØ, Borch J, Højrup P, Cox RP, Miller M. (2006) The light-harvesting antenna of *Chlorobium tepidum*: interactions between the FMO protein and the major chlorosome protein CsmA studied by surface plasmon resonance. *Photosynth Res.* 89: 63-69.
15. Wen J, Huang R, Gross ML, Blankenship RE (2010) The binding sites, affinity and stoichiometry of CsmA/FMO revealed by H/D exchange. (In preparation)
16. Wen J, Harada J, Buyle K, Yuan K, Tamiaki H, Oh-oka H, Loomis RA, Blankenship RE (2010) Pigment mutants of the FMO antenna protein from green photosynthetic bacteria. (Under review)
17. Tsukatani Y, Wen J, Blankenship RE, and Bryant DA (2010) Characterization of the FMO protein from the aerobic chlorophototroph, *Candidatus Chloracidobacterium thermophilum*. *Photosyn Res* DOI 10.1007/s11120-009-9517-0
18. Wen J, Tsukatani Y, Bryant DA, Blankenship RE (2010) Electronic structure of FMO protein from the aerobic chlorophototroph, *Candidatus Chloracidobacterium thermophilum*. (In preparation)
19. Zhou W, LoBrutto R, Lin S, Blankenship RE (1994) Redox effects on the bacteriochlorophyll a-containing Fenna-Matthews-Olson protein from *Chlorobium tepidum*. *Photosyn Res* 41: 89-96

20. Hauska G, Schoedl T, Remigy H, Tsiotis G (2001) The reaction center of green sulfur bacteria. *Biochim Biophys Acta* 1507: 260-277
21. Modesto-Lopez LB, Thimsen EJ, Collins AM, Blankenship RE, and Biswas P (2009). Electrospray-assisted characterization and deposition of chlorosomes to fabricate a lightharvesting biomimetic device. *Energy Environ. Sci.* 3: 216-222.
22. Modesto-Lopez LB, Collins AM, Wen J, Blankenship RE, Biswas P (2010) Measuring the size and charge of natural photosynthetic antenna aerosols. (In preparation)
23. Hernández H, Robinson CV (2007) Determining the stoichiometry and interactions of macromolecular assemblies from mass spectrometry. *Nature Protocols* 2:715-726
24. Rémy HW, *et al* (1999) The reaction center complex from the green sulfur bacterium *Chlorobium tepidum*: a structural analysis by scanning transmission electron microscopy. *J Mol Biol* 290:851–858.

Visualization of Excitonic Structure in the Fenna-Matthews-Olson Photosynthetic Complex by Polarization-Dependent Two-Dimensional Electronic Spectroscopy

Elizabeth L. Read,^{*,†} Gabriela S. Schlau-Cohen,^{*,†} Gregory S. Engel,^{*,†} Jianzhong Wen,[‡] Robert E. Blankenship,[‡] and Graham R. Fleming^{*,†}

^{*}Department of Chemistry, University of California, Berkeley, California 94720; [†]Physical Biosciences Division, Lawrence Berkeley National Laboratory, Berkeley, California 94720; and [‡]Department of Biology, Department of Chemistry, Washington University, St. Louis, Missouri 63130

ABSTRACT Photosynthetic light-harvesting proceeds by the collection and highly efficient transfer of energy through a network of pigment-protein complexes. Interchromophore electronic couplings and interactions between pigments and the surrounding protein determine energy levels of excitonic states, and dictate the mechanism of energy flow. The excitonic structure (orientation of excitonic transition dipoles) of pigment-protein complexes is generally deduced indirectly from x-ray crystallography, in combination with predictions of transition energies and couplings in the chromophore site basis. We demonstrate that coarse-grained, excitonic, structural information in the form of projection angles between transition dipole moments can be obtained from the polarization-dependent, two-dimensional electronic spectroscopy of an isotropic sample, particularly when the nonrephasing or free polarization decay signal, rather than the photon echo signal, is considered. This method provides an experimental link between atomic and electronic structure, and accesses dynamical information with femtosecond time resolution. In an investigation of the Fenna-Matthews-Olson complex from green sulfur bacteria, the energy transfer connecting two particular exciton states in the protein was isolated as the primary contributor to a crosspeak in the nonrephasing two-dimensional spectrum at 400 femtoseconds under a specific sequence of polarized excitation pulses. The results suggest the possibility of designing experiments using combinations of tailored polarization sequences to separate and monitor individual relaxation pathways.

INTRODUCTION

Photosynthesis begins with the harvesting of sunlight by antenna pigments that rapidly funnel energy to reaction centers. The spectral coverage and energy transfer characteristics of light-harvesting systems are determined by the structural arrangement of pigments and their interactions with the surrounding environment, which is often the interior of a protein. Even among organisms with chlorophyll as the primary light absorber, the architecture of antenna systems varies widely in nature (1). Investigation of these specialized light-harvesting structures, which evolved under different light environments to fuel photosynthesis with optimal efficiency, could have applications in solar-energy conversion devices, and such investigations become increasingly important as we search for clean energy alternatives.

The Fenna-Matthews-Olson (FMO) pigment-protein complex is found in low light-adapted green sulfur bacteria, which harvest light primarily in a large antenna structure called the chlorosome. The FMO complex is tasked with transporting energy collected in the chlorosome to the reaction center, thereby initiating the photochemistry that ulti-

mately leads to the chemical storage of energy. The FMO complex was the first chlorophyll protein structure solved by x-ray crystallography, and comprises three identical subunits, each containing seven bacteriochlorophyll (BChl) pigments nested within beta sheets (2,3). The closest center-to-center distance between neighboring intrasubunit BChls is 11 Å, with the largest coupling energies between them estimated to be on the order of 100 cm⁻¹. The closest approach of inter-subunit BChls is ~24 Å, with corresponding coupling energies of <20 cm⁻¹ (4). For this reason, it has been assumed (and borne out by spectroscopic studies) that the exciton wave function is rapidly localized on individual subunits upon excitation (5). Compared to the highly symmetric ring structures of the light-harvesting apparatus in the similarly widely studied purple photosynthetic bacteria, the asymmetric arrangement of the seven pigments in FMO is more reminiscent of light harvesting in higher plants. Because of its lack of symmetry and the early availability of x-ray structure information in conjunction with its relatively small size, FMO has been considered a model system for the investigation of photosynthetic energy transfer.

A number of spectroscopic experiments and theoretical studies have contributed to a good understanding of the energetic landscape in FMO (5–7). The lack of symmetry within the FMO subunit has presented a challenge for researchers modeling experimental spectra, because each of the seven BChls experiences a different local environment due to, for example, the proximity of charged residues or bowing

Submitted December 23, 2007, and accepted for publication February 21, 2008.

Address reprint requests to Graham R. Fleming, Dept. of Chemistry, University of California, Berkeley, CA 94720. E-mail: grfleming@lbl.gov. Gregory S. Engel's present address is the Dept. of Chemistry, University of Chicago, Chicago, IL 60637.

Editor: Klaus Schulten.

© 2008 by the Biophysical Society
0006-3495/08/07/847/10 \$2.00

doi: 10.1529/biophysj.107.128199

Role of the AcsF Protein in *Chloroflexus aurantiacus*^{∇†}

Kuo-Hsiang Tang, Jianzhong Wen, Xianglu Li, and Robert E. Blankenship*

Departments of Biology and Chemistry, Campus Box 1137, Washington University, St. Louis, Missouri 63130

Received 26 January 2009/Accepted 27 March 2009

The green phototrophic bacteria contain a unique complement of chlorophyll pigments, which self-assemble efficiently into antenna structures known as chlorosomes with little involvement of protein. The few proteins found in chlorosomes have previously been thought to have a primarily structural function. The biosynthetic pathway of the chlorosome pigments, bacteriochlorophylls *c*, *d*, and *e*, is not well understood. In this report, we used spectroscopic, proteomic, and gene expression approaches to investigate the chlorosome proteins of the green filamentous anoxygenic phototrophic bacterium *Chloroflexus aurantiacus*. Surprisingly, Mg-protoporphyrin IX monomethyl ester (oxidative) cyclase, AcsF, was identified under anaerobic growth conditions. The AcsF protein was found in the isolated chlorosome fractions, and the proteomics analysis suggested that significant portions of the AcsF proteins are not accessible to protease digestion. Additionally, quantitative real-time PCR studies showed that the transcript level of the *acsF* gene is not lower in anaerobic growth than in semiaerobic growth. Since the proposed enzymatic activity of AcsF requires molecular oxygen, our studies suggest that the roles of AcsF in *C. aurantiacus* need to be investigated further.

The unique chlorosome antenna complexes found in green phototrophic bacteria are the most densely packed pigmented light-harvesting complexes known and contain self-assembled bacteriochlorophyll (BChl) *c*, *d*, or *e* aggregates (1). Chlorosomes are central to the ability of green bacteria to carry out photosynthesis under very low light conditions (2). While most of the enzymes that contribute to the biosynthesis of BChl in protein-pigment light-harvesting antenna complexes have been investigated in detail, there have been few studies of the enzymes involved in synthesis of chlorosome pigments.

Chlorosomes contain relatively few proteins compared to other photosynthetic antenna systems. The functions of most of the chlorosome proteins remain to be understood. For example, while *Chloroflexus aurantiacus* is one of the most investigated green filamentous anoxygenic phototrophic (FAP) bacteria, the functions of the chlorosome proteins are completely unknown, except for CsmA, which is known to function as the baseplate pigment-binding protein and to mediate energy transfer from BChl *c* to BChl *a* in the integral light-harvesting complexes (13, 25).

The genome of *C. aurantiacus* has been completely sequenced (http://genome.jgi-psf.org/finished_microbes/chlau/chlau.home.html), so combinations of biochemical and genetic studies have recently become possible. In this work, we used spectroscopic, proteomic, and gene expression approaches to investigate the chlorosome proteins and unexpectedly identified Mg-protoporphyrin IX monomethyl ester aerobic cyclase (AcsF) in chlorosomes under anaerobic growth conditions. Two cyclase enzymes are capable of forming the isocyclic ring ("E ring") that is found in all (bacterio)chlorophylls: AcsF and Mg-protoporphyrin IX

monomethyl ester anaerobic cyclase (BchE). The roles of the AcsF and BchE proteins have been suggested to be conversion of Mg-protoporphyrin IX monomethyl ester into Mg-divinyl-protoporphyrin IX monomethyl ester into Mg-divinyl-protoporphyrin IX monomethyl ester (PChlide) by catalyzing the isocyclic ring formation under aerobic and anaerobic conditions, respectively (Fig. 1) (21, 22). The *acsF*-like gene can be detected in diverse organisms, from bacteria to algae and higher plants, whereas the gene encoding BchE is found strictly in anaerobic bacteria. Interestingly, both the *acsF* and *bchE* genes exist in *C. aurantiacus*. As a result, alternative roles for AcsF in the chlorosomes and in anaerobic growth need to be considered, and some hypotheses are reported in this work.

MATERIALS AND METHODS

Materials. DNA oligomers used in this work were purchased from Integrated DNA Technologies and used without further purification. Enzymes and kits for the reported molecular biology studies are described below.

Cell cultures. *Chloroflexus aurantiacus* J-10-fl cells were cultured in "D" medium as reported previously (7) under anaerobic and semiaerobic growth conditions at 48°C in low-intensity light (6 W/m²). Only one small air bubble in the incubation bottle was allowed for anaerobic growth, whereas approximately half of the volume in the 200-ml bottle was filled with medium for semiaerobic growth (see Fig. 2A). The cultures were harvested after 3 days, when the *A*₈₆₃ and *A*₇₄₂ values were 0.46 and 1.57 for anaerobic growth and 0.48 and 0.97 for the semiaerobic growth, respectively.

Isolation and characterization of chlorosomes. *C. aurantiacus* cells were harvested by centrifugation at 5,471 × *g* for 15 min. After sonication and removal of the cell debris by centrifugation at 20,000 × *g* for 30 min, the membrane fraction was separated from the soluble fraction by ultracentrifugation at 200,000 × *g* for 2 h. The chlorosomes, located in the membrane fractions, were fractionated using a 15 to 45% sucrose density gradient as reported earlier (4, 26). The purified chlorosome fraction was characterized by the UV/visible spectrum and also subjected to sodium dodecyl sulfate-polyacrylamide gel electrophoresis (SDS-PAGE) analysis (12% Tris-glycine).

SDS-PAGE analysis. For SDS-PAGE analysis, the chlorosome fraction was incubated in methanol at room temperature for 10 min and centrifuged, and the supernatant liquid was removed to release the pigments and soluble components from the chlorosome envelope. The pellet (the chlorosome envelope) was then subjected to SDS-PAGE analysis.

Protein identification by MALDI-TOF fingerprinting. In-gel protein digestion by trypsin for matrix-assisted laser desorption ionization-time-of-flight (MALDI-TOF) analysis was used, following the procedure reported previously (6, 23). Briefly, the Coomassie G-250-stained SDS-PAGE (12.5% Tris-glycine) gel was

* Corresponding author. Mailing address: Departments of Biology and Chemistry, Campus Box 1137, Washington University, St. Louis, MO 63130. Phone: (314) 935-7971. Fax: (314) 935-4432. E-mail: blankenship@wustl.edu.

† Supplemental material for this article may be found at <http://jib.asm.org/>.

∇ Published ahead of print on 3 April 2009.

The structural basis for the difference in absorbance spectra for the FMO antenna protein from various green sulfur bacteria

Dale E. Tronrud · Jianzhong Wen ·
Leslie Gay · Robert E. Blankenship

Received: 23 January 2009 / Accepted: 23 April 2009 / Published online: 13 May 2009
© Springer Science+Business Media B.V. 2009

Abstract The absorbance spectrum of the Fenna–Matthews–Olson protein—a component of the antenna system of Green Sulfur Bacteria—is always one of two types, depending on the species of the source organism. The FMO from *Prosthecochloris aestuarii* 2K has a spectrum of type 1 while that from *Chlorobaculum tepidum* is of type 2. The previously reported crystal structures for these two proteins did not disclose any rationale that would explain their spectral differences. We have collected a 1.3 Å X-ray diffraction dataset of the FMO from *Prosthecochloris aestuarii* 2K, which has allowed us to identify an additional Bacteriochlorophyll-*a* molecule with chemical attachments to both sides of the central magnesium atom. A new analysis of the previously published X-ray data for the *Chlorobaculum tepidum* FMO shows the presence of a Bacteriochlorophyll-*a* molecule in an equivalent location but with a chemical attachment from only one side. This difference in binding is shown to be predictive of the spectral type of the FMO.

Keywords FMO · Bacteriochlorophyll · Crystal structure · Absorbance spectra · Bidentate ligation

D. E. Tronrud (✉) · L. Gay
Howard Hughes Medical Institute, Institute of Molecular
Biology, University of Oregon, Eugene, OR 97403, USA
e-mail: det101@daletronrud.com

J. Wen · R. E. Blankenship
Departments of Biology and Chemistry, Washington University,
St Louis, MO 63130, USA

Present Address:
D. E. Tronrud
Department of Biochemistry and Biophysics, Oregon State
University, Corvallis, OR 97331, USA

Abbreviations

Bchl- <i>a</i>	Bacteriochlorophyll- <i>a</i>
<i>Cbl</i>	<i>Chlorobaculum</i>
FMO	Fenna–Matthews–Olson Protein
PDB	Protein Data Bank
<i>Pel</i>	<i>Pelodictyon</i>
<i>Ptc</i>	<i>Prosthecochloris</i>
r.m.s.	Root mean square

Introduction

Fenna–Matthews–Olson protein (Olson 2004) is a bacteriochlorophyll-*a* containing protein that exclusively occurs in photosynthetic bacteria with a chlorosome light antenna system (Blankenship and Matsuura 2003). It is of interest, because it is a rare example of an antenna system component that is water soluble. This property has made it an attractive target for spectroscopic studies (Olson et al. 1974; Louwe et al. 1997a; Whitten et al. 1980; van Mourik et al. 1994; Francke and Amesz 1997; Vulto et al. 1998a, 1998b; Brixner et al. 2005; Engle et al. 2007), theoretical studies (Pearlstein 1992; Louwe et al. 1997b; Savikhin et al. 1997; Vulto et al. 1998a; Wendling et al. 2002; Müh et al. 2007), and X-ray diffraction structure studies (Tronrud and Matthews 1993; Camara-Artigas et al. 2003; BenShem et al. 2004). In fact, the FMO from *Prosthecochloris aestuarii* 2K was the first protein containing some type of chlorophyll to have its atomic structure known (Tronrud et al. 1986) and stood as the highest resolution model in this class for over 20 years. The review by Savikhin et al. (1998) is an informative recap of the spectroscopic work done up to that point.

Membrane orientation of the FMO antenna protein from *Chlorobaculum tepidum* as determined by mass spectrometry-based footprinting

Jianzhong Wen^a, Hao Zhang^b, Michael L. Gross^b, and Robert E. Blankenship^{a,1}

^aDepartments of Biology and Chemistry, ^bDepartment of Chemistry, Washington University in St. Louis, St. Louis, MO 63130

Communicated by Graham R. Fleming, University of California, Berkeley, CA, February 23, 2009 (received for review October 15, 2008)

The high excitation energy-transfer efficiency demanded in photosynthetic organisms relies on the optimal pigment-protein binding orientation in the individual protein complexes and also on the overall architecture of the photosystem. In green sulfur bacteria, the membrane-attached Fenna-Matthews-Olson (FMO) antenna protein functions as a “wire” to connect the large peripheral chlorosome antenna complex with the reaction center (RC), which is embedded in the cytoplasmic membrane (CM). Energy collected by the chlorosome is funneled through the FMO to the RC. Although there has been considerable effort to understand the relationships between structure and function of the individual isolated complexes, the specific architecture for *in vivo* interactions of the FMO protein, the CM, and the chlorosome, ensuring highly efficient energy transfer, is still not established experimentally. Here, we describe a mass spectrometry-based method that probes solvent-exposed surfaces of the FMO by labeling solvent-exposed aspartic and glutamic acid residues. The locations and extents of labeling of FMO on the native membrane in comparison with it alone and on a chlorosome-depleted membrane reveal the orientation. The large differences in the modification of certain peptides show that the Bchl *a* #3 side of the FMO trimer interacts with the CM, which is consistent with recent theoretical predictions. Moreover, the results also provide direct experimental evidence to confirm the overall architecture of the photosystem from *Chlorobaculum tepidum* (*C. tepidum*) and give information on the packing of the FMO protein in its native environment.

chemical labeling | energy transfer | FMO protein | mass spectrometry | protein footprinting

Photosynthesis is a fundamental biological process that harvests solar energy to power life on Earth (1). A diverse family of pigment-protein complexes and elegant architectures accomplish the necessary light-harvesting and energy-storage processes (2–5). In photosynthetic green sulfur bacteria, light absorbed by a large antenna complex known as a chlorosome (6–8) is transferred through a protein called Fenna-Matthews-Olson (FMO) (9) to the reaction center, which is embedded in the cytoplasmic membrane (CM). Together, they form a funnel-like architecture to facilitate energy transfer. The specific orientation of the critical linker, the FMO protein, however is unknown (Fig. 1A).

The structure of the FMO protein was the first (bacterio)chlorophyll binding protein to be determined by X-ray crystallography. Structures of this protein from 2 species, *Prosthecochloris aestuarii* 2K (10, 11) and *Chlorobaculum tepidum* (12) are now available, and they show strong structural and spectral similarities. The FMO protein consists of 3 identical subunits of mass 40 kDa related by a 3-fold axis of symmetry. The 3 monomers form a disc with a C3 symmetry axis perpendicular to the disc plane (Fig. 1B). There are 7 BChl *a* molecules in a monomer, although an eighth pigment has been resolved in newly solved structures (13, 14). Each pigment experiences a different local environment (Fig. 1C), and their site energies are fine-tuned by specific interactions with the protein. Bchl *a* #3 and Bchl *a* #1, for example, are on the opposite sides of the FMO protein from the side view of the FMO trimer (Fig. 1C).

Given that the FMO protein plays a critical role in the energy transfer pathway, significant effort has been made to understand its electronic structure. Quantum effects (15–20), which were recently discovered in this complex, may function to improve the energy-transfer efficiency. A defined energy-transfer pathway was also elucidated by both 2D electronic spectroscopy (21) and novel theoretical calculations (20). The pigment with the lowest site energy, the assignment of which was historically controversial (22–24), is predicted to be Bchl *a* #3 on the basis of coupling with the dipole of adjacent alpha helices (19). This energy-sink pigment is expected to be close to the CM to ensure efficient energy transfer from the FMO protein to the reaction center (RC) (20). Thus, this side of the FMO trimer (Bchl *a* #3 side) should be in close contact with the RC in the CM.

The opposite orientation, however, was predicted from the structure and properties of the isolated protein. Hydrophobicity analysis of the FMO protein favors an interaction of the Bchl *a* #1 side of the protein with the CM (12), in accord with another suggestion based on the existence of an eighth pigment (13). In this latter model, the extra pigment forms an energy transfer bridge between the FMO and the RC.

The experimental evidence for the orientation of the FMO comes from linear dichroism (25) and 3D reconstitution data based on STEM images (26). Both suggest that the FMO disc sits flat on the CM with its C3 symmetry axis perpendicular to the plane of the membrane. However, the specific orientation of the disc (i.e., which side interacts with the CM), cannot be determined by using these methods.

Moreover, the overall architecture of the photosystem, including the relative orientation and the extent of the interaction between the individual antenna complexes, is also poorly understood. The interaction between the flat surface of the FMO trimer and the RC, shown by the STEM image (26), is not as strong as proposed on the basis of protein hydrophobicity, suggesting that the FMO is probably partially buried in the CM (12). On the chlorosome side, the detailed interaction between the FMO and the CsmA protein is not clear, although surface plasmon resonance (27) and cross-linking data (28) suggest that FMO protein directly interacts with the CsmA protein and is probably partially buried in the CsmA layer (28). In short, a comprehensive interaction map of the various components, chlorosome, FMO, and RC, at the molecular level is still needed.

We report here a method that combines carboxyl group modification with mass spectrometry to afford surface mapping or footprinting (29, 30) of the protein, revealing the interaction of proteins associated with membranes. We chose the reagent, glycine

Author contributions: J.W., H.Z., M.L.G., and R.E.B. designed research; J.W. and H.Z. performed research; J.W., H.Z., M.L.G., and R.E.B. contributed new reagents/analytic tools; J.W., H.Z., M.L.G., and R.E.B. analyzed data; and J.W. wrote the paper.

The authors declare no conflict of interest.

¹To whom correspondence should be addressed. E-mail: blankenship@wustl.edu.

This article contains supporting information online at www.pnas.org/cgi/content/full/0901691106/DCSupplemental.

Characterization of the FMO protein from the aerobic chlorophototroph, *Candidatus Chloracidobacterium thermophilum*

Yusuke Tsukatani · Jianzhong Wen ·
Robert E. Blankenship · Donald A. Bryant

Received: 15 October 2009 / Accepted: 7 December 2009 / Published online: 22 January 2010
© Springer Science+Business Media B.V. 2010

Abstract *Candidatus Chloracidobacterium* (Cab.) thermophilum is a recently discovered aerobic chlorophototroph belonging to the phylum *Acidobacteria*. From analyses of genomic sequence data, this organism was inferred to have type-1 homodimeric reaction centers, chlorosomes, and the bacteriochlorophyll (BChl) *a*-binding Fenna–Matthews–Olson protein (FMO). Here, we report the purification and characterization of Cab. thermophilum FMO. Absorption, fluorescence emission, and CD spectra of the FMO protein were measured at room temperature and at 77 K. The spectroscopic features of this FMO protein were different from those of the FMO protein of green sulfur bacteria (GSB) and suggested that exciton coupling of the BChls in the FMO protein is weaker than in FMO of GSB especially at room temperature. HPLC analysis of the pigments extracted from the FMO protein only revealed the presence of BChl *a* esterified with phytol. Despite the distinctive spectroscopic properties, the residues known to bind BChl *a* molecules in the FMO of GSB are well conserved in the primary structure of the Cab. thermophilum FMO protein. This suggests that the FMO of Cab. thermophilum probably also binds seven or possibly eight BChl *a*(P) molecules. The results imply that, without changing pigment composition or structure dramatically, the FMO protein has acquired properties that allow it to perform light harvesting efficiently under aerobic conditions.

Keywords *Acidobacteria* · *Chloracidobacterium thermophilum* · Chlorosome · Exciton coupling · FMO protein

Introduction

The Fenna–Matthews–Olson protein (FMO) is a bacteriochlorophyll (BChl) *a*-binding protein found in green sulfur bacteria (GSB; phylum *Chlorobi*), which have homodimeric type-1 reaction centers and a light-harvesting apparatus comprising chlorosomes and FMO (Blankenship et al. 1995; Blankenship and Matsuura 2003; Bryant and Frigaard 2006; Frigaard and Bryant, 2006). Chlorosomes, which serve as the major light-harvesting antennae in GSB, can contain up to 250,000 BChl *c*, *d*, or *e* molecules; the supramolecular organization of these BChls has recently been determined (Ganapathy et al. 2009). The baseplate, BChl-*a* binding protein CsmA ($\lambda_{\max} \sim 795$ nm) (Pedersen et al. 2008) traps light energy harvested by the BChls in chlorosomes and transfers that energy to the reaction centers by the way of FMO ($\lambda_{\max} \sim 809$ nm).

As FMO is a rare example of a water-soluble antenna protein that binds BChls, it occupies a special place in the history of photosynthesis. FMO was first isolated from the GSB *Prosthecochloris aestuarii* strain 2K in 1962 by John Olson, and soon thereafter Olson and co-workers showed that the protein carried BChl *a* as the pigment (for a review of the history concerning this protein, see Olson 2004). The water-soluble nature of the protein, and the early availability of a structure (see below), have made FMO a favorite subject of spectroscopists and theorists, who have sought to explain the absorption, fluorescence, circular dichroism, and excitonic properties of FMO from a theoretical perspective (for references, see Olson 2004; Tronrud et al.

Y. Tsukatani · D. A. Bryant (✉)
Department of Biochemistry and Molecular Biology,
The Pennsylvania State University, S-235 Frear Building,
University Park, PA 16802, USA
e-mail: dab14@psu.edu

J. Wen · R. E. Blankenship
Departments of Biology and Chemistry, Washington University,
St. Louis, MO 63130, USA

Characterization of an FMO Variant of *Chlorobaculum tepidum* Carrying Bacteriochlorophyll *a* Esterified by Geranylgeraniol[†]

Jianzhong Wen,^{‡,§} Jiro Harada,^{||,@} Kenny Buyle,[§] Kevin Yuan,^{‡,§} Hitoshi Tamiaki,^{||} Hirozo Oh-oka,[⊥] Richard A. Loomis,[§] and Robert E. Blankenship^{*,‡,§}

[‡]Department of Biology, and [§]Department of Chemistry, Washington University, St. Louis, Missouri 63130, ^{||}Department of Bioscience and Biotechnology, Faculty of Science and Engineering, Ritsumeikan University, Kusatsu, Shiga 525-8577, Japan, and [⊥]Department of Biological Sciences, Graduate School of Science, Osaka University, Osaka 560-0043, Japan. [@]Present address: Department of Medical Biochemistry, Kurume University School of Medicine, Fukuoka 830-0011, Japan.

Received May 2, 2010; Revised Manuscript Received June 1, 2010

ABSTRACT: The Fenna–Matthews–Olson light-harvesting antenna (FMO) protein has been a model system for understanding pigment–protein interactions in the energy transfer process in photosynthesis. All previous studies have utilized wild-type FMO proteins from several species. Here we report the purification and characterization of the first FMO protein variant generated via replacement of the esterifying alcohol at the C-17 propionate residue of bacteriochlorophyll (BChl) *a*, phytol, with geranylgeraniol, which possesses three more double bonds. The FMO protein still assembles with the modified pigment, but both the whole cell absorption and the biochemical purification indicate that the mutant cells contain a much less mature FMO protein. The gene expression was checked using qRT-PCR, and none of the genes encoding BChl *a*-binding proteins are strongly regulated at the transcriptional level. The smaller amount of the FMO protein in the mutant cell is probably due to the degradation of the apo-FMO protein at different stages after it does not bind the normal pigment. The absorption, fluorescence, and CD spectra of the purified FMO variant protein are similar to those of the wild-type FMO protein except the conformations of most pigments are more heterogeneous, which broadens the spectral bands. Interestingly, the lowest-energy pigment binding site seems to be unchanged and is the only peak that can be well resolved in 77 K absorption spectra. The excited-state lifetime of the variant FMO protein is unchanged from that of the wild type and shows a temperature-dependent modulation similar to that of the wild type. The variant FMO protein is less thermally stable than the wild type. The assembly of the FMO protein and also the implications of the decreased FMO/chlorosome stoichiometry are discussed in terms of the topology of these two antennas on the cytoplasmic membrane.

In the photosynthetic green sulfur bacteria, light absorbed by the large peripheral antenna complex called the chlorosome (*I–4*) is transferred through the baseplate protein CsmA (*5–7*) and the FMO¹ protein (*8*) to the reaction center (RC) where charge separation occurs (*9*). The FMO protein forms a bridge to connect the chlorosome to the cytoplasmic membrane structurally and functionally to direct the excitation energy collected from the

chlorosome to the RC (*10, 11*). Ever since the FMO protein was first discovered in the early 1960s (*12*) and its atomic-resolution structure was determined in the 1970s (*13*), the analysis of this protein has been a major source of our understanding of how pigments bind to photosynthetic proteins and the nature of pigment–pigment interactions.

The FMO protein is a water-soluble protein that is remarkably stable. This makes it a very attractive system for structural and functional studies. The X-ray structures of the FMO protein have been determined from two species of green sulfur bacteria, *Prosthecochloris aestuarii* and *Chlorobaculum tepidum* (*14–18*), and a third FMO protein structure from *Pelodictyon phaeum* in which bacteriochlorophyll *e* is the dominant chlorosomal pigment has recently been completed in collaboration with J. Allen and co-workers (unpublished data). The FMO protein forms a compact trimer with 3-fold symmetry (Figure 1A). A large portion of the protein scaffold is β -sheet secondary structure, which forms a “taco shell” to create a highly hydrophobic cavity to hold seven BChl *a* molecules in each monomer. Three monomers join together by both electrostatic and hydrophobic interactions to form a stable structure (*16*). The seven BChl *a* molecules hold very specific conformations inside the protein with their bacteriochlorin rings forming hydrogen bonds and axial ligation with the surrounding protein and water. The tails of

[†]This work was supported by U.S. Department of Energy Grant DE-FG02-07ER15846 to R.E.B., a Grant-in-Aid for Scientific Research (A) (22245030) from the Japan Society for the Promotion of Science to H.T., a Grant-in-Aid for Scientific Research (C) (21570168) from the Ministry of Education, Culture, Sports, Science, and Technology (MEXT) of Japan to H.O., and a David and Lucile Packard Foundation Fellowship in Science and Engineering to R.A.L. This research is from the Photosynthetic Antenna Research Center (PARC), an Energy Frontier Research Center funded by the U.S. Department of Energy, Office of Science, Office of Basic Energy Sciences, via Grant DE-SC 0001035.

*To whom correspondence should be addressed: Departments of Biology and Chemistry, Campus Box 1137, Washington University, St. Louis, MO 63130. Phone: (314) 935-7971. Fax: (314) 935-4432. E-mail: blankenship@wustl.edu.

Abbreviations: FMO, Fenna–Matthews–Olson bacteriochlorophyll *a*; BChl *a*, bacteriochlorophyll *a*; CD, circular dichroism; RC, reaction center; BChl *a*_P, BChl *a* with a phytol tail; BChl *a*_{GG}, BChl *a* with a geranylgeraniol tail; OD, optical density; TCSPC, time-correlated single-photon counting; fwhm, full width at half-maximum; qRT-PCR, quantitative real-time PCR; RT, room temperature; IRF, instrument response function; PDB, Protein Data Bank.

Structural Analysis of Alternative Complex III in the Photosynthetic Electron Transfer Chain of *Chloroflexus aurantiacus*[†]

Xinliu Gao,[‡] Yueyong Xin,^{‡§} Patrick D. Bell,[‡] Jianzhong Wen,[‡] and Robert E. Blankenship^{*‡}

[‡]Departments of Biology and Chemistry, Washington University in St. Louis, St. Louis, Missouri 63130, and [§]College of Life and Environmental Sciences, HangZhou Normal University, HangZhou, 310036 P. R. China

Received May 27, 2010; Revised Manuscript Received July 6, 2010

ABSTRACT: The green photosynthetic bacterium *Chloroflexus aurantiacus*, which belongs to the phylum of filamentous anoxygenic phototrophs, does not contain a cytochrome *bc* or *bf* type complex which is found in all other known groups of phototrophs. This suggests that a functional replacement exists to link the reaction center photochemistry to cyclic electron transfer as well as respiration. Earlier work identified a potential substitute of the cytochrome *bc* complex, now named alternative complex III (ACIII), which has been purified from *C. aurantiacus*, identified, and characterized. ACIII functions as a menaquinol:auracyanin oxidoreductase in the photosynthetic electron transfer chain, and a related but distinct complex functions in respiratory electron flow to a terminal oxidase. In this work, we focus on elucidating the structure of photosynthetic ACIII. We found that ACIII is an integral membrane protein complex of ~300 kDa that consists of eight subunits of seven different types. Among them, there are four metalloprotein subunits, including a 113 kDa iron–sulfur cluster-containing polypeptide, a 25 kDa penta-heme *c*-containing subunit, and two 20 kDa monoheme *c*-containing subunits in the form of a homodimer. A variety of analytical techniques were employed in determining the ACIII substructure, including HPLC combined with ESI-MS, metal analysis, potentiometric titration, and intensity analysis of heme staining SDS–PAGE. A preliminary structural model of ACIII is proposed on the basis of the analytical data and chemical cross-linking in tandem with mass analysis using MALDI-TOF, as well as transmembrane and transit peptide analysis.

Bacterial electron transport pathways largely fall into two major categories: the light-driven photosynthetic electron transfer chain and the aerobic or anaerobic respiratory electron transfer chain. Despite the vast differences between photophosphorylation and oxidative phosphorylation, they both couple the chemical reactions between electron donors and electron acceptors to the translocation of protons across the membrane, which then drives ATP formation and other energy-dependent processes (1). As a result, the common feature of all electron transport chains is the presence of a proton pump to create the transmembrane proton gradient. In respiratory electron transfer pathways, there may be as many as three types of proton pumping protein complexes reminiscent of mitochondria, depending on environmental factors (2). In contrast, the proton pump in all the photosynthetic electron transfer chains was until recently believed to involve a cytochrome *bc*₁ or *b₆f* complex, which resembles mitochondrial complex III in terms of overall structure and mechanism (3).

In the species tree of bacteria based on 16S rRNA analysis (4), the phylum of filamentous anoxygenic phototrophs (FAPs) is not closely related to the other phyla that contain organisms that

carry out chlorophyll-based photosynthesis: purple bacteria, cyanobacteria, heliobacteria, green sulfur bacteria, and chloroacidobacteria. Instead, it exhibits a much deeper branching position to the other five bacterial phyla that contain phototrophic representatives (5, 6). Because of this distinctive feature, the study of FAPs may shed an interesting light on the evolutionary development of photosynthesis. The FAPs make up a very diverse and unique phylum of bacteria, including several genera: *Chloroflexus* (7), *Oscillochloris* (8), *Chloronema* (9), *Heliothrix* (10), and several *Chloroflexus*-like bacteria found in marine environments (11). Among them, *Chloroflexus aurantiacus*, a prominent microorganism of hot spring microbial mat communities, was the first described and is the most extensively studied representative of FAPs in terms of its photosynthetic and other metabolic pathways. The photosynthetic apparatus of *C. aurantiacus* exhibits an interesting combination of characteristics found in very different and diverse groups of phototrophic prokaryotes. They have a type II photoreaction center and integral membrane antenna complex reminiscent of purple bacteria (12, 13). In addition, they have a peripheral chlorosome antenna complex (14) and a chlorophyll biosynthesis pathway that are both similar to those found in green sulfur bacteria (15, 16). *C. aurantiacus* also contains a unique autotrophic carbon fixation pathway different from that found in any other phototrophs, the 3-hydroxypropionate cycle (17, 18). Therefore, the phylogenetic characterization and the versatile photosynthetic apparatus of *C. aurantiacus* suggest that it occupies an important place in the origin and evolution of photosynthesis (19).

[†]This work was supported by Grant MCB-0646621 to R.E.B. from the Molecular Biochemistry Program of the National Science Foundation. The mass spectrometry research was supported by the National Center for Research Resources (NCRR) of the National Institutes of Health (Grant 2P41RR00954).

^{*}To whom correspondence should be addressed: Washington University in St. Louis, One Brookings Drive, CB 1137, St. Louis, MO 63130. Telephone: (314) 935-7971. Fax: (314) 935-4432. E-mail: blankenship@wustl.edu.

Long-lived quantum coherence in photosynthetic complexes at physiological temperature

Gitt Panitchayangkoon^a, Dugan Hayes^a, Kelly A. Fransted^a, Justin R. Caram^a, Elad Harel^a, Jianzhong Wen^b, Robert E. Blankenship^b, and Gregory S. Engel^{a,1}

^aDepartment of Chemistry and The James Franck Institute, University of Chicago, Chicago, IL 60637; and ^bDepartments of Biology and Chemistry, Washington University, St. Louis, MO 63130

Communicated by Graham R. Fleming, University of California, Berkeley, CA, May 3, 2010 (received for review January 26, 2010)

Photosynthetic antenna complexes capture and concentrate solar radiation by transferring the excitation to the reaction center that stores energy from the photon in chemical bonds. This process occurs with near-perfect quantum efficiency. Recent experiments at cryogenic temperatures have revealed that coherent energy transfer—a wave-like transfer mechanism—occurs in many photosynthetic pigment-protein complexes. Using the Fenna–Matthews–Olson antenna complex (FMO) as a model system, theoretical studies incorporating both incoherent and coherent transfer as well as thermal dephasing predict that environmentally assisted quantum transfer efficiency peaks near physiological temperature; these studies also show that this mechanism simultaneously improves the robustness of the energy transfer process. This theory requires long-lived quantum coherence at room temperature, which never has been observed in FMO. Here we present evidence that quantum coherence survives in FMO at physiological temperature for at least 300 fs, long enough to impact biological energy transport. These data prove that the wave-like energy transfer process discovered at 77 K is directly relevant to biological function. Microscopically, we attribute this long coherence lifetime to correlated motions within the protein matrix encapsulating the chromophores, and we find that the degree of protection afforded by the protein appears constant between 77 K and 277 K. The protein shapes the energy landscape and mediates an efficient energy transfer despite thermal fluctuations.

biophysics | photosynthesis | quantum beating | ultrafast spectroscopy | quantum biology

Energy transfer through photosynthetic pigment-protein complexes operates with exceptionally high quantum efficiency (1). Recent studies have demonstrated that energy moves through antennae using not only a classical hopping mechanism but also a manifestly quantum mechanical wave-like mechanism at cryogenic temperatures (2–5). Theoretical studies of this process within the Fenna–Matthews–Olson antenna complex (FMO) show that this quantum transport mechanism requires a balance between unitary (oscillatory) and dissipative (dephasing) dynamics; further, this balance appears to be optimized near room temperature and contributes to the robustness of the process (6–9). This theory demands that quantum coherence persist long enough to affect transport, but quantum beating has never been observed in FMO at physiological temperature.

The FMO pigment-protein complex from *Chlorobium tepidum* serves as a model system for photosynthetic energy transfer processes (2, 10–13). This complex conducts energy from the larger light-harvesting chlorosome to the reaction center in green sulfur bacteria (14, 15). Each noninteracting FMO monomer contains seven coupled bacteriochlorophyll-*a* chromophores arranged asymmetrically, yielding seven nondegenerate, delocalized molecular excited states called excitons (11, 16). The small number of distinct states makes this particular complex attractive for theoretical studies of transport dynamics. As shown by Ishizaki and Fleming (13), the arrangement of the chromophores in FMO results in a downhill, rugged energetic landscape with two distinct routes

through which an excitation can travel to reach the lowest energy state. While classical trajectories can navigate such funnel-like landscapes, the wave-like motion through the complex improves efficiency by avoiding kinetic traps. In higher plants, this mechanism likely becomes more important because the landscape is more rugged without a downhill arrangement (17).

Recent investigations of photosynthetic systems at 77 K have found evidence of coherent energy transfer in many antenna complexes and even in the reaction center of purple bacteria (2–4). This wave-like energy transfer mechanism, however, can contribute to the near-perfect quantum efficiency of photosynthesis only if coherences survive in these systems during energy transfer at physiological temperatures. As temperature increases, thermally excited vibrational modes of the protein bath drive larger energetic fluctuations, thereby accelerating decoherence (14, 18). Although this dephasing seems unfavorable, Mohseni et al. (6) and Plenio and Huelga (7) have independently shown that the delicate interplay between quantum coherence and dephasing can create fast and unidirectional transfer pathways within these complexes, resulting in highly efficient electronic energy transfer (8, 9, 19). This scheme exploits quantum coherence to overcome an energy barrier, but subsequent dephasing processes trap the excitation at the target site. Optimal transport therefore requires both dephasing and coherent energy transfer.

The initial excitation or transfer event necessarily creates quantum coherence because both the dipole and site operators do not commute with the system Hamiltonian. For a system of two excitons described by $\Psi(t) = c_1\phi_1 + c_2\phi_2$, the time evolution of the density matrix is given by

$$|\Psi(t)\rangle\langle\Psi(t)| = |c_1|^2|\phi_1\rangle\langle\phi_1| + |c_2|^2|\phi_2\rangle\langle\phi_2| + c_1c_2^*e^{-i(E_1-E_2)t/\hbar}|\phi_1\rangle\langle\phi_2| + c_1^*c_2e^{i(E_1-E_2)t/\hbar}|\phi_2\rangle\langle\phi_1|. \quad [1]$$

The first two terms represent populations in the excitonic basis, whereas the latter two describe coherences. The phase factors in the coherence terms are responsible for quantum beating, which appears as a periodic modulation of population in the site basis and peak amplitude. The frequency of this beating corresponds to the energy difference between the two excitons giving rise to that particular quantum coherence. Traditionally this phenomenon is ignored in transport dynamics because fast electronic dephasing generally destroys quantum coherence before it can impact the transport process. For example, at cryogenic temperature, coherences between ground and excited states in FMO dephase in approximately 70 fs. In contrast, coherences among excited states have been shown to persist beyond 660 fs—long enough to

Author contributions: G.P., K.A.F., and G.S.E. designed research; G.P., D.H., K.A.F., and J.R.C. performed research; J.W. and R.E.B. contributed reagents; G.P., D.H., J.R.C., E.H., and G.S.E. analyzed data; and G.P., D.H., and G.S.E. wrote the paper.

The authors declare no conflict of interest.

¹To whom correspondence should be addressed at: Gordon Center for Integrative Science, 929 East 57th Street, GCIS E119, Chicago, IL 60637. E-mail: gsel@uchicago.edu.

Dynamics of electronic dephasing in the Fenna–Matthews–Olson complex

Dugan Hayes¹, Gitt Panitchayangkoon¹, Kelly A Fransted¹,
Justin R Caram¹, Jianzhong Wen², Karl F Freed¹
and Gregory S Engel^{1,3}

¹ Department of Chemistry and The James Franck Institute,
The University of Chicago, 929 East 57th Street, Chicago, IL 60637, USA

² Departments of Biology and Chemistry, Washington University,

1 Brookings Drive, St Louis, MO 63130, USA

E-mail: gsengel@uchicago.edu

New Journal of Physics **12** (2010) 065042 (12pp)


Received 18 February 2010

Published 30 June 2010

Online at <http://www.njp.org/>

doi:10.1088/1367-2630/12/6/065042

Abstract. Electronic coherence has been shown to persist in the Fenna–Matthews–Olson (FMO) antenna complex from green sulfur bacteria at 77 K for at least 660 fs, several times longer than the typical lifetime of a coherence in a dynamic environment at this temperature. Such long-lived coherence was proposed to improve energy transfer efficiency in photosynthetic systems by allowing an excitation to follow a quantum random walk as it approaches the reaction centre. Here we present a model for bath-induced electronic transitions, demonstrating that the protein matrix protects coherences by globally correlating fluctuations in transition energies. We also quantify the dephasing rates for two particular electronic coherences in the FMO complex at 77 K using two-dimensional Fourier transform electronic spectroscopy and find that the lifetimes of individual coherences are distinct. Within the framework of noise-assisted transport, this result suggests that the FMO complex has been locally tuned by natural selection to optimize transfer efficiency by exploiting quantum coherence.

 Online supplementary data available from stacks.iop.org/NJP/12/065042/mmedia

³ Author to whom any correspondence should be addressed.





温建忠

荣获二〇〇九年度国家优秀自费留学生
奖学金，特颁证嘉奖，以资鼓励。

CHINA SCHOLARSHIP COUNCIL

Presents the

**2009 Chinese Government Award
for Outstanding Self-financed
Students Abroad**

to

Wen Jianzhong

A handwritten signature in black ink, consisting of the Chinese characters '刘敬辉' (Liu Jinghui).

Dr. Liu Jinghui
Secretary-General
China Scholarship Council

Jianzhong Wen

Departments of Chemistry and Biology
Washington University in St. Louis
St. Louis, Missouri 63130

Tel (314) 229-2750
Fax (314) 935-5125
Email: jwen@artsci.wustl.edu

EDUCATION:

- 08/2005-08/2010 Ph.D in Biochemistry, Departments of Chemistry & Biology, **Washington University in St. Louis**, MO, 63130 USA
(Thesis advisor: Prof. Robert E. Blankenship)
- 08/2004-06/2005 Visiting student in the National Key Laboratory of Optical Physics and Soft Matter Physics, **Institute of Physics, Chinese Academy of Science**, Beijing, 100080, China. (Advisor: Prof. Yu-xiang Weng)
- 09/2000-07/2004 B.S. in Physics (with honor), Dept. of Physics, **Wuhan University**, Wuhan, Hubei, 430072, China. (Advisor: Prof. Guo-ping Wang)

ACHIEVEMENTS AND AWARDS:

- Undergraduate Student Scholarship. (Sponsored by *Wuhan University*, 2000-2004)
- National 1st Prize in the *China Undergraduate Contest in Mathematical Model Building*. (Sponsored by the *Higher Education Commission of P. R. China*, & *Chinese Industry and Applied Mathematics Society*, 2003)
- National First-Place Scholarship. (Sponsored by the *State Council of P. R. China*, 2003)
- The Young Investigator Award. (Gordon Research Conference, USA 2008)
- Chinese Government Award for Outstanding Self-financed Students Abroad (Sponsored by the *China Scholarship Council, the Ministry of Education, China*, 2009)

SOCIETIES and MEMBERSHIPS:

- * International Society for Photosynthesis Research
- * American Association for the Advancement of Science
- * American Society of Mass Spectrometry

PRESENTATIONS:

- 04/2004 Proceedings of 2004's General Congress of Chinese Optical Society (*oral*)
- 09/2006 2006 Washington University Biophysics and Biochemistry retreat (*poster*)
- 10/2006 32nd Midwest photosynthesis meeting (*poster*)
- 07/2007 14th International congress in photosynthesis (*poster*)
Satellite Antenna complex meeting (*selected poster presentation*)
- 10/2007 33rd Midwest photosynthesis meeting (*selected poster presentation*)
- 09/2007 2007 Washington University Biophysics and Biochemistry retreat (*oral*)

06/2008	Photosynthesis Gordon Conference. (<i>the young investigator award presentation</i>)
10/2008	34 th Midwest photosynthesis meeting (<i>oral</i>)
06/2009	57 th ASMS Conference on Mass Spectrometry (<i>poster</i>)
08/2009	Carbon fixation and renewable energy workshop
09/2009	11 th Donald Danforth Plant Science Center symposium on cellular signaling
11/2009	35 th Midwest photosynthesis meeting (<i>poster</i>)
11/2009	2009 Washington University Biophysics and Biochemistry retreat (<i>poster</i>)
05/2010	58 th ASMS Conference on Mass Spectrometry (<i>poster</i>)

PUBLICATIONS:

1. Xie J, **Wen J-Z**, Wang G-P, and Wang J-B (2005) Large area deposition of homogeneous metallic nanoparticles on polymer film and the storage property, *Acta Physica Sinica*, 54(01):242-245.
2. Read EL, Schlau-Cohen G, Engel GS, **Wen J-Z**, Blankenship RE, Fleming GR (2008) Visualization of excitonic structure in the Fenna-Matthews-Olson photosynthetic complex by polarization-dependent two-dimensional electronic spectroscopy. *Biophys J.* 95(2):847-56. (highlighted by *Sciencedaily et al*)
3. Tang KH, **Wen J-Z**, Li X, Blankenship RE (2009) Role of the AcsF protein in *Chloroflexus aurantiacus*. *J Bacteriol.* 191(11):3580-7.
4. **Wen J-Z**, Zhang H, Gross ML, Blankenship RE (2009) Membrane orientation of the FMO antenna protein from *Chlorobaculum tepidum* as determined by mass spectrometry-based footprinting. *Proc Natl Acad Sci USA* 106(15):6134-9. (highlighted by *Sciencedaily et al*)
5. Tronrud DE, **Wen J-Z**, Gay L, Blankenship RE (2009) The structural basis for the difference in absorbance spectra for the FMO antenna protein from various green sulfur bacteria. *Photosynth Res* 100(2):79-87.
6. Tsukatani Y, **Wen J-Z**, Blankenship RE, Bryant DA (2010) Characterization of the FMO protein from the aerobic chlorophototroph, *Candidatus Chloracidobacterium thermophilum*. *Photosynth Res* 104:201-209.
7. **Wen J-Z**, Harada J, Buyle K, Yuan K, Tamiaki H, Oh-oka H, Loomis RA, Blankenship RE (2010) Characterization of an FMO variant of *Chlorobaculum tepidum* carrying bacteriochlorophyll *a* esterified by geranylgeraniol. *Biochemistry* 49:5455-5463
8. Panitchayangkoon G, Hayes D, Fransted KA, Caram JR, Harel E, **Wen J-Z**, Blankenship RE, Engel GS (2010) Quantum coherence in photosynthetic complexes at physiological temperature. *Proc Natl Acad Sci USA* doi:10.1073/pnas.1005484107
9. Hayes D, Panitchayangkoon G, Fransted KA, Caram JR, **Wen J-Z**, Freed KF, Engel GS (2010) Dynamics of electronic dephasing in the Fenna–Matthews–Olson complex. *New J. Phys.* 12 065042 (10.1088/1367-2630/12/6/065042)
10. Tang J, Urban V, **Wen J-Z**, Xin YY, Blankenship RE (2010) Small-angle neutron scattering (SANS) investigation of the structure and assembly of the photosynthetic machinery of the green bacterium *Chloroflexus aurantiacus*. *Biophys. J* (under review)

11. Zhang H, Cui W, **Wen J-Z**, Blankenship RE, Gross ML (2010) Nanospray and electron-capture dissociation in FTICR mass spectrometry provide top-down sequencing of an intact protein complex. (under review)
12. **Wen J-Z**, Tsukatani Y, Cui W, Zhang H, Buyle K, Loomis RA, Gross ML, Bryant DA, Blankenship RE (2010) Structural and spectral insights into the FMO protein from the aerobic chlorophototroph, *Candidatus Chloracidobacterium thermophilum*. (under review)
13. Larson CR, Seng C, Lauman L, Matthies HJ, **Wen J-Z**, Blankenship RE, Allen JP (2010) The three dimensional structure of the FMO protein from *Pelodictyon phaeum* and the implications for energy transfer. (under review)
14. Gao X, Xin Y, Bell PD, **Wen J-Z**, Blankenship RE (2010) Structural analysis of alternative complex III in the photosynthetic electron transfer chain of *Chloroflexus aurantiacus*. *Biochemistry* DOI: 10.1021/bi100858k
15. **Wen J-Z**, Zhang H, Gross ML, Blankenship RE (2010) Nature and stoichiometry of pigments in the FMO protein revealed by native spray mass spectrometry. (In preparation)
16. **Wen J-Z**, Huang R, Gross ML, Blankenship RE (2010) Architecture of a photosynthetic membrane revealed by hydrogen/deuterium exchange and mass spectrometry. (In preparation)
17. Zhang H, **Wen J-Z**, Blankenship RE, Gross ML (2010) Structural mass spectrometry by specific carboxyl group labeling. (In preparation)
18. Modesto-Lopez LB, Collins AM, **Wen J-Z**, Blankenship RE, Biswas P (2010) Measuring the size and charge of natural photosynthetic antenna aerosols. (In preparation)

Book Chapter

1. **Wen J-Z**, Collins AM, Blankenship RE (2010) Photosynthetic light-harvesting complexes. In: *Molecular Solar Fuels*, Wydrzynski T, Hillier W, ed., The Royal Society of Chemistry (In preparation)